Frauenklinik und Poliklinik der Technischen Universität München

Klinikum rechts der Isar

Kallikrein-related peptidase 10: a novel independent prognostic marker in advanced high-grade serous ovarian cancer and triple-negative breast cancer

Yueyang Liu

Vollständiger Abdruck der von der Fakultät für Medizin
der Technischen Universität München zur Erlangung des akademischen Grades eines

Doktors der Medizin (Dr. med.)

genehmigten Dissertation.

Vorsitzender: Prof. Dr. Jürgen Schlegel

Prüfer der Dissertation:

1. apl. Prof. Dr. Viktor Magdolen
2. apl. Prof. Dr. Birgit Luber

Die Dissertation wurde am 12.11.2018 bei der Technischen Universität München eingereicht und durch die Fakultät für Medizin am 19.03.2019 angenommen.

For my family

Table of Contents

Tables

Figures

1 Introduction

1.1 Ovarian cancer

According to the global cancer statistics of 2012, ovarian cancer is one of the most frequently diagnosed malignancies. It is the eighth leading cause of cancer death among females worldwide, followed by cancers of the breast, lung, colon, cervix, stomach, liver, and pancreas (Torre et al., 2015). In Europe, the age-standardized incidence rate of ovarian cancer is 10.2 per 100,000, approaching that of kidney cancer (10.5/100,000). However, due to its high fatality, ovarian cancer has twice the age-standardized mortality rate (7.0/100,000) compared to kidney cancer (3.2/100,000), which makes ovarian cancer the fifth deadliest female malignancy (Ferlay et al., 2013).

Ambiguous symptoms, the lack of an effective screening strategy, and late presentation are the characteristics of ovarian cancer, leading to its high fatality. Hence, early ovarian cancer commonly shows no apparent symptoms such as pelvic discomfort, abdominal swelling, weight gain or loss or persisting fatigue (Paulsen et al., 2005). So far, the major screening approaches in the clinical practice of ovarian cancer including transvaginal ultrasonography and detection of CA125 have shown limited sensitivity and specificity concerning the detection of early ovarian cancer, which are still the major screening approaches in the clinical practice of ovarian cancer. Thus, in the past two decades the prior screening strategy failed in providing a survival benefit (Kurman, 2013). The majority of the newly diagnosed ovarian cancer cases are already in an advanced stage when detected, thus contributing to the poor prognosis of the disease (Kipps et al., 2013). Therefore, it is not surprising that the prognosis of this lethal gynecologic malignancy has not obviously improved in recent years (Kurman, 2013).

Based on the guidelines of the Féderation Internationale de Gynécologie et d'Obstétrique (FIGO), ovarian cancer staging is achieved surgically and pathologically, taking into account the major prognostic factors of ovarian cancer (Zeppernick and Meinhold-Heerlein, 2014). Patients suffering from ovarian cancer FIGO stage IA/IB have a 5-year survival rate of up to 91.5 %, whereas only 25-30% of advanced stage (FIGO stage III/IV) ovarian cancer patients live longer than 5 years (Howlader et al., 2015). Hence, early detection is the key to decrease the mortality of ovarian cancer. Accordingly, it is of critical importance to develop accurate and reliable screening methods for the early detection of ovarian cancer.

Histologically, ovarian cancer is classified into epithelial tumors, germ cell tumors and stromal tumors, according to the origin of cancer cells (Au et al., 2015). Epithelial ovarian cancer (EOC) accounts for 90% of malignant ovarian tumors, including serous carcinomas (70-80%) as the major subtype and the rarer types, *i.e.* endometrioid (<5%), mucinous (<3%), and clear cell cancer (3%) (Sundar et al., 2015). EOC exhibits tremendous heterogeneity with respect to the histopathology, clinical features, molecular genetic patterns, and the putative precursor lesions. Based on the current morphologic and molecular research, EOC is divided into the two categories type I (25%) and type II (75%) ovarian cancer (Shih and Kurman, 2004; Walker et al., 2015). The type I subgroup is characterized by high differentiation, containing low-grade serous, low-grade endometrioid, low-grade mucinous and clear cell carcinomas (Jayson et al., 2014). These tumors are mainly derived from typical precursor lesions like cystadenomas and borderline tumors and observed to be clinically indolent and genomically stable (Meinhold-Heerlein and Hauptmann, 2014; Walker et al., 2015). Typically, type II EOCs are more common and more lethal than type I EOCs. Type II tumors are poorly differentiated and described as aggressive, typically presenting at an advanced stage, and exhibiting marked chromosomal aberrations, with a 5-year survival rate of 25% (Kurman and Shih, 2011). Type II EOCs consist of about 70% high-grade serous carcinomas or, less often, high-grade endometrioid adenocarcinomas, undifferentiated carcinomas, and carcinosarcomas (Kurman, 2013; Walker et al., 2015). Thus advanced high-grade serous ovarian cancer is the most common ovarian cancer and constitutes the majority of ovarian cancer-related death (Bast, 2011). Hence, the current study focuses on this most common and lethal subtype of ovarian cancer.

Generally, the cornerstones of ovarian cancer treatment comprise surgery and platinum-containing adjuvant chemotherapy. Individual treatment of ovarian cancer patients depends on FIGO stage and the extent of surgical debulking (Jelovac and Armstrong, 2011; Sundar et al., 2015). At an early stage, the ovarian tumor confines to the ovary (FIGO I) or pelvis (FIGO II). For this subset, comprehensive staging laparotomy plus platinum-based chemotherapy dramatically improves the prognosis. However, it should be noted that only a little portion of ovarian cancer cases are diagnosed early, whereas the majority of patients present at an advanced stage (FIGO III or IV), when the tumors are spread within the abdominal cavity or the patient has distant metastatic disease. For these advanced-stage ovarian cancer patients, standard treatment includes debulking surgery with the goal of removal of all visible tumor, followed by platinum-based

chemotherapy plus an inhibitor of angiogenesis (bevacizumab). In more recent cohorts, 80% of the patients with optimal debulking were disease-free for 5 years (Harter et al., 2017), but those with residual tumor left in the abdomen after surgery, showed a 5-survival rate of 30% or less (Jelovac and Armstrong, 2011). Additionally, residual tumor mass after standard debulking surgery is the only and essential prognostic indicator to be affected by the gynecologist so far (Dorn et al., 2015). Therefore, besides early detection, identification of valid biomarkers for the most common and lethal subtype, advanced high-grade serous ovarian cancer, is an imperative and alternative way to better predict the outcome of patients and develop corresponding targeting therapies, improving the prognosis of these patients.

1.2 Breast cancer

Breast cancer is the most frequent malignancy among females and the second most common cancer worldwide, following lung cancer. In the year of 2012, approximately 1.7 million women were newly diagnosed with breast cancer on the worldwide scale, accounting for 25% of all new cancer cases (Ferlay et al., 2015). It has been assumed that 10-12% of women around the world will be afflicted with breast cancer during their lifetime (Harbeck and Gnant, 2017).

Besides advanced age, risk factors for breast cancer include major inheritance susceptibility (*e.g.*, BRCA1/2), alcohol intake, menstrual history (early menarche/late menopause), nulliparity, older age at first birth, hormone therapy history, obesity (postmenopausal), and benign breast disease history (Harbeck and Gnant, 2017). Based on the risk factors, screening strategies for asymptomatic women are established through clinical trials.

When breast cancer is suspected clinically or in screening mammography, the patient will be referred to biopsy for diagnosis confirmation. Depending on the tumor biology and stage, the breast cancer patients will be recommended an adapted and individual therapy, possibly including surgery, systemic therapy, and radiation therapy. In surgery of breast cancer, the concept of sentinel lymph node biopsy is well established, and could remarkably decrease the necessity of full axillary lymph node dissection and thus minimize suffering from surgery (Giuliano et al., 2011). Systemic therapy includes chemotherapy (neoadjuvant or adjuvant), endocrine therapy and HER2 targeted therapy, which performs the anti-tumor effects via blood circulatory system, whereas simultaneously influence the normal parts of human body. Preoperative systemic

therapy, also known as neoadjuvant therapy, is more frequently applied to shrink the tumor volume before surgery, thus increasing the possibility for breast-conserving surgery (Mauri et al., 2005).

Owing to (i) the increased awareness, (ii) powerful screening programs leading to earlier detection, and (iii) effective systemic therapies, the mortality of breast cancer has been moderately reduced in the past two decades around the world. Nevertheless, it should be recognized that breast cancer is still a big challenge for the present, even in the developed countries. In the United States, an estimated 252,710 women are expected to be diagnosed with breast cancer and more than 40,610 women are supposed to die from the disease in the year of 2017. This accounts for 30% of new cancer diagnoses and 14% of cancer deaths among women, respectively (Siegel et al., 2017).

The main cause leading to this scenario is attributed to the fact that breast cancer is very heterogenous malignant disease displaying great heterogeneity in morphology, biology, clinical feature, and treatment sensitivity (Geyer et al., 2009). Several biomarkers have been introduced to determine the molecular subtypes of breast cancer, like estrogen receptor (ER), progesterone receptor (PR), and the human epidermal growth factor receptor 2 (HER2), as well as the tumor proliferation factor Ki67. HER2 is a transmembrane tyrosine kinase receptor and has been identified to be involved in tumorigenesis of breast cancer (Moasser, 2007). Moreover, amplification of HER2 has been reported to happen in around 15-20% of breast cancer patients and be remarkably associated with an increased recurrence risk and poor outcomes (Ross et al., 2009; Krishnamurti and Silverman, 2014).

Based on the expression or amplification of the above-named markers in formalin-fixed paraffin-embedded tumor samples, breast cancer is classified into four clinically relevant molecular subtypes (**Table 1**): luminal A, luminal B, HER2-positive, and triple-negative (Senkus et al., 2015).

According to their molecular features, the targeted therapies for luminal A, luminal B, and HER2-positive subtypes have been developed appropriately and applied in daily clinical practice of breast cancer, bringing steady improvements in outcome. Luminal A and luminal B subgroups are sensitive to endocrine therapy, *e.g.* selective estrogen receptor modulators and aromatase inhibitors, moreover luminal B displays good sensitivity to routine chemotherapy of breast cancer (Krishnamurti and Silverman, 2014). HER2-targeting therapies, *e.g.* the monoclonal antibody trastuzumab

(Herceptin®) and the tyrosine kinase inhibitor lapatinib (Tykerb®) have been specially developed for HER2-positive breast cancer and have proven to significantly decrease the risk of disease recurrence and cancer-related death (Romond et al., 2005; Cameron et al., 2010).

Table 1. Intrinsic subtypes of breast cancer based on the status of ER, PR, HER2, and Ki67

Subtypes	ER, PR, HER2, and Ki67 status
Luminal A	ER-positive HER2-amplification negative Ki67 low PR high (> 20%) low-risk molecular signature (if available)
Luminal B (HER2-negative)	ER-positive HER2-amplification negative Ki67 high or PR low (≤ 20%) high-risk molecular signature (if available)
Luminal B (HER2-positive)	ER-positive HER2-amplification positive any Ki67 any PR
HER2-positive	HER2-positive ER and PR absent
Triple-negative	ER and PR absent HER2-amplification negative

ER estrogen receptor; HER2 human epidermal growth factor 2 receptor; PR progesterone receptor. Adapted from (Senkus et al., 2015).

Nevertheless, in case of triple-negative breast cancer (TNBC), the improvements in outcome presently seem to plateau. Like for the other three molecular subtypes, the prognosis of TNBC has been notably improved in the past two decades, owing to improvement in (neo-)adjuvant chemotherapy. However, only few additional systemic therapies have been introduced into the management of TNBC (Palma et al., 2015). As shown in **Table 1**, TNBC is characterized by the lack of ER and PR expression as well as the absence of HER2 amplification, excluding TNBC patients from the available targeted, anti-hormonal or HER2-targeting therapies. This, together with an aggressive spread (see below) explains the fact that TNBC patients have the worst prognosis among all subtypes (Foulkes et al., 2010).

Generally, TNBC accounts for about 17% of breast cancers, is associated with a higher histopathological grade, more commonly occurs in younger women (<50 years), and more likely shows distant recurrence (Millikan et al., 2008; Foulkes et al., 2010; Bonzanini et al., 2012). TNBC is very aggressive and tends to disseminate to visceral organs in the early course of the disease. It is observed that unlike the other subtypes of breast cancer that preferentially metastasize to axillary nodes and bones, TNBC tends to disseminate to brain, lungs, and liver (Hicks et al., 2006; Reis-Filho and Tutt, 2008). Patients afflicted with metastatic TNBC have been previously reported to have a median survival time of less than 13 months (Kassam et al., 2009). This is also due to the fact that besides adjuvant chemotherapy (anthracycline-based), there is no tailored treatment available for TNBC yet. Therefore, valid biomarkers for either developing individualized treatment or improving the management of TNBC are urgently needed.

1.3 Kallikrein-related peptidases

Prostate-specific antigen (PSA) is a well-established biomarker in prostate cancer, applied in screening, staging, treatment, and monitoring for recurrence. PSA, also known as kallikrein-related peptidase 3 (KLK3), is a serine protease of the family of kallikrein-related peptidases. The kallikrein-related peptidase family encompasses 15 closely related serine proteases. The first member of this family, tissue kallikrein (KLK1), was identified in the 1930s as a protease in pancreatic extracts with kininogenase activity, participating in the regulation of blood pressure (Schedlich et al., 1987). Subsequently, 14 serine proteases have been discovered with a conserved structure and enzymatic protease function compared to KLK1. These enzymes, however, lack kininogenase activity and, therefore, are accordingly named kallikrein-related peptidase 2-15 (Lundwall et al., 2006).

The human KLK proteins are encoded by the genes KLK1-15 located on the long arm of chromosome 19q13.4 (**Figure 1**), with lengths ranging from 4.3 to 10.5 kb (Borgono and Diamandis, 2004). The 15 KLK genes are tightly arranged in a contiguous cluster without non-KLK gene insertion, comprising the largest tandem protease gene cluster of the human genome (Clements et al., 2001). The KLK genes share a great similarity in sequence and structure. KLK1-3 share 61-79% of sequence identity with each other, while 38-57% for KLK4-15 (Goettig et al., 2010). The KLK genes are divided into the classical KLKs (KLK1-3) and the new KLKs (KLK4-15) (Harvey et al., 2000). All KLK genes encompass five highly conserved coding exons (**Figure 1**), while KLK4-

15 additionally contain 1 or 2 non-coding exons in the 5′ untranslated region (Borgono et al., 2004). The codons for the three amino acids constituting KLK catalytic triad, histidine (H), aspartic acid (D), and serine (S), are well conserved at the end of coding-exon 2, middle of coding exon 3, and the beginning of coding exon 5, respectively (**Figure 1**) (Lawrence et al., 2010). Unlike the coding exons, the intervening introns of KLKs are highly variable in lengths and sequences (Kryza et al., 2015). Alternative splicing of mRNA transcripts is commonly observed among KLKs.

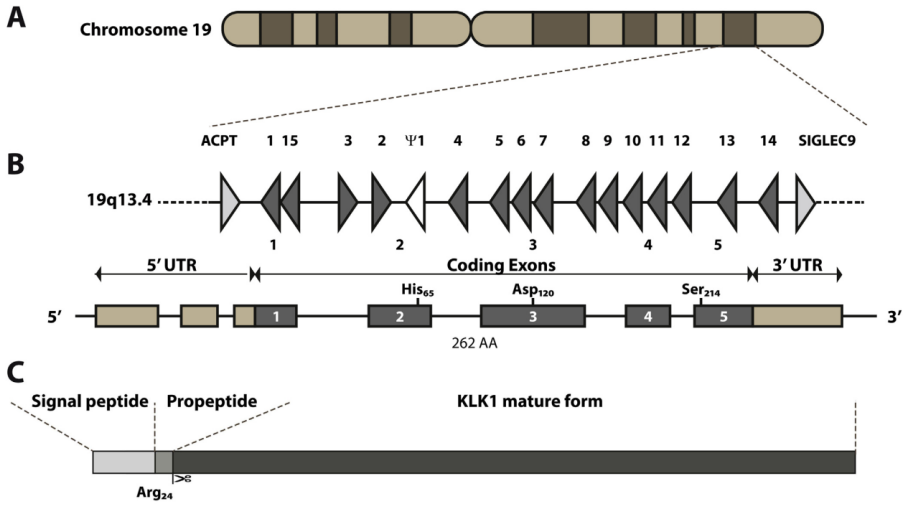

Figure 1. Gene, mRNA, and protein characteristics of kallikrein-related peptidases
A. The KLK locus is located on chromosome 19q13.3-13.4 and flanked by the genes for testicular acid phosphatase (ACPT) and sialic acid-binding Ig-like lectin 9 (SIGLEC9). **B**. Typically, KLKs comprise five coding exons (dark gray boxes), of which exon 2 contains the codons of catalytic His65, exon 3 of Asp120, and exon 5 of Ser214, as exemplified here by KLK1 mRNA. **C**. KLKs are first synthesized as single-chain pre-pro-enzyme comprising three domains: a signal peptide, a propeptide, and a core domain accomplishing the catalytic activity. Adapted from (Kalinska et al., 2016).

In hormone-related tissues, most KLKs are regulated by steroid hormones, such as androgen, estrogen, and progestin (Shaw and Diamandis, 2008). Also, it is highlighted that epigenetic-related mechanisms are involved in the transcriptional and post-transcriptional regulation of KLKs, such as DNA methylation, histone modification, and miRNA-mediated control of mRNA levels (Pasic et al., 2012; Samaan et al., 2014; Pasic et al., 2015). Moreover, single nucleotide polymorphisms (SNP), variations occurring on the DNA level, have been demonstrated to influence the mRNA and protein expression of KLKs or alter the proteolytic activity of the resulting KLK proteases (Michael et al., 2005; Lai et al., 2007).

According to their structure and proteolytic mechanism, KLK proteases belong to the S1 peptidase family and are secreted serine endopeptidases. KLK proteins display a molecular weight of about 25-30 kDa and are composed of 244-253 amino acids (Kalinska et al., 2016). The pre-pro-enzymes of the KLKs are composed of three domains: a signal peptide, 16 to 30 amino acids long, guiding the pre-pro-enzyme into the endoplasmatic reticulum for secretion; a propeptide, four to nine amino acids long, rendering the proteases as inactive form; a core domain (mature form), encompassing the invariant catalytic triad of histidine, aspartic acid, and serine (Clements et al., 2001). Similar to most of the members of the S1 clade, KLKs are synthesized as single-chain pre-pro-enzyme with active sites sterically masked the zymogen forms. After activation, the enzymes display with chymotrypsin-like activity or trypsin-like activity (Lawrence et al., 2010).

Extracellular activation is a critical step in regulation of the levels of active KLKs. Firstly, guided by the signal (pre-) peptide, the newly synthesized pre-pro-KLKs are transported into the endoplasmic reticulum, followed by proteolytic removal of the signal peptide. The resulting proteins, pro-KLKs or zymogens are still enzymatically inactive. For activation, the propeptides of pro-KLKs have to be extracellularly removed via specific proteolytic cleavage, thus completing the conversion of pro-KLKs to the mature forms (Guo et al., 2014; Kalinska et al., 2016). Proteolytic removal of the pro-peptides is mediated by proteases, and may vary from KLK to KLK. The list of pro-KLK-activating enzymes includes plasmin, matrix metalloproteinases (MMP), tissue-type plasminogen activator (tPA), urokinase plasminogen activator (uPA), thrombin, factor Xa and mature KLK proteins (Yoon et al., 2008, 2013). The cross-activation relationships of KLKs have been reported by Yoon and co-workers (Yoon et al., 2007, 2009) using 12 different mature KLKs to process the 15 different pro-KLK peptides, indicative of the potential for KLK activation cascades. Furthermore, extracellular activation of KLK2, 6 and 13 has been reported to be performed by autolytic activation (Yoon et al., 2007).

In humans, KLKs are widely expressed in various tissues and can be detected in most of the physiological fluids (Shaw and Diamandis, 2007), suggesting that KLKs are broadly involved in physiologic and pathological processes. In fact, KLKs have been described to be associated with most crucial mechanistic pathways like angiogenesis, skin desquamation, seminal liquefaction, wound healing, viral infections, and tumorigenicity (Kalinska et al., 2016).

1.4 Kallikrein-related peptidases in cancer

Accumulating evidence has revealed that KLKs are dysregulated in various malignancies, including ovarian, breast, prostate, bladder, salivary, colon, gastric, and lung cancer (Planque et al., 2006; Dorn et al., 2014; Linardoutsos et al., 2014). Via different *in vitro* and *in vivo* strategies, KLKs have been demonstrated to be involved in the modulation of tumor-relevant processes, both as autocrine and paracrine factors impacting components of the tumor microenvironment. KLK-mediated pericellular proteolysis influences growth factors, cell adhesion molecules, cell surface receptors, and extracellular matrix proteins, which are associated with proliferation, angiogenesis, migration, invasion, and chemo-resistance (Kryza et al., 2015).

1.4.1 Impact of KLKs on cancer cell proliferation

Cell proliferation as the initial and critical step of cancer development, has been reported to be modulated by KLKs through protease-activated receptors (PARs), growth factors and some components of the extracellular matrix (ECM). When the extracellular N-terminus of PARs is cleaved by the serine endopeptidase activity of e.g. KLK1, 2, 4, 5 and 6, the new N-terminal sequence of PARs binds intramolecularly to itself and initiates signal pathway, leading to increased cell proliferation (Yu et al., 2014). In prostate cancer cells, recombinant KLK2 and KLK4 proteases are capable of activating PAR1 and PAR2, whose downstream mitogens can further initiate the mitogen-activated protein kinase (MAPK) pathway, thereby promoting proliferation of prostate cancer cells (Mize et al., 2008). Enhanced KLK6 expression in lung cancer cells has been shown to favor proliferation and decrease the apoptosis rate by mediating the PAR2-dependent epidermal growth factor receptor (EGFR) signaling pathway (Michel et al., 2014). Moreover, KLKs have been reported to be implicated in tumorigenesis by modulating the activity and bioavailability of growth factors. Insulin-like growth factor binding proteins (IGFBPs) can be directly degraded by KLK1-5, 11, and 14, resulting in the release of insulin-like growth factor (IGF). This process diminishes the tumor suppression activity of IGFBPs, but also elevates the availability of IGF (Michael et al., 2006; Sano et al., 2007). The released IGF can interact with the corresponding receptors on tumor cells to induce cell proliferation. Furthermore, modulation of growth factor bioavailability can also be attributed to the KLK enzymatic activity towards components of the extracellular matrix (ECM), which is associated with the insulation of growth factors. For example, KLKs can degrade ECM

components to release the sequestrated growth factors like fibroblast growth factor (FGF), epidermal growth factor (EGF), and transforming growth factor beta (TGF-ß) (Lawrence et al., 2010).

In contrast, some members of the KLK family are also supposed to exert an anti-proliferative effect during tumorigenesis as exemplified by KLK4, which suppresses proliferation in the prostate cancer cell line PC-3 (Veveris-Lowe et al., 2005). Besides, the *in vitro* study of Zheng and co-workers (Zheng et al., 2012) has demonstrated that elevated KLK10 can inhibit cell proliferation and invasiveness in tongue cancer. Moreover, transfection of ES-2 ovarian cancer cells with KLK5 or KLK10 expression plasmids resulted in an obvious reduction of tumor growth and colony formation in a nude mouse model (Pepin et al., 2011).

1.4.2 Impact of KLKs on cancer cell migration

KLKs are involved in migration and invasion in various types of cancer cells, via (i) degradation of ECM components, (ii) modulation of adhesion and junction proteins, and (iii) control of epithelial-mesenchymal transition (EMT). ECM is indispensable with regard to constituting a physical barrier prohibiting the dissemination of cancer cells. KLKs can directly cleave the components of ECM including fibronectin, vitronectin, collagens, and laminins, but can also induce ECM degradation induced by activating matrix metalloproteinases (MMPs) (Lawrence et al., 2010). Overexpression of KLK13 in lung adenocarcinoma cells was shown to enhance laminin degradation *in vitro* and to increase the number of lung metastasis in a xenograft model (Chou et al., 2011). Cell-cell adhesion molecules like corneodesmin, desmocollin, desmoglein 1 and 2, and E-cadherin, have been demonstrated as substrates of KLKs *in vitro*, revealing that KLKs can enhance tumor cell motility through proteolytic processing of these adhesion proteins (Lawrence et al., 2010). In addition, KLKs have been observed to regulate expression of adhesion molecules. When subjected to exogenous recombinant KLK6 protein, gastric and colon cancer cells showed a reduced promoter activity of E-cadherin (Kim et al., 2011, 2012). Last but not least, KLKs are implicated in the process of EMT, where epithelial cells transform into mesenchymal-like cells for reinforcement of cell motility (Veveris-Lowe et al., 2005; Thiery et al., 2009). KLK3 and KLK4 have been shown to promote the EMT-like changes in prostate cancer cells as evidenced by an increase in mesenchymal markers and the absence of epithelial markers (Veveris-Lowe et al., 2005).

Nevertheless, some KLKs also display an anti-metastatic effect in some types of cancer. KLK6 overexpression in MDA-MB-231 breast cancer cells led to a negative impact on cancer cell migration and impaired tumorigenesis in a xenograft model (Pampalakis et al., 2009). CL1-5 lung adenocarcinoma cells with KLK8 overexpression have been associated with a reduction in cell invasion and migration *in vivo* as well. This might be due to the fact that KLK8 induced fibronectin degradation can suppress tumor cell motility by inhibition of actin polymerization (Sher et al., 2006).

1.4.3 Impact of KLKs on cancer angiogenesis

Angiogenesis is supposed to be the cornerstone of tumorigenesis, owing to the fact that neovascularization can provide sufficient nutrients and oxygen for tumor growth, and also promote spread of cancer cells. Gastrointestinal stromal cancer cells have been found to express and secret KLK1, which enhanced the secretion of vascular endothelial growth factor (VEGF) and further increased neovascularization (Dominek et al., 2010). KLK3 has been reported to induce expression of proangiogenic factors through activation of the latent TGF-β, thus contributing to angiogenesis (Seoane and Gomis, 2017). Besides, KLKs can support angiogenesis via degradation of ECM components as mentioned above. Conversely, KLK5, 6 and 13 were reported to exert an anti-angiogenic effect by the generation of antiangiogenic peptides. The three KLKs degraded plasminogen, resulting in the release of angiostatin-like peptides, which in turn suppressed proliferation of endothelial cells during angiogenesis (Bayés et al., 2004; Michael et al., 2005).

1.5 Kallikrein-related peptidases as biomarkers in ovarian and breast cancer

Concerning their effects on tumorigenesis, KLKs are supposed to serve as suitable biomarkers in various types of cancer. Many members of the KLK family have been found to be possibly utilized as diagnostic and prognostic markers in several types of tumors, primarily in hormone-related cancers like testicular, prostate, ovarian, and breast cancer. To exemplify the relevance of KLKs as biomarkers in hormone-related malignancies, detailed clinical data of KLKs in ovarian and breast cancer is summarized in **Table 2** and **Table 3**.

In ovarian cancer, most KLKs have been reported to be upregulated (**Table 2**). Compared with normal ovaries, mRNA expression of KLK4-8, 14, and 15 are elevated in ovarian cancer tissues. Elevated expression has also been observed at the protein

level for KLK4, 6, 10, 11, and 13. ELISA analysis of KLK proteins in serum of healthy and cancerous cohorts suggested that the concentrations of KLK5, 6, 8, 10, 11, and 14 were enhanced in ovarian cancer patients. These results are again indicative that KLKs have a high potential as screening and/or diagnostic biomarkers in ovarian cancer.

In breast cancer, KLK5-8 and KLK10-13 are downregulated at the mRNA level, compared to noncancerous breast tissues. On the other hand, KLK4 has been observed to be overexpressed in breast cancer tissues both at the mRNA and protein levels. There are contradictory reports in as much as KLK5, 10 and 14 were found to be upregulated in serum of breast cancer patients while they are downregulated in cancer tissue (**Table 3**). This discrepancy can be attributed to the fact that glandular destruction and angiogenesis may facilitate the release of KLK protein into serum during tumorigenesis.

As summarized in **Table 2** and **Table 3**, KLKs are often associated with patient prognosis in ovarian and breast cancer. In ovarian cancer, upregulation of KLK4-7 and 10 implies an unfavorable prognosis, while upregulation of KLK9, 13, and 14 is indicative of a favorable prognosis. In breast cancer, elevated levels of KLK4, 5, 8, 10, and 14 are associated with unfavorable outcome, whereas higher levels of KLK3, 9, 12, 13, and 15 are indicative of a favorable outcome. Interestingly, previous studies have reported controversial results of KLKs on the prognosis of ovarian and breast cancer. While Shigemasa et al. (Shigemasa et al., 2004) showed that elevated KLK11 mRNA levels are correlated with a shortened overall survival in ovarian cancer, Diamandis et al. (Diamandis et al., 2004) observed that patients with KLK11-positive tumors have a longer overall and progression-free survival, compared to KLK11-negative cases. Similar results have been reported in the case of KLK7 for breast cancer (**Table 3**). These conflictive findings are speculated to be attributed to the heterogeneous patient cohorts previously analyzed, including mixed histological subtypes and clinical stages. As exemplified by the work of Diamandis and co-workers (Diamandis et al., 2004), the heterogeneous cohort of ovarian cancer patients investigated, consisted of all stages, low/high grade, and various histological subtypes. Therefore, in the current study, a homogeneous cohort of patients with advanced high-grade serous ovarian cancer FIGO stage III/IV was analyzed to investigate the impact of KLKs on prognosis. Analogously, in the breast cancer setting, we analyzed a homogeneous cohort consisting of triple-negative breast cancer patients only.

Table 2. Expression and clinical relevance of KLKs in ovarian cancer

KLK	Expression in ovarian cancer tissue or serum compared to normal	Prognosis		Reference
		Favorable	Unfavorable	
4	↑ mRNA and protein in tissue		PFS and OS	(Obiezu and Diamandis, 2005) (Dong et al., 2001) (Obiezu et al., 2001)
5	↑ mRNA in tissue ↑ protein in serum and ascitic fluid		PFS and OS	(Yousef et al., 2003) (Dong et al., 2003) (Diamandis et al., 2003)
6	↑ mRNA and protein in tissue ↑ protein in serum		OS PFS and OS OS	(Yousef et al., 2003) (Diamandis et al., 2000) (Kountourakis et al., 2008) (Shan et al., 2007) (Ahmed et al., 2016)
7	↑ mRNA in tissue		OS PFS	(Adib et al., 2004) (Psyrri et al., 2008) (Shan et al., 2006)
8	↑ mRNA in tissue ↑ protein in serum	OS and DFS; PFS and OS	DFS	(Adib et al., 2004) (Kishi et al., 2003) (Kountourakis et al., 2009) (Magklara et al., 2001) (Borgoño et al., 2006)
9	ND	PFS and OS		(Yousef et al., 2001)
10	↑ protein in tissue ↑ protein in serum		PFS and OS	(Luo et al., 2001, 2003) (Luo et al., 2001)
11	↑ protein in tissue ↑ protein in serum	PFS and OS; PFS and OS	OS	(Diamandis et al., 2002; Borgoño et al., 2003) (Geng et al., 2017) (Shigemasa et al., 2004) (Diamandis et al., 2004)
13	↑ protein in tissue	PFS and OS		(Kapadia et al., 2003) (Scorilas et al., 2004)
14	↑ mRNA in tissue ↑ protein in serum ↓ protein in tissue	PFS and OS		(Yousef et al., 2001) (Borgoño et al., 2003) (Yousef et al., 2003)
15	↑ mRNA in tissue	OS	PFS and OS	(Yousef et al., 2003) (Geng et al., 2017)

↑ upregulated; ↓ downregulated; ND not determined; OS overall survival; PFS progression-free survival; DFS disease-free survival.

Table 3. Expression and clinical relevance of KLKs in breast cancer

KLK	Expression in ovarian cancer tissue or serum compared to normal	Prognosis		Reference
		Favorable	Unfavorable	
3	↓ Protein in tissue	OS and DFS		(Black and Diamandis, 2000) (Yu et al., 1998)
4	↑ mRNA and protein in tissue		DFS	(Mangé et al., 2008) (Yang et al., 2017)
5	↓ mRNA in tissue ↓ mRNA in tissue ↑ protein in serum		OS and DFS OS and DFS	(Yousef et al., 2004) (Li et al., 2009) (Yousef et al., 2003) (Yousef et al., 2002)
6	↓ mRNA in tissue	ND	ND	(Yousef et al., 2004)
7	↓ mRNA in tissue	DFS	OS and DFS	(Li et al., 2009) (Holzscheiter et al., 2006) (Talieri et al., 2004)
8	↓ mRNA in tissue		DFS	(Yousef et al., 2004) (Michaelidou et al., 2015)
9	ND	OS and DFS		(Yousef et al., 2003)
10	↓ mRNA in tissue ↓ mRNA in tissue ↑ protein in serum ↑ DNA methylation	OS (methylation)	OS DFS	(Yousef et al., 2004) (Dhar et al., 2001) (Ewan King et al., 2007) (Kioulafa et al., 2009) (Wang et al., 2016) (Luo et al., 2002)
11	↓ mRNA in tissue	ND	ND	(Yousef et al., 2004)
12	↓ mRNA in tissue	DFS		(Yousef et al., 2000) (Yousef et al., 2004) (Talieri et al., 2012)
13	↓ mRNA in tissue	OS and DFS		(Yousef et al., 2000) (Chang et al., 2002)
14	↓mRNA in tissue ↑ mRNA in tissue ↑ protein in serum		OS and DFS	(Mangé et al., 2008) (Borgoño et al., 2003) (Papachristopoulou et al., 2011) (Yousef et al., 2002)
15	ND	OS and DFS		(Yousef et al., 2002)

↑ upregulated; ↓ downregulated; ND not determined; OS overall survival; PFS progression-free survival; DFS disease-free survival.

1.6 Kallikrein-related peptidases 9 (KLK9) and 10 (KLK10)

KLK9, also known as KLK-L3, localizes immediately upstream of the KLK8 and downstream of the KLK10 on the KLK locus of chromosomal region 19q13.3–q13.4 (Yousef and Diamandis, 2000). Like other members of the KLK family, KLK9 encodes a 27.5 kDa pre-pro-peptide, which includes an N-terminal signal peptide, a propeptide and the protease domain (Lawrence et al., 2010). Following secretion and extracellular removal of the pro-peptide, the mature KLK9 protein is supposed to show a chymotrypsin-like activity, whereas its exact enzymatic activity and endogenous substrates have not yet been confirmed (Yousef and Diamandis, 2001; Filippou et al., 2017). Besides, the expression of KLK9 has been identified to be modulated by estrogens, progestin, and androgens (Yousef and Diamandis, 2000).

Prior studies have shown that KLK9 is implicated in several pathophysiological processes such as cardiovascular diseases, neurological diseases, and cancerous disorders. Blazquez-Medela and co-workers (Blazquez-Medela et al., 2015) have found that urinary KLK9 is strongly associated with cardiac hypertrophy, hypertensive cardiac and vascular damage. Elevated levels of KLK9 have been identified to contribute to neurodegenerative changes during spinal cord injury, representing a potential target in the improvement of neuroprotection (Radulovic et al., 2013). Furthermore, Drucker et al. (Drucker et al., 2015) revealed an association of high KLK9 expression with higher grade gliomas and poor prognosis of this tumor entity. Conversely, in case of breast cancer, KLK9 overexpression has been observed to be related with smaller tumor mass, improved disease-free and overall survival (Yousef et al., 2003). Furthermore, it has been reported that in ovarian cancer KLK9 mRNA expression is significantly associated with early disease stage and inversely coupled to CA125 levels. Moreover, ovarian cancer patients with KLK9-positive expression displayed a significantly prolonged progression-free and overall survival (Yousef et al., 2001).

KLK10 was originally identified as NES1 (normal epithelial cell-specific 1), due to its selective expression in normal human mammary epithelial cells (Zhang et al., 2006). Further work demonstrated that this gene is located immediately upstream of the KLK9 and downstream of the KLK11 on the KLK locus of chromosomal region 19q13.3–q13.4, encoding a 30.14 kDa serine protease with high homology to the KLK family (Yousef et al., 2005). Therefore, it was renamed KLK10. The KLK10 gene comprises

six exons, of which the first exon is noncoding and the third exon has a large CpG island (Elliott et al., 2006; Pasic et al., 2012). The KLK10 protein is composed of 276 amino acids, possessing a 33-residue signal peptide, followed by a 13-residue activating peptide, and a 230-residue catalytic domain (Lundwall and Brattsand, 2008). Expression of KLK10 is controlled by steroid hormones, DNA hypermethylation, and miRNAs (White et al., 2010; Pasic et al., 2012).

KLK10 is widely distributed in various human organs and biological fluids (Luo et al., 2001) and broadly involved in pathophysiological processes. Cumulative evidence indicates that KLK10 has a cancer-specific impact on tumor progression. KLK10 has been described to exert a tumor-suppressing role in diverse human cancers like breast, esophageal, prostate, testicular, and tongue cancer (Luo et al., 2001; Yunes et al., 2003; Zheng et al., 2012; Hu et al., 2015; Li et al., 2015). However, in ovarian, gastric, colon, and endometrial cancer, KLK10 overexpression has been observed to be associated with unfavorable prognosis (Luo et al., 2003; Feng et al., 2006; Santin et al., 2006; Jiao et al., 2013). Luo et al. (Luo et al., 2003) have quantified serum levels of KLK10 in 146 ovarian cancer patients, demonstrating that patients with high KLK10 expression was associated with serous epithelial type, late-stage, and advanced grade tumors, suboptimal debulking, and resistance to chemotherapy.

Altogether, accumulative evidence strongly indicates that KLK9 and KLK10 may serve as diagnostic and prognostic biomarkers in ovarian and breast cancer. Of note, as mentioned above, ovarian and breast cancer both represent heterogeneous diseases and are composed of several distinct subtypes. Thus, in the present study, we focused on the analysis of KLK9 and/or KLK10 expression in homogenous ovarian cancer (advanced high-grade serous ovarian cancer) and breast cancer (triple-negative breast cancer) cohorts and evaluated their clinical relevance in these well-defined subgroups.

2 Aims of the study

Accumulating evidence has revealed that most KLKs are dysregulated in malignancies and involved in the modulation of tumor-relevant processes. Many members of the KLK family have been proposed to be utilized as diagnostic and prognostic markers in ovarian and breast cancer. Nevertheless, the prognostic impact of KLKs on these tumor entities was previously reported to be paradoxical. Recently, this was speculated to be attributed to the heterogeneous patient cohorts analyzed in former researches. Therefore, the current project aimed at investigating tumor-relevant expression of KLK9 and KLK10 in homogenous ovarian cancer cohorts (advanced high-grade serous ovarian cancer) and breast cancer cohort (triple-negative breast cancer) and correlating the expression levels with clinical outcome.

To achieve our purpose, the following steps were performed:

1. Establishment of PCR-based assays for quantification of KLK9 and/or KLK10 mRNA expression levels in ovarian and breast cancer tumor tissue specimens.
2. Establishment of immunohistochemical (IHC) assays for detection of KLK9 and/or KLK10 protein expression levels in tumor tissue of both cancer types.
3. Correlation of KLK10 mRNA expression levels with its corresponding protein expression levels in tumor tissue of both cancer types.
4. Association of KLK9 and/or KLK10 mRNA and protein expression, respectively, with clinical parameters of advanced high-grade serous ovarian cancer and triple-negative breast cancer patients.
5. Association of KLK9 and/or KLK10 mRNA and protein expression, respectively, with the clinical outcome of patients afflicted with advanced high-grade serous ovarian cancer and triple-negative breast cancer.

3 Patients, Materials, and methods

3.1 Advanced high-grade serous ovarian cancer patients

The ovarian tumor tissue samples enrolled in the current study were obtained from patients afflicted with advanced (FIGO stage III/IV) high-grade serous ovarian cancer, treated between 1990 and 2013 at the Department of Obstetrics and Gynecology, Klinikum rechts der Isar, Technical University of Munich (TUM), Germany. All patients received standard stage-related primary radical debulking surgery. Following surgery, platinum-based adjuvant treatment was performed based on consensus recommendations at that time. Patients receiving any neoadjuvant therapy prior to surgery were excluded. The assessment of KLK expression in the collected tissues of ovarian cancer patients was approved by the Ethics Committee of the Medical Faculty of TUM (number of Ethics Committee: 491/17 S). Written informed consent from patients authorized the utilization of collected tumor tissues for research purposes.

Tumor tissues were collected during surgery, inspected for malignancy by pathologists, and validated tumor tissues stored in liquid nitrogen until extraction. RNA was isolated from 139 frozen tumor specimens of advanced high-grade serous ovarian cancer (cohort 1, n = 139) and stored at –80 °C until analysis. Simultaneously, the Department of Pathology and Pathological Anatomy routinely worked on the preparation of formalin-fixed, paraffin-embedded (FFPE) ovarian cancer tissues. FFPE blocks were used for the preparation of the tissue microarrays (TMAs), encompassing 159 cases of tumor tissue of advanced high-grade serous ovarian cancer patients (cohort 2, n = 159). 60 patients of cohort 1 overlapped with cohort 2. The clinical data of the advanced high-grade serous ovarian cancer patients of cohort 1 and 2 are documented in **Table 4** and **Table 5**, respectively.

Table 4. Clinical data of advanced high-grade serous ovarian cancer patients in cohort 1 (n = 139).

Clinical parameters	Number	Percentage
All patients	139	
Median age (range)	64 (33-88) years	
Median observation time of patients alive (range)	29 (2-279) months	
Age		
≤ 60 years	58	41.7
> 60 years	81	58.3
Residual tumor mass		
0 mm	70	50.4
> 0 mm	67	48.2
No data	2	1.4
Ascitic fluid volume		
≤ 500 ml	78	56.1
> 500 ml	54	38.9
No data	7	5.0
FIGO stage		
III	109	78.4
IV	30	21.6
Disease recurrence		
Yes	76	54.7
No	33	23.7
no data	30	21.6
Alive recurrence		
Yes	78	56.1
No	47	33.8
no data	14	10.1

Table 5. Clinical data of advanced high-grade serous ovarian cancer patients in cohort 2 (n = 159).

Clinical parameters	Number	Percentage
All patients	159	
Median age (range)	65 (33-88) years	
Median observation time of patients alive (range)	29 (1-270) months	
Age		
≤ 60 years	57	35.8
> 60 years	102	64.2
Residual tumor mass		
0 mm	75	47.2
> 0 mm	80	50.3
No data	4	2.5
Ascitic fluid volume		
≤ 500 ml	88	55.4
> 500 ml	66	41.5
No data	5	3.1
FIGO stage		
III	120	75.5
IV	39	24.5
Disease recurrence		
Yes	95	59.7
No	33	20.8
no data	31	19.5
Alive		
Yes	65	40.9
No	85	53.5
no data	9	5.6

3.2 Triple-negative breast cancer patients

One-hundred and twenty-seven patients afflicted with triple-negative breast cancer (TNBC, cohort 3, n = 127) were enrolled in the study conducted between the year 1988 and 2012 at the Department of Obstetrics and Gynecology, Klinikum rechts der Isar, Technical University of Munich (TUM). As mentioned above for the ovarian cancer patients, tumor tissues were collected after inspection and immediately stored in liquid nitrogen and also routinely tested by pathologists for ER, PR, and HER2 expression. Tumor specimens were categorized as triple-negative breast cancer by the following rules (Yang et al., 2017): Lack of estrogen receptor (ER) and progesterone receptor (PR) protein expression and absence of or low HER2 expression (immunohistochemically determined score 0, 1+; or score 2+ with negative fluorescence in situ hybridization [FISH] test for testing HER2 amplification).

In the TNBC cohort, all patients primarily underwent standard surgical procedures including mastectomy or breast conservation surgery and none of them had primary metastasis after surgery. Invasive ductal carcinoma subtype accounted for 91% (115/127) of all carcinomas and the rest were rare subtypes like medullary, lobulary, and others. Regarding treatment, adjuvant therapy was administered based on consensus recommendations at that time. 74% (94/127) of the patients were treated with anthracycline- or cyclophosphamide-based chemotherapy; 16% (20/127) received endocrine therapy along; 75% (95/127) of the patients were given radiotherapy. The histomorphologic parameters and clinical data were documented in **Table 6**.

We also analyzed mRNA levels in 27 hormone receptor-positive breast cancer specimens (HRPBC, n = 27). Tumor specimens were categorized as HRPBC by the following rules: positive expression of ER and PR and absence of HER2 expression (immunohistochemically determined score 0, 1+; or score 2+ with negative FISH test).

The biomarker study in breast tumor tissues was approved by the local Ethics Committee (number of Ethics Committee: 491/17 S) and written informed consent of the study was available for all patients.

Table 6. Clinical characteristics of TNBC patients in cohort 3 (n = 127).

Clinical parameters	Number	Percentage
All patients	127	
Median age (range)	55 (30-96) years	
Median observation time of patients alive (range)	79 (4-286) months	
Age		
≤ 60 years	69	54.3
> 60 years	58	45.7
Menopausal status		
Pre-menopausal	42	33.1
Peri-menopausal	3	2.4
Post-menopausal	82	64.5
Histological subtype		
Invasive ductal	115	90.5
Medullary	2	1.6
Lobular	1	0.8
other	9	7.1
Tumor size		
pT1	35	27.6
pT2	76	59.8
pT3	7	5.5
pT4	9	7.1
Nodal status		
pN0	72	56.7
pN1	39	30.7
pN2	9	7.1
pN3	4	3.1
unknown	3	2.4
Metastasis		
Yes		
No	95	74.8
unknown	32	25.2
Histological grade		
G1	1	0.8
G2	20	15.7
G3	106	83.5
Disease recurrence		
Yes	59	46.5
No	64	50.4
unknown	4	3.1
Adjuvant treatment		
Chemotherapy	94	74.0
Endocrine therapy	20	15.7
radiotherapy	95	74.8
unknown	1	0.8

3.3 Reagents and materials

Cell culture	
Cell culture flask (25 cm^2, 75 cm^2)	Greiner Bio-one GmbH, Frickenhausen, Germany
Cell culture microscope	CK30, Olympus, Tokyo, Japan
Centrifuge	Rotina 48R, Andreas Hettich, Tuttlingen, Germany
CO^2 incubator	Heraeus Function Line Serie 7000
Cryogenic vials	Thermo Fisher Scientific Inc., Rochester, NY, USA
DMEM (dulbecco's modified eagle's medium)	#61965-026, Gibco, Invitrogen, Paisley, United Kingdom
DMSO (dimethyl sulfoxide)	#317275, Merck Chemicals, Darmstadt, Germany
EDTA (ethylenediaminetetraacetic acid), 1% (w/v)	#L2113, Biochrom GmbH, Berlin, Germany
FBS (fetal bovine serum)	#10270-106, Invitrogen, Carlsbad, USA
Hemocytometer	0.1 mm, Neubauer improved chamber, Laboroptik Ltd, United Kingdom
HEPES (4-(2-hydroxyethyl)-1-piperazineethanesulfonic acid)	#15630-080, Gibco, Invitrogen, Darmstadt, Germany
Laminar flow cabinet (Hera Safe)	M1199, Heraeus, Hanau, Germany
L-arginine	#A8094, Sigma, Munich, Germany
L-asparagine	#A7094, Sigma, Munich, Germany
PBS (phosphate-buffered saline)	#10010-015**,** Gibco, Invitrogen, Carlsbad, CA, USA
Serological pipette	Greiner Bio-one GmbH, Frickenhausen, Germany

qPCR	
AllPrep DNA/RNA/miRNA Universal Kit	#80224, Qiagen, Hilden, Germany
Brilliant III Ultra-Fast RT-PCR Master Mix with Low ROX	#600890, Agilent Technologies, USA
Cloned AMV first-strand cDNA synthesis kit	#12328-032, Invitrogen, Darmstadt, Germany
Filter-Tips, 1000 µl	#943540178, Qiagen, Hilden, Germany
Mx3000p 96-well plate, skirted	#401334, Agilent Technologies, Great Britain
Nanodrop	Thermo Scientific, Peqlab, Erlangen, Germany
Primers	Metabion, Martinsried, Germany
QIAcube	Qiagen, Hilden, Germany
QIAshredder	#79654, QIAGEN, Hilden, Germany
Stratagene Mx3005P	Agilent Technologies, Boeblingen, Germany
Thermal cycler	Qiagen, Hilden, Germany
Universal ProbeLibray probes	Roche, Penzberg, Germany

Immunohistochemistry	
10 x TBS (Tris-buffered saline, 7.6)	60.5g Trizma Base, 90g sodium chloride, 1 L distilled H_2O. Adjust pH to 7.6 with hydrogen chloride.
Antibody diluent 500 ml ready to use	ZUX025-500, Zytomed Systems GmbH, Berlin, Germany
Citric acid	#C1909, Sigma-Aldrich GmbH, Taufkirchen, Germany
Coverslip	#1130287, R. Langenbrinck, Teningen, Germany
DAB (diaminobenzidine)	#DAB 5000 plus, Zytomed Systems GmbH, Berlin, Germany
Ethanol	Provided by Department of Pathology, Technical University of Munich, Germany
HCl 37% (hydrochloric acid)	#3957.2, Carl Roth, Karlsruhe, Germany
Hydrogen peroxide 30% (H_2O_2)	#8070.4, Carl Roth, Karlsruhe, Germany
Isopropanol	Provided by Department of Pathology, Technical University of Munich, Germany
KLK10 rabbit polyclonal antibody	#HPA017195, Sigma, Steinheim, Germany
Light microscope	Axioskop, Carl Zeiss, Jena, Germany
Mayer's Hematoxylin solution	#254766.1611, Applichems, Darmstadt, Germany
$Na_2HPO_4 \cdot 2\ H_2O$ (sodium phosphate dibasic dihydrate)	#2370, Carl Roth, Karlsruhe, Germany
NaCl (sodium chloride)	#1.06404, Merck, Darmstadt, Germany
NanoZoomer Virtual Microscope and software NDP2.0	Hamamatsu Photonics, Hamamatsu, Japan
NaOH (sodium hydroxide)	#S-0899, Sigma-Aldrich, Taufkirchen, Germany
Pertex (mounting medium)	#PER3000, Medite Pertex, Burgdorf, Germany
pH Meter	SCHOTT Instruments Analytics, Mainz, Germany
Trizma Base	#T1503, Sigma-Aldrich GmbH, Taufkirchen, Germany
Tween-20	#P1379, Sigma-Aldrich GmbH, Taufkirchen, Germany
Xylene	Provided by Department of Pathology, Technical University of Munich, Germany
Zytochem plus HRP One-Step polymer anti-rabbit	#ZUC053-100, Zytomed Systems, Berlin, Germany

WB	
10 x TBS (Tris-buffered saline, pH 7.4)	12.1g Trizma base, 81.8g NaCl, 1 L distilled H_2O. Adjust pH to 7.4 with hydrogen chloride.
Acrylamide/bisacrylamide (29:1)	#A121.1, Roth, Karlsruhe, Germany
APS (Ammoniumpersulfate)	#MKBN6480V, Sigma, Saint Louis, USA
Centrifuge 5417C	Eppendorf, Hamburg, Germany

Chemiluminescent HRP Substrate	#WBKLS0100, Immobilon, Millipore, Billerica, USA
Electrophoresis device	PowerPac Basic, Bio-Rad, Singapore
KLK10 antibody	#HPA017195, Sigma, Steinheim, Germany
PageRuler Prestained Protein ladder	#26616, Thermo Scientific, Lithuania
PVDF (polyvinylidene difluoride) membrane	#IPVH00010, Immobilon, Millipore, Billerica, USA
Rabbit anti-Histone H3 antibody	#441190G, Invitrogen, USA
SDS (sodium dodecyl sulfate)	#2326.1, Carl Roth, Karlsruhe, Germany
Semi-dry transfer apparatus	Whatman Biometra, Göttingen, Germany
Skimmed milk	#70166, Fluka, Sigma, Munich, Germany
Tank blotting device	#07S73289, Bio-Rad, Italy
TEMED (tetramethylethylenediamine)	#A1148,0100, Applichem, Omnilab, Munich, Germany
Thermomixer 5436	Eppendorf, Hamburg, Germany
Tween-20	#P1379, Sigma-Aldrich GmbH, Taufkirchen, Germany
V3 Western Workflow	Bio-Rad, Munich, Germany
β-Mercaptoethanol	#444203, Merck Chemicals, Darmstadt, Germany

3.4 Cell culture

3.4.1 Thawing of OV-MZ-6 cells

OV-MZ-6 cells in cryogenic vials from liquid nitrogen were rapidly thawed and immediately transferred to a 15 ml Falcon tube containing 5-6 ml complete medium (Dulbecco's Modified Eagle Medium [DMEM] with 10% fetal bovine serum [FBS], 10 mM 4-(2-hydroxyethyl)-1-piperazineethanesulfonic acid [HEPES]). Then, the Falcon tube was centrifuged (1, 300 rpm, 3 min, RT) and the supernatant was discarded. Fresh medium was added to the Falcon tube for resuspension of cells and then the centrifuge step was performed again. After all steps above, cells were gently resuspended in complete medium and the cell suspension was transferred into a new cell culture flask for cultivation. Four hours after thawing, the culture medium was carefully removed and fresh one was added.

3.4.2 Cultivation of OV-MZ-6 cells

OV-MZ-6 cells were adherently grown in 75 cm^2 cell culture flasks with complete medium at the condition of 5% CO^2 (v/v), 95% humidity and 37 °C. Every 2-3 days culture medium was replaced and every 6-7 days a cell passage was performed. For the detachment, cells were treated with EDTA/PBS (1% w/v) for 5 min. After washing with

PBS, the cell suspension was transferred to a 15 ml Falcon tube for centrifuging (1, 300 rpm, 3 min, RT) and then the supernatant was discarded. Finally, cells were resuspended in fresh medium and the cell suspension was transferred to new flasks.

3.4.3 Freezing of OV-MZ-6 cells

For cell cryopreservation, freezing medium (FBS containing 10% dimethylsulfoxid [DMSO]) was prepared ($1x10^6$ cells/ml). OV-MZ-6 cells were detached and collected in a 15 ml Falcon tube (see **3.4.2**). The freezing medium was applied to resuspend the cells and then the cell suspension was transferred into cryogenic micro tubes (Thermo Fisher). The cryogenic micro tubes were frozen at -80 °C for 24 h and further transferred to liquid nitrogen -196 °C for storage.

3.5 Quantitative PCR analysis

3.5.1 RNA isolation from cell lines and tumor tissues

The automated QIAcube sample preparation device (Qiagen) and the all Prep DNA/RNA Universal kit for RNA and DNA extraction (Qiagen) were employed for simultaneous purification of total DNA and RNA from cell lines and tumor tissues. Deep-frozen tumor tissues stored in liquid nitrogen were obtained from the Tumor Bank of the Medical Faculty of TUM. 10–20 µg of still-frozen tumor tissue material were sliced off the clinical specimens, which were immediately homogenized in 600 µl of RLT plus buffer (Qiagen) supplemented with 6 µl 2-mercaptoethanol. Tissue lysates were transferred to QIAshredder spin columns (Qiagen), which were further centrifuged at full speed (3 min, RT). The flow-through was inserted into the QIAcube for RNA and DNA extraction. The manufacturer's recommendations were exactly followed.

Concentration and purity of the extracted RNA were determined by the Nano Drop 2000c spectrophotometer (Thermo Scientific). All RNA samples were stored at -80 °C until further use.

3.5.2 Reverse transcription and cDNA synthesis

The cloned AMV first strand cDNA Synthesis Kit (Invitrogen) was used for reverse transcription. According to the manufacturer's recommendations, the steps of cDNA synthesis were done as follows:

Annealing of primers

Components	
RNA	1000 ng (cell line) or 500 ng (tumor tissues)
dNTP (10 mM)	2.0 µl
Random hexamer primers (50 ng/µl)	1.0 µl
H_2O	x µl
Total	12.0 µl

The PCR reaction tubes containing the RNA/primers mixture was incubated at 65 °C for 5 min in a thermal cycler and then transferred on ice.

Reverse transcription

Components	
5x cDNA Synthesis Buffer	4.0 µl
1 DTT (0.1 M)	1.0 µl
DEPC-treated H_2O	1.1 µl
RNaseOUT (40 U/µl)	1.0 µl
Cloned AMV RT (15 units/µl)	0.9 µl
Total	8.0 µl

Per reaction, 8 µl of the master reaction mix were added into the PCR reaction tube from the primer annealing step. The reaction tubes were then transferred to a thermal cycler (Qiagen) and the following PCR program performed:

Step 1: 10 min at 25 °C
Step 2: 50 min at 50 °C
Step 3: 5 min at 85 °C

Finally, the resulting cDNA from cell lines, which was prepared for dilution series and calibrator, as well as the cDNA from frozen tumor tissues was diluted with 80 µl RNase-free water. All cDNA samples were stored at -20 °C until further use.

3.5.3 qPCR analysis using Universal ProbeLibray probes

Universal ProbeLibray probes (Roche) were used in the quantitative polymerase chain reaction (qPCR). These probes are short hydrolysis probes (8-9 nucleotides), which are labeled at the 5' end with fluorescein (FAM) and the 3' end with a dark quencher dye. These fluorogenic probes specifically target to the genes of interest and are hydrolyzed

by the DNA polymerase during amplification, releasing the fluorescein of the probes.

Gene-specific primers were designed with the Universal Probe Library Assay Design Center software (https://lifescience.roche.com). The following primers (Metabion) and hydrolysis probes from the Universal Probe Library (Roche) were used:

KLK9 (NM_012315.1):

Forward: 5'- TCCACCTTACTCGGCTCTTCT-3' (209-229);

Reverse: 5'- AAGGCGGACCCACAGATAC-3' (288-306);

KLK9-probe: 5'-FAM-GCTGCCCA-3'-dark quencher; amplicon size: 98 bp.

The assay detects the KLK9 mRNA NM_012315.1, encoding full-length KLK9.

KLK10 (NM_002776.4, NM_145888.2, and NM_001077500.1):

Forward: 5'-CAGGTCTCGCTCTTCAACG-3' (397-415, 259-277, 298-316);

Reverse: 5'-GAGCCCACAGTGGCTTGT-3' (485-502, 347-364, 386-403);

KLK10-probe: 5'-FAM-TCCACTGC-3'-dark quencher; amplicon size: 106 bp.

The assay detects the three major KLK10 mRNA transcript variants 1, 2 and 3, all encoding full-length KLK10.

HPRT1 (NM_000194):

Forward: 5'-TGACCTTGATTTATTTTGCATACC-3' (218-241);

Reverse: 5'-CGAGCAAGACGTTCAGTCCT-3' (300-319);

HPRT1-probe: 5'-FAM-GCTGAGGA-3'-dark quencher; amplicon size: 102 bp.

The assay detects the HPRT1 mRNA NM_000194, encoding full-length HPRT1.

The Stratagene Mx3005P qPCR System (Agilent) was employed for qPCR analysis. 3 µl of cDNA from synthesis step were used per well.

The experimental reaction was prepared as follows:

Components	
2x Brilliant III qPCR master mix with low ROX	10.0 µl
UPL Probe (10 µM)	0.4 µl
Primer forward (20 µM) 0.4 µl	0.4 µl
Primer reverse (20 µM)	0.4 µl
H_2O	5.8 µl
cDNA	3.0 µl
Total	20.0 µl

All qPCR reactions were performed in triplicates, including calibrator (cDNA from OV-MZ-6 cells overexpressing target gene was used as the calibrator and positive control). Negative controls included a no-template control (water as substrate), genomic DNA (OV-MZ-6 cells), and a no reverse transcriptase control (lack of reverse transcriptase during a reverse transcription reaction).

The reaction mixture was transferred to a 96-well qPCR reaction plate (Agilent Technologies), which was further centrifuged (3, 000 rpm, 3 min) to remove bubbles. Then the plate was transferred to the Mx3005P instrument for qPCR analysis. The following qPCR cycling program was applied:

- Step 1: 3 min at 95 °C
- Step 2: 15 s at 95 °C
- Step 3: 1 min at 60 °C

3.5.4 Standard dilution series for assay establishment

In order to exclude specimen heterogeneity and extraction/conversion efficiency variation, dilution series were performed to evaluate the efficiency of target gene and reference gene amplification. A 2-fold dilution series was created with the cDNA from a positive control cell line (OV-MZ-6 cells overexpressing the target gene). Five serial dilution steps of cDNA (cDNA0 30 ng, cDNA1 15 ng, cDNA2 7.5 ng, cDNA3 3.75 ng, cDNA4 1.875 ng) was applied for the establishment of the standard dilution curves of the target and reference genes, respectively. The cycle threshold (Ct) value was plotted against the corresponding logarithm of cDNA input (30-1.875 ng, log input 1.477-0.273) for each serial dilution sample. The slope of the standard dilution series was obtained according to linear regression analysis and further used for the calculation of efficiency (E) by the following formula: $E = 10^{(-1/slope)}$. Under ideal condition, the efficiency of qPCR assays is 100%, with a corresponding E-value of 2. A ΔE between target gene and reference gene was employed to evaluate error margins associated with Δ efficiency. The 2-fold dilution series for each gene was analyzed by qPCR in three independent experiments,

3.5.5 qPCR calculation methods

Accounting for fact that the efficiency of KLK9 amplification, but not of KLK10, approximated that of HPRT, relative KLK9 mRNA expression was performed using

the comparative threshold cycle ($2^{-\Delta\Delta Ct}$) method (Pfaffl, 2012):

$$\Delta Ct = Ct_{KLK9} - Ct_{HPRT}$$

$$\Delta\Delta Ct = \Delta Ct_{sample} - \Delta Ct_{calibrator}$$

$$R = 2^{-\Delta\Delta Ct}$$

For KLK10, relative target gene expression was calculated using the following formula (Pfaffl, 2012):

$$\Delta Ct = Ct_{sample} - Ct_{calibrator}$$

$$R = \frac{E_{KLK10}^{-\Delta Ct\,(KLK10)}}{E_{HPRT}^{-\Delta Ct\,(HPRT)}}$$

Relative error propagation (EP) was calculated for each ΔCt analysis step by the following formula (STDEV: standard deviation):

$$EP\,(\Delta Ct) = \sqrt{\frac{(STDEV_{marker})^2 + (STDEV_{HPRT})^2}{2}}$$

$$EP\,(\Delta\Delta Ct) = \sqrt{\frac{(EP_{\Delta Ct_{sample}})^2 + (EP_{\Delta Ct_{calibrator}})^2}{2}}$$

Absolute error propagation was calculated using (ln: natural logarithm):

$$EP\,(\text{absolute error}) = \ln 2 \times EP(\Delta\Delta Ct) \times 2^{-\Delta\Delta Ct}$$

Considering the limitations of the qPCR analysis and the variations of specimen qualities, the following exclusion criteria were introduced in the current study to ensure reproducible results: the Ct value for HPRT was higher than 35; the $2^{-\Delta\Delta Ct}$ error progression % was more than 30% even after repetition; the % STDEV of the $2^{-\Delta\Delta Ct}$ for 2 valid runs was higher than 47.1% (Ahmed et al., 2016).

3.6 Western blot analysis to test specificity of a KLK10-directed antibody

3.6.1 Preparation of protein samples, SDS-PAGE gels, and buffers

The samples for SDS-PAGE (polyacrylamide gel electrophoresis) were prepared as follows and then denatured by using SDS-PAGE loading buffer and heating at 95 °C for 5 min:

Marker: 4ul Prestained Protein Ladder (Thermo Scientific) plus 20 µl 8M urea + 8 µl SDS-PAGE loading buffer (4X)
Samples: approximately 50 ng of KLK proteins adjusted with 8M urea up to total 24 µl +8 µl SDS-PAGE loading buffer (4X)

The 5% PAA stacking gel was prepared as follows:

Components	
H_2O	17.2 ml
1.5 M Tris HCl (pH6.8)	7.2 ml
40% acryl / bis (acrylamide-bisacrylamide 29:1)	3.6 ml
10% SDS (sodium dodecyl sulfate)	0.28 ml
The stacking gel solution was stored at 4 °C (maximum 4 weeks). For each 1 mm thickness gel, 2 ml solution was mixed with 20 µl APS (Ammoniumpersulfate) and 2 µl TEMED (tetramethylethylenediamine).	

The 12% PAA (polyacrylamide) separating gel was prepared freshly as follows:

Components	
H_2O	4.4 ml
1.5 M Tris HCl (pH8.8)	2.5 ml
40% acryl / bis (acrylamide-bisacrylamide, 29:1)	3 ml
10% SDS (sodium dodecyl sulfate)	0.1 ml
APS (ammonium persulfate)	80 µl
TEMED (tetramethylethylenediamine)	8 µl

Semi-dry buffer A for blotting:

Components	
H_2O	150 ml
99.9% ethanol	50 ml
0.25 M boric acid	50 ml

Semi-dry buffer B for blotting:

Components	
H_2O	187.5 ml
99.9% ethanol	12.5 ml
0.25 M boric acid	50 ml

Membrane stripping buffer：

Components	
SDS	0.15 g
glycine	2.25 g
Tween 20	1.5ml

All ingredients were first dissolved with 100 ml H_2O. The solution was adjusted pH to 2.2 with HCL and then filled up to 150 ml with H_2O.

3.6.2 SDS-PAGE, blotting and protein detection

Each slot of the stacking gel was loaded with about 50 ng of KLK sample, which was concentrated by the stacking gel at 90 V for 20 min and then separated on the separating gel at 130 V for 1 h. A Prestained Protein Ladder ranging from 11 to 170 kDa (Thermo Scientific) was applied for evaluating the relative molecular mass of the separated proteins.

A (sandwich) semi-dry transfer apparatus (Whatman Biometra) was used to transfer the proteins from the gel to a polyvinylidene difluoride (PVDF) membrane (Millipore). In this blotting system, three filter papers and the resulting gel were saturated with blotting buffer B and the PVDF membrane plus other three filter papers with blotting buffer A, respectively. Then, the above-named materials were placed between the dry anode and cathode plates in the following order: the three filter papers with blotting buffer A, gel, PVDF membrane, and the three filter papers with blotting buffer B. The blotting process was performed at 150 mA for 2h.

The PVDF membrane was washed in TBST for 5 min at RT and then incubated with blocking buffer [TBST; 5% (w/v) milk powder] for 1 h at RT. After that, the membrane were incubated with KLK10 primary rabbit polyclonal antibody (HPA017195, Sigma; dilution, 1:1000) in blocking buffer [TBST; 5% (w/v) milk powder] overnight at 4 °C. After washing with TBST (5 min ×3, RT), the membrane was incubated for 1 h at RT with HRP-conjugated Goat-Anti-Rabbit secondary antibody (Jackson ImmunoResearch; dilution, 1:10000) in blocking buffer [TBST; 1% (w/v) milk powder]. Finally, Chemiluminescent HPR Substrate (Millipore) and V3 Western Workflow (Bio-Rad) were applied for the visualization of antigen-antibody complexes.

After washing the PVDF membrane with stripping buffer, the same blots were

incubated with Rabbit anti-Histone H3 (#441190G, Invitrogen; dilution, 1:2000) for validating that the samples were prepared appropriately.

3.7 Immunohistochemical (IHC) analysis of KLK10 expression

3.7.1 Tissue microarrays (TMA)

Tissue microarrays (TMA) have several advantages, e.g. increased capacity of tissue specimens, precise positioning of areas of interest, and a high-degree standardization. A previously established method was used for the construction of TMA (Skacel et al., 2002; Waziri et al., 2009). Using hematoxylin-eosin (H&E) stained slides as reference, the tumor regions were identified and pre-marked by pathologists in the corresponding FFPE specimens. Then, three different tissue punches (1 mm) were retrieved from the marked areas of each donor block and positioned into the recipient array block. In addition, the core biopsies of normal tissues like kidney and lung were placed between tumor core samples for reference and orientation of histological specimens. Finally, 3 µm thick sections were cut from the tissue microarray blocks for further H&E staining or immunohistochemistry (IHC).

3.7.2 Immunohistochemical staining for KLK10

The paraffin-embedded TMA slides were heated at 60 °C overnight and then immersed into xylene twice for 10 min at RT for deparaffinization. Rehydration of the slides was performed in a descending row of graded alcohols, including 100 % isopropanol twice, 96% and 70% ethanol, for 5 min each. After blocking in 3% hydrogen peroxide for 20 min at RT, the slides were subjected to pressure cooking for 4 min in citrate buffer (citric acid 2.1 g, H_2O 1 l, pH 6.0) for antigen retrieval. Then, they were incubated with a KLK10-directed primary antibody (HPA017195, Sigma; dilution, 1:200) overnight at 4 °C in a wet chamber. After washing in TBST, a HRP-conjugated anti-rabbit secondary antibody (Zytomed Systems) was applied to the slides for 30 min at RT in a wet chamber. Subsequently, a mixture of DAB high substrate buffer and liquid DAB chromogen (Zytomed Systems) was added to the slides for 8 min at RT. The resulting slides were counterstained with haematoxylin for 3 min, rinsed under tap water for 10 min, and then transferred to distilled water for 1 min. For dehydration the slides were subjected to an ascending alcohol series: 70% ethanol, 96% ethanol, 100 % isopropanol twice and xylene twice, for 3 min each. At last, they were mounted with PERTEX (Histolab).

3.7.3 Quantification of immunostaining

To evaluate the immunostaining, the software ImageJ (Java 1.8.0, 64 bit), downloaded from the NIH website (https://imagej.nih.gov/ij), plus the IHC Profiler plugin, from Sourceforge website (https://sourceforge.net/projects/ihcprofiler/), were applied. Stained TMA slides were scanned using a Hamamatsu NanoZoomer Digital Pathology virtual microscope (Hamamatsu) with a 100×objective (**Figure 2 A**). The image of each tumor core was captured and further loaded into the software ImageJ. With the assistance of the IHC Profiler plugin, color deconvolution was performed to separate the antibody DAB signal from the hematoxylin counterstain (**Figure 2 B, C**). The details of the related theory and guidelines for ImageJ and its plugin were previously reported by Varghese (Varghese et al., 2014). In the current study, we selected the analysis pattern for DAB stained cytoplasmic proteins in the IHC Profiler plugin, which was constrained to the default setting threshold and scale of ImageJ. Tumor areas of interest on each TMA core were manually selected by consensus of two independent observers. To assign an objective and automated score for each core based on DAB staining density, a formula below was applied in the study:

$$Score = 255 - \sum_{i=1}^{n} InD_i \Big/ \sum_{i=1}^{n} A_i$$

In this formula, InD describes the integrated gray density and A represents the area of tumor regions in pixels. The mean value of DAB gray density on each core is calculated by dividing the total integrated gray density by the area sum, as a continuous variable ranging from 0-255. A gray density value of 0 represents the darkest color shade while 255 represent the brightest color shade in the image. For convenience, a subtraction of 255 minus the resulting mean value is added in the formula, thereby the score positively associated with DAB staining density.

In addition to digital analysis, the TMAs were manually scored by a pathologist (Dr. E. Drecoll, Institute of Pathology, TUM). KLK10 staining intensity was classified on a scale of 0 to 3 (0: no staining; 1: weak staining; 2: moderate staining; 3: strong staining). Comparison of digital and manual scores showed an excellent overlap, with the digital scores displaying a higher resolution.

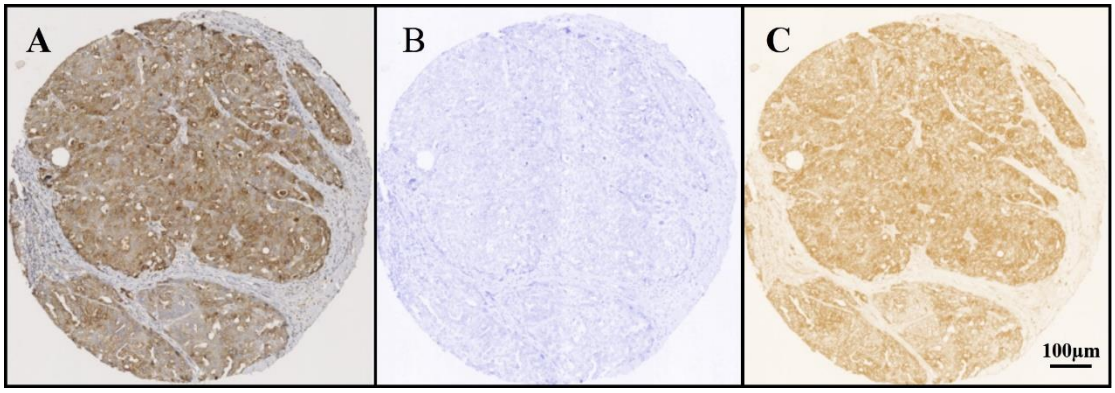

Figure 2. Exemplary color deconvolution of the tumor core image via ImageJ plus IHC Profiler plugin

The image of tumor core was captured (A) and further loaded into the software ImageJ. With the assistance of the IHC Profiler plugin, color deconvolution was carried out to separate the antibody DAB signal from the hematoxylin counterstain (B, C).

3.8 Statistics

The association of IHC and mRNA expression levels of KLKs with clinicopathological parameters of the patients was assessed by the Chi-square test. Survival analyses were performed by constructing Kaplan–Meier curves. The log-rank test is proposed to evaluate group differences of the survival functions. Associations of KLKs and clinical parameters with patients' survival were additionally determined by univariate and multivariable Cox regression analysis and expressed as hazard ratio (HR) as well as its 95% confidence interval (95% CI). The database from The Cancer Genome Atlas (TCGA) was utilized to validate *in silico* the prognostic power of KLKs in advanced high-grade serous ovarian cancer (not available for TNBC).

The correlations between continuous variables of KLKs were examined with the Mann-Whitney U test and the Spearman rank correlation (r_s). The Mann–Whitney U test was also employed to scrutinize the differences of KLK10 expression between distinct groups of breast cancer samples and analyze the relationship between its protein and mRNA expression. Box plots were drawn to indicate differences.

All calculations were performed with the SPSS statistical analysis software (version 20.0; SPSS Inc., Chicago, IL, USA). P values of less than 0.05 were considered statistically significant.

4 Results

4.1 mRNA expression of KLK9 and KLK10 determined by qPCR in advanced high-grade serous ovarian cancer

4.1.1 Establishment of quantitative PCR assays for KLK9 and KLK10

Due to fact that amplification efficiencies vary among different qPCR assays, dilution series were employed to determine the differences concerning efficiency between the assays for the target genes and the housekeeping gene HPRT1 (Bustin and Nolan, 2013). Theoretically, the efficiency of the qPCR assay should be 100%, with an E-value of 2, while in fact the efficiency of qPCR assays typically range between 95-100%, corresponding to E values ranging from 1.6 to 2 (Ruijter et al., 2013).

2-fold dilution series for KLK9, 10 and HPRT, respectively, were generated with cDNA derived from positive control cells (OVMZ6-KLK9 or OVMZ6-KLK10), comprising five serial dilution steps (input: cDNA0 30 ng, cDNA1 15 ng, cDNA2 7.5 ng, cDNA3 3.75 ng, cDNA4 1.875 ng). As exemplified by the dilution series of KLK9 and KLK10 (**Figure 3**), the cycles of threshold (Ct) values were plotted against the corresponding logarithm of the cDNA input (30-1.875 ng, log input 1.477-0.273). Three independent experiments were performed for each dilution series.

In the three independent repetitions, the slope of the fitted line for the KLK9 dilution series (slope: 1^{st} -3.54; 2^{nd} -3.57; 3^{rd} -3.48) was parallel with that of HPRT (slope: 1^{st} -3.33; 2^{nd} -3.38; 3^{rd} -3.40); further, the efficiencies of KLK9 amplification (E: 1^{st} 1.92; 2^{nd} 1.90; 3^{rd} 1.94) approximated that of HPRT (E: 1^{st} 1.99; 2^{nd} 1.98; 3^{rd} 1.96). Thus, efficiency correction was not necessary for normalization and, therefore, the 2ΔΔCt method was applied for the calculation of relative KLK9 mRNA expression.

In the case of the KLK10 assay, the fitted lines of KLK10 dilution series (slope: 1^{st} -4.18; 2^{nd} -3.17; 3^{rd} -3.83) did not always parallel those of the HPRT expression (slope: 1^{st} -3.38; 2^{nd} -3.15; 3^{rd} -3.20); furthermore, the efficiencies of KLK10 amplification (E: 1^{st} 1.74; 2^{nd} 2.07; 3^{rd} 1.82) were not comparable to those of HPRT (E: 1^{st} 1.98; 2^{nd} 2.08; 3^{rd} 2.05). Hence, relative KLK10 mRNA expression was quantitatively accessed using the efficiency correction method instead of 2ΔΔCt method (see chapter 3.5 for details).

After normalization with the HPRT and setting the cDNA0 values to 1.0, standard deviations (SDs) of relative KLK9 mRNA expression of cDNA1-4 were calculated (**Figure 4).** All SDs were lower than 20%. Similarly, all SDs of relative KLK10 mRNA

expression were lower than 20% in sample cDNA1-4 after normalization and efficiency correction (**Figure 5**).

For the pretest of clinical specimens, three ovarian cancer tissues were randomly selected to validate the established qPCR assays. Each of the samples was quantified in triplicates by KLK9, 10, and HRPT mRNA expression and three independent qPCR assays including the three samples were performed. In the three repetitions, Ct values for HPRT were lower than 35 and the $2^{-\Delta\Delta Ct}$ error progression values were less than 30% in OVC1, 2, and 4; SDs of relative KLK9/10 mRNA expression were lower than 47.1% in the three samples (**Figure 6)**. According to our exclusion criteria (see chapter 3.5.5 qPCR calculation methods), none of the three clinical specimens would have to be excluded for further analysis.

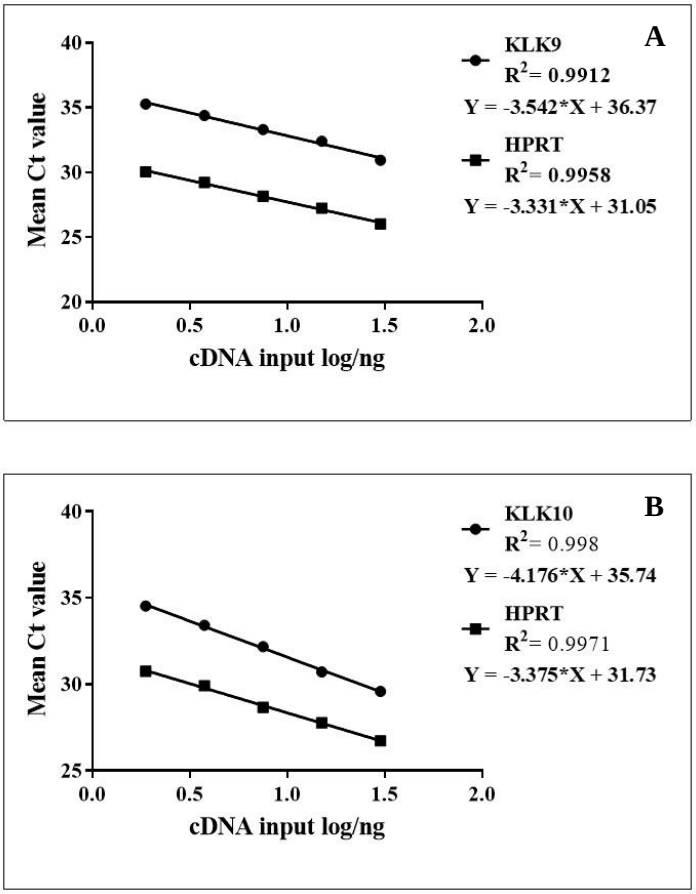

Figure 3. Representative dilution series of KLKs and HPRT obtained by qPCR.
The two types of dots represent 2-fold dilution series for KLKs and HPRT respectively (dots from left to right: cDNA4, cDNA3, cDNA2, cDNA1, cDNA0). Based on that, the fitted lines for KLKs and HPRT were plotted, which were applied for the efficiency calculation. Slope: (A) KLK9 -3.54, HPRT -3.33; (B) KLK10 -4.18, HPRT -3.38. Efficiency (E): KLK9 1.92, HPRT 1.99; KLK10 1.74, HPRT 1.98.

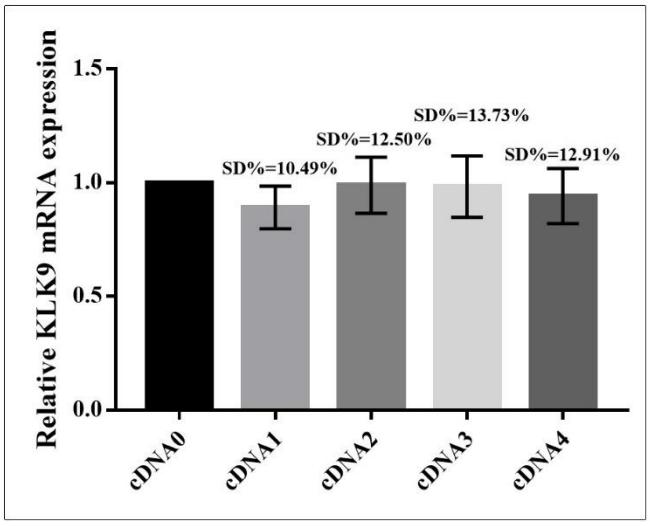

Figure 4. **Mean values and standard deviations of relative KLK9 mRNA expression (normalized against HPRT and cDNA0) of cDNA1-4 in three independent qPCR experiments.**

With normalization against HPRT and cDNA0, mean values of relative KLK9 mRNA expression were in close proximity among cDNA1-4; SDs of relative KLK9 mRNA expression were lower than 20% in cDNA1-4.

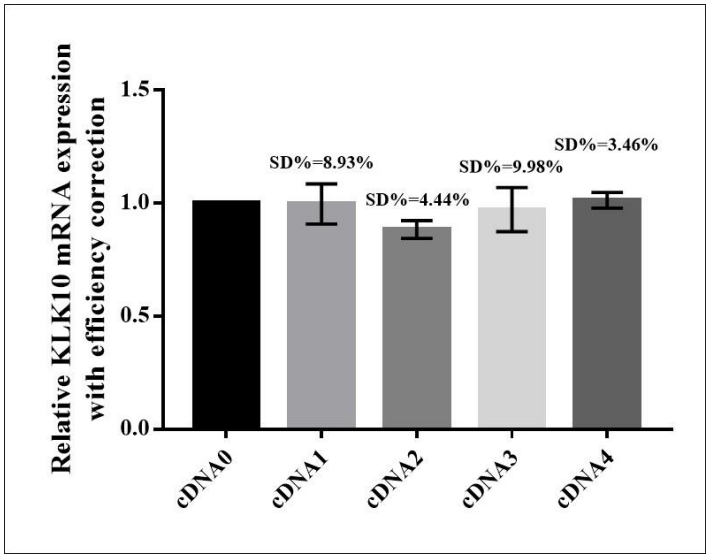

Figure 5. **Mean values and standard deviations of relative KLK10 mRNA expression (normalized against HPRT and cDNA0, with efficiency correction) of cDNA1-4 in three independent qPCR experiments.**

With the normalization and efficiency correction, mean values of relative KLK10 mRNA were in close proximity among cDNA1-4; SDs of relative KLK10 mRNA expression were lower than 20% in cDNA1-4.

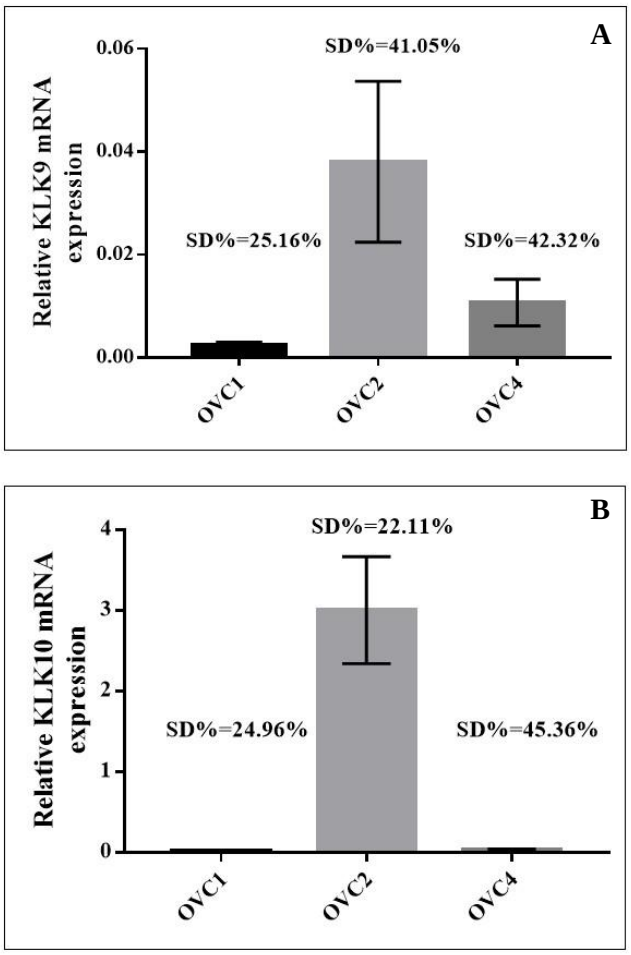

Figure 6. **Mean values and standard deviations of relative KLK mRNA expression in three ovarian cancer tissues.**
In three independent repetitions, SDs of relative KLK9 (A) and KLK10 (B) mRNA expression were lower than 47.1% in OVC1, 2, and 4. cDNA from OVMZ6-KLK9 and OVMZ6-KLK10 cells, were employed as calibrators for normalization of relative KLK9 or KLK10 mRNA expression, respectively. OVC: ovarian cancer tissues.

4.1.2 mRNA expression of KLK9 and KLK10 in advanced high-grade serous ovarian cancer tissues and their association with clinical parameters

The mRNA expression levels of KLK9 and KLK10 were quantitatively accessed by the established qPCR assays in a homogenous cohort including 139 cases of patients with advanced high-grade serous ovarian cancer (FIGO stage III/IV; cohort 1: for details see chapter 3.1; Geng et al., 2017). After normalization against HPRT and calibrators, the values of relative KLK9 mRNA expression ranged from 0.00 to 26.59 (median: 0.14); in case of KLK10, the values ranged from 0.01 to 15.43 (median: 1.24). The majority of the ovarian cancer samples displayed low KLK9 expression (**Figure 7**), but robust KLK10 expression at the mRNA level was observed (**Figure 8**). According to this

expression pattern, KLK9 mRNA levels (and initially also KLK10 mRNA levels; see Geng et al., 2017) were dichotomized into a low-expressing group (quartiles 1+2+3) versus a high-expressing group (quartile 4) by the 75th percentile (**Figure 7**). In the present work, the KLK10 low-expressing group was defined by the first tertile, versus the high-expressing group consisting of tertiles 2+3 (**Figure 8**), which is comparable with the dichotomization in the clinical protein expression study (see chapter 4.2).

Including mRNA expression data of KLK11 and KLK15 in the same cohort (X. Geng, pers. comm.), Spearman correlation analysis was performed among these KLKs (Geng et al., 2017). KLK10 mRNA expression was significantly and positively associated with KLK11 mRNA expression ($r_s = 0.647$, $p < 0.001$); also, a similar correlation was observed between KLK9 and KLK15 mRNA levels ($r_s = 0.716$, $p < 0.001$). This relationship is also evident in box plot analysis **(Figure 9)**, where KLK11 mRNA levels are remarkably elevated in the KLK10 high group ($p < 0.001$, Mann-Whitney test), and, similarly, enhanced KLK15 mRNA expression is observed in the KLK9 high group ($p < 0.001$, Mann-Whitney test), confirming coordinate expression of distinct pairs of KLKs in advanced high-grade serous ovarian cancer. The association of the dichotomized KLK9 and KLK10 mRNA expression levels (low/high) with established clinical parameters in ovarian cancer including age, pre-operative ascitic fluid volume, and post-operative residual tumor mass was investigated (**Table 7**; Geng et al., 2017). KLK9 or KLK10 mRNA levels did not show any significant association with the mentioned clinical parameters.

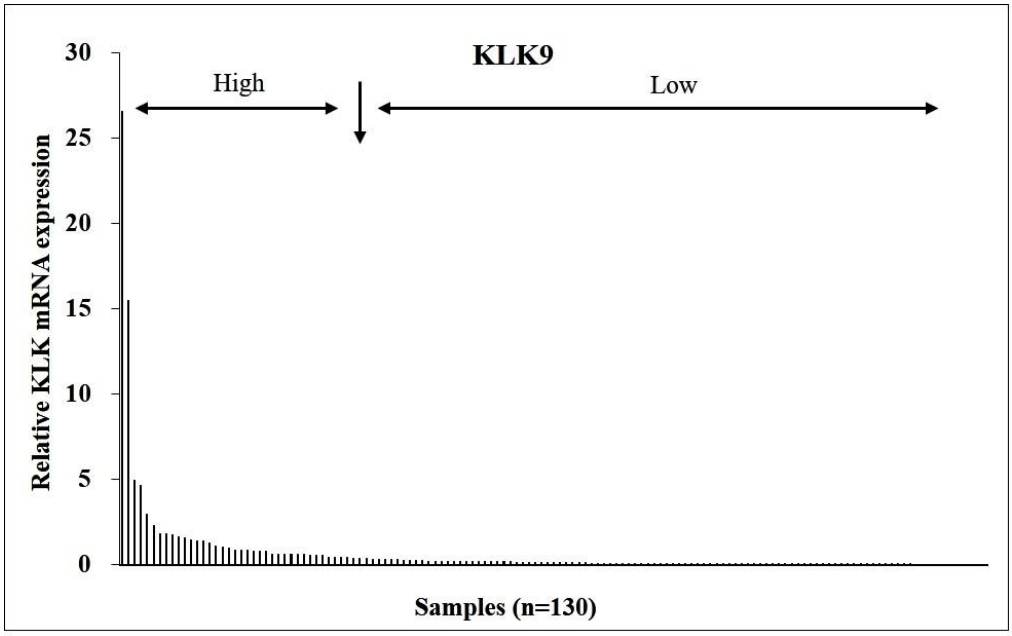

Figure 7. **mRNA expression levels of KLK9 in advanced high-grade serous ovarian cancer (FIGO III/IV)**

The majority of the ovarian cancer samples displayed low KLK9 mRNA expression. KLK9 mRNA levels were dichotomized into a low-expressing group (quartiles 1+2+3) and a high-expressing group (quartile 4) by the 75th percentile (data published in Geng et al., 2017).

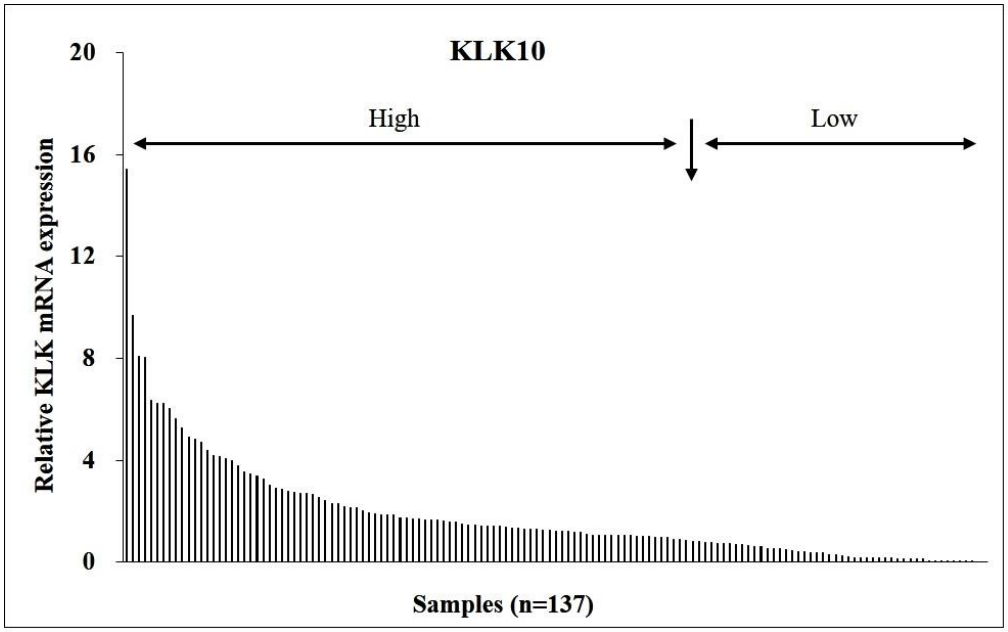

Figure 8. **mRNA expression levels of KLK10 in advanced high-grade serous ovarian cancer (FIGO III/IV)**

The majority of the ovarian cancer samples showed robust KLK10 expression (data published in Geng et al., 2017). KLK10 mRNA levels were dichotomized into a low-expressing group (tertile 1) and a high-expressing group (tertiles 2+3) by the 33rd percentile.

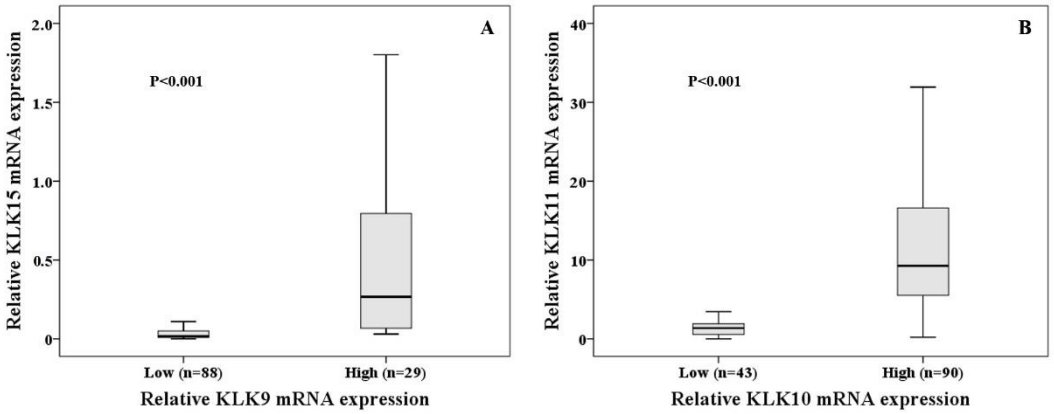

Figure 9. Correlations of KLK mRNA expression levels in tumor tissues of advanced high-grade serous ovarian cancer patients (FIGO III/IV).
(A) Enhanced KLK15 mRNA expression was significantly associated with upregulated KLK9 mRNA level ($p < 0.001$, Mann-Whitney test; data published in Geng et al., 2017). (B) KLK11 mRNA levels were remarkably elevated in the KLK10 high group ($p < 0.001$, Mann-Whitney test). Relative KLK mRNA levels were quantified by qPCR with normalization against HPRT expression.

Table 7. Association of KLK9 and KLK10 mRNA expression with clinical parameters in advanced high-grade serous ovarian cancer patients (FIGO III/IV)

Clinical parameters	KLK9[a] Low/high	KLK10[a] Low/high
Age	p = 0.686	p = 0.169
≤ 60 years	37/15	15/42
> 60 years	58/20	30/50
Residual tumor mass	p = 0.165	p = 0.224
0 mm	50/14	26/42
> 0 mm	43/21	19/48
Ascitic fluid volume	p = 0.316	p = 0.465
≤ 500 ml	56/17	28/49
> 500 ml	35/16	16/37

[a] Chi-square test, cut-off point: KLK9 = 75th percentile (Geng et al., 2017), KLK10 = 33rd percentile.

4.1.3 Association of clinical parameters and tumor biological factors with progression-free survival (PFS) and overall survival (OS)

Univariate Cox regression analysis was applied for evaluating the association of clinical parameters and KLK9/10 mRNA expression with patients` PFS and OS (observation

time: 5 years; **Table 8**). Among the clinical parameters, residual tumor mass left after debulking surgery and pre-operative amounts of ascitic fluid displayed prognostic power for PFS and OS. Compared to the tumor-free group, the risk of cancer-related death was distinctly increased in the group with residual tumor mass (>0 mm) (HR, 3.77; 95% CI, 2.18-6.51; p <0.001). Similarly, the risk for tumor progression was significantly increased (HR, 2.53; 95% CI, 1.60-4.02; p <0.001). Patients with ascitic fluid volume >500 ml displayed an elevated probability of cancer-related death (HR, 1.94; 95% CI, 1.17-3.21; p =0.011) and disease progression (HR, 1.78; 95% CI, 1.10-2.87; p =0.018), respectively (Geng et al., 2017).

Table 8. Univariate Cox regression analysis of KLK9/10 mRNA levels and clinical parameters for the prediction of clinical outcome in advanced high-grade serous ovarian cancer patients (FIGO III/IV)

Clinical parameters	PFS			OS		
	No[a]	HR (95% CI)[b]	p	No[a]	HR (95% CI)[b]	p
Age			0.627			0.358
≤ 60 years	43	1		50	1	
> 60 years	65	1.12 (0.70-1.79)		75	1.26 (0.77-2.08)	
Residual tumor mass			**< 0.001**			**< 0.001**
0 mm	59	1		64	1	
> 0 mm	49	2.53 (1.60-4.02)		59	3.77 (2.18-6.51)	
Ascitic fluid volume			**0.018**			**0.011**
≤ 500 ml	63	1		72	1	
> 500 ml	39	1.78 (1.10-2.87)		46	1.94 (1.17-3.21)	
KLK9 mRNA[c]			0.530			0.311
low	73	1		86	1	
high	28	0.85 (0.50-1.43)		32	0.75 (0.43-1.31)	
KLK10 mRNA[d]			0.947			0.662
low	38	1		44	1	
high	69	1.02 (0.63-1.64)		81	1.13 (0.66-1.91)	

[a] Number of patients;

[b] HR: hazard ratio (CI: confidence interval) of univariate Cox regression analysis;

[c] Dichotomized into low and high levels by the 75th percentile;

[d] Dichotomized into low and high levels by the 33rd percentile;

Bold value indicates statistical significance (p < 0.05).

The data concerning age, residual tumor mass, ascitic fluid volume, and KLK9 mRNA (cut-off: 75th percentile) are presented in Geng et al., 2017.

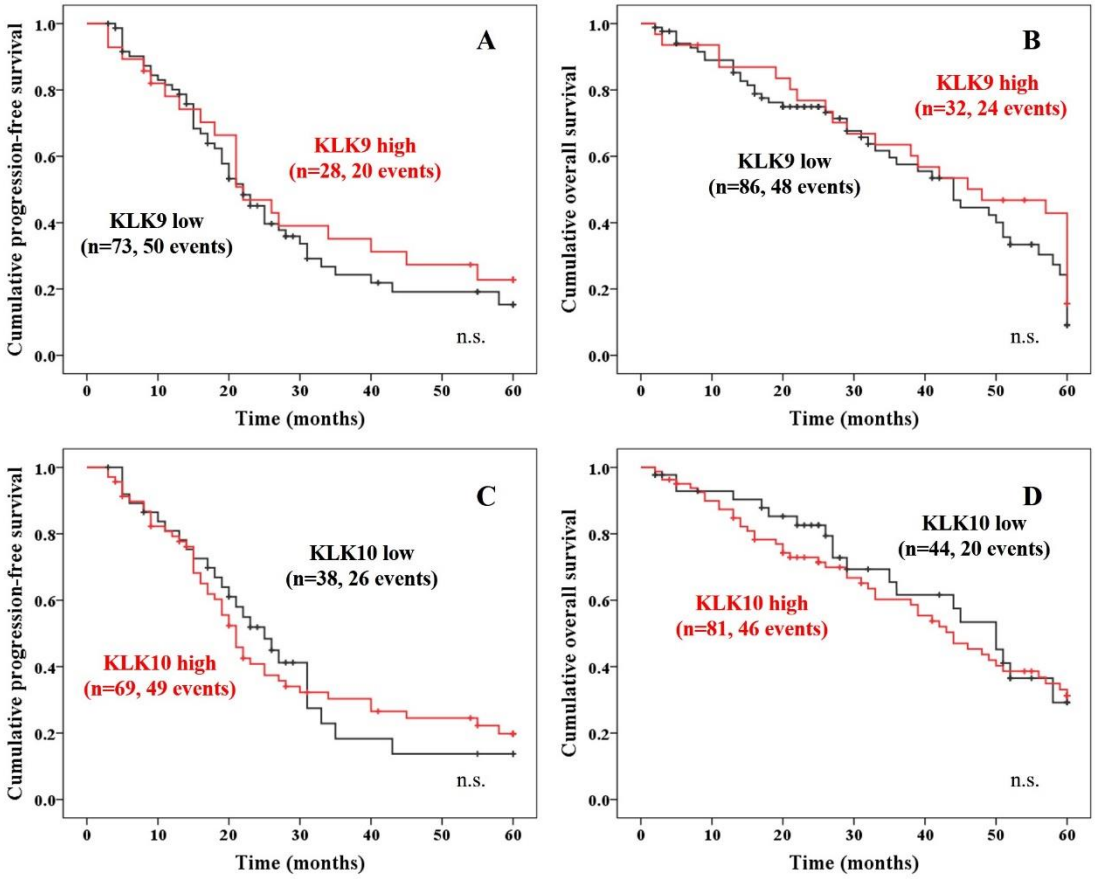

Figure 10. Kaplan–Meier survival curves for the cohort of advanced high-grade serous ovarian cancer patients (FIGO III/IV).
Neither KLK9 (A, B) nor KLK10 (C, D) mRNA levels are associated with progression-free survival and overall survival in advanced high-grade serous ovarian cancer patients (FIGO III/IV).

However, neither KLK9 nor KLK10 mRNA levels contributed to the prognosis in this tumor entity (**Table 8**; Geng et al., 2017). The impact of KLK9 and KLK10 mRNA expression on clinical outcome was further validated by Kaplan-Meier survival analysis (**Figure 10**), confirming that both KLK9 and KLK10 mRNA expression were not associated with the prognosis of advanced high-grade serous ovarian cancer patients.

4.1.4 In silico analysis of KLK9 and KLK10 expression in advanced high-grade serous ovarian cancer

To further validate the obtained results of KLK9 and KLK10 in advanced high-grade serous ovarian cancer, the Kaplan-Meier Plotter, a biomarker assessment tool, was utilized to analyze the publicly available Affymetrix-based mRNA data of ovarian cancer patients, deposited by The Cancer Genome Atlas (TCGA) (Gyorffy et al., 2012). In the *in silico* analysis, patients afflicted with high-grade (grade 3), serous, and

advanced-stage (FIGO III+IV) ovarian cancer, receiving platinum-based chemotherapy (follow up: 5 years), were enrolled for Kaplan-Meier survival analysis. As visualized in **Figure 11**, neither KLK9 nor KLK10 mRNA levels showed any predictive power for the prognosis of advanced high-grade serous ovarian cancer patients.

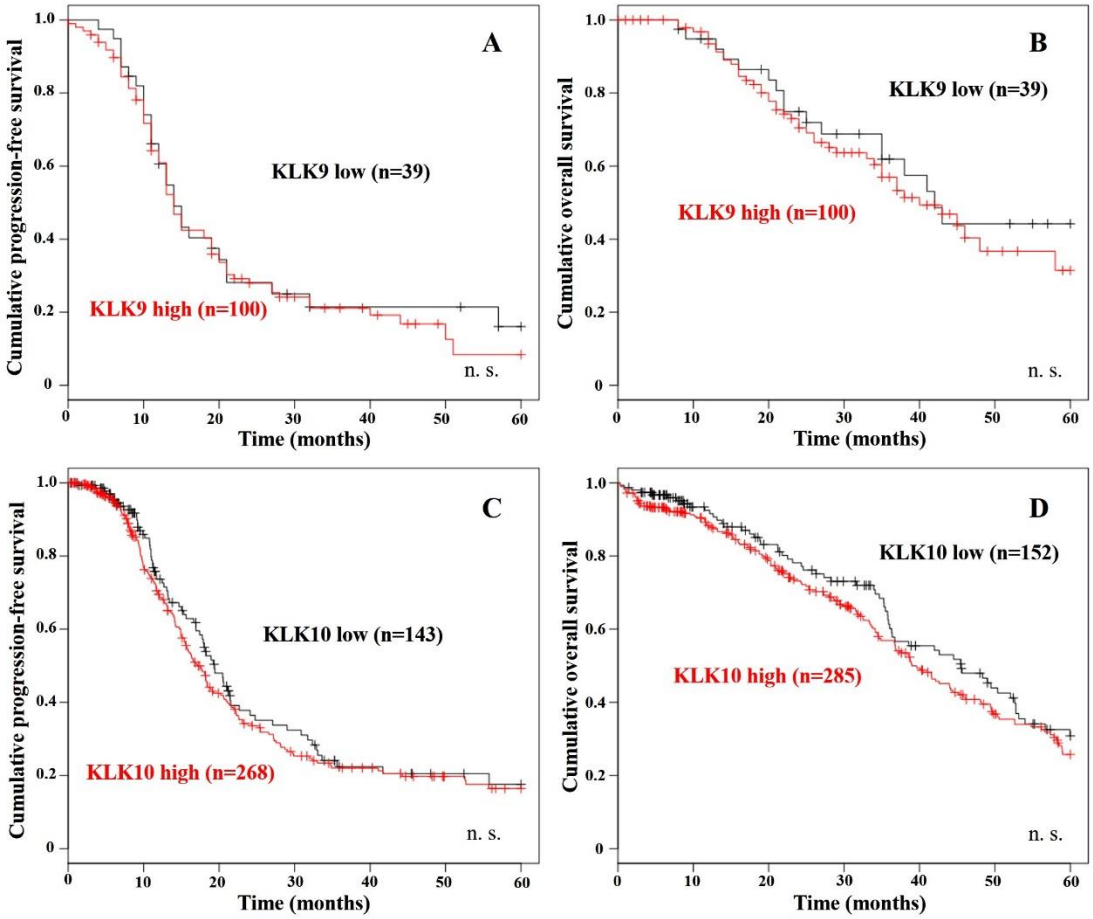

Figure 11. *In silico* analysis for the associations of KLK9 and KLK10 mRNA with the prognosis of advanced high-grade serous ovarian cancer patients.
Kaplan-Meier analysis based on a microarray data set from TCGA shows that neither KLK9 nor KLK10 mRNA levels display any predictive power for prognosis in advanced high-grade serous ovarian cancer patients. In the *in silico* analysis, patients afflicted with high-grade (grade 3), serous, and advanced-stage (FIGO III+IV) ovarian cancer, receiving platinum-based chemotherapy (follow up: 5 years), were enrolled for Kaplan-Meier survival analysis.

4.2 Protein expression of KLK10 determined by immunohistochemistry in advanced high-grade serous ovarian cancer

4.2.1 Establishment of an immunohistochemical assay for detection of KLK10 protein expression

First, Western blot analysis and cell microarrays (CMAs) were applied to validate the

specificity of the KLK10-directed polyclonal antibody (pAb) HPA017195 for protein detection. His-tagged, recombinant human KLK1-15 proteins (rec-KLK1-15) have been previously produced in-house as depicted in the prior study of our lab (Seiz et al., 2010). Approximately 50 ng of rec-KLK1-15 were separately subjected to SDS-PAGE and Western blot analysis applying the KLK10-directed pAb HPA017195. Also, CMAs were employed for estimating the cross-reactivity of the KLK10-directed pAb HPA017195 with other KLK proteins. The cell microarrays (CMAs) included thirteen OV-MZ-6 cell lines separately transfected with KLK3-15 and had been established by other colleagues of the laboratory before. KLK-transfected OV-MZ-6 tumor cells in the CMAs served as tumor tissue models overexpressing different KLKs.

In Western blot analysis, only rec-KLK10 (30 kDa) was strongly detected by pAb HPA017195 (**Figure 12**). The result indicates that pAb HPA017195 specifically binds to KLK10 and does not cross-react with other KLK proteins. After stripping, a polyclonal antibody directed against the His-Tag of all of the recombinant proteins was applied for Western blot analysis to test for equal transfer of KLK1-15 (data not shown). In the CMA tests, positive staining was only observed in KLK10-overexpressing OV-MZ-6 cells applying pAb HPA017195, while the OV-MZ-6 cells transfected with other KLKs did not show any staining (**Figure 13**), further validating the specificity and reliability of antibody HPA017195 in detecting KLK10 protein.

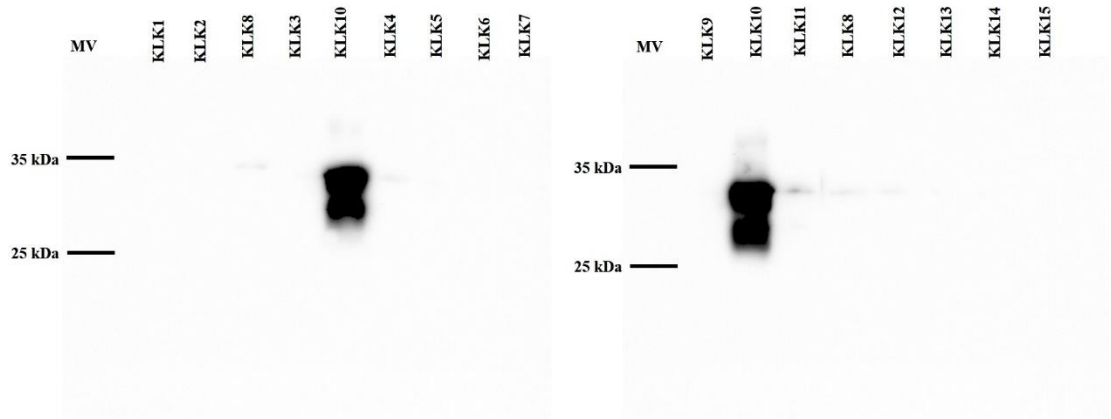

Figure 12. Western blot analysis demonstrating the specificity of the KLK10-directed pAb HPA017195

Rec-KLK1-15 were separately subjected to SDS-PAGE and Western blot analysis was performed with pAb HPA017195 (1:1000). Only rec-KLK10 loading (30 kDa) was detected with a strong band among rec-KLK1-15 proteins.

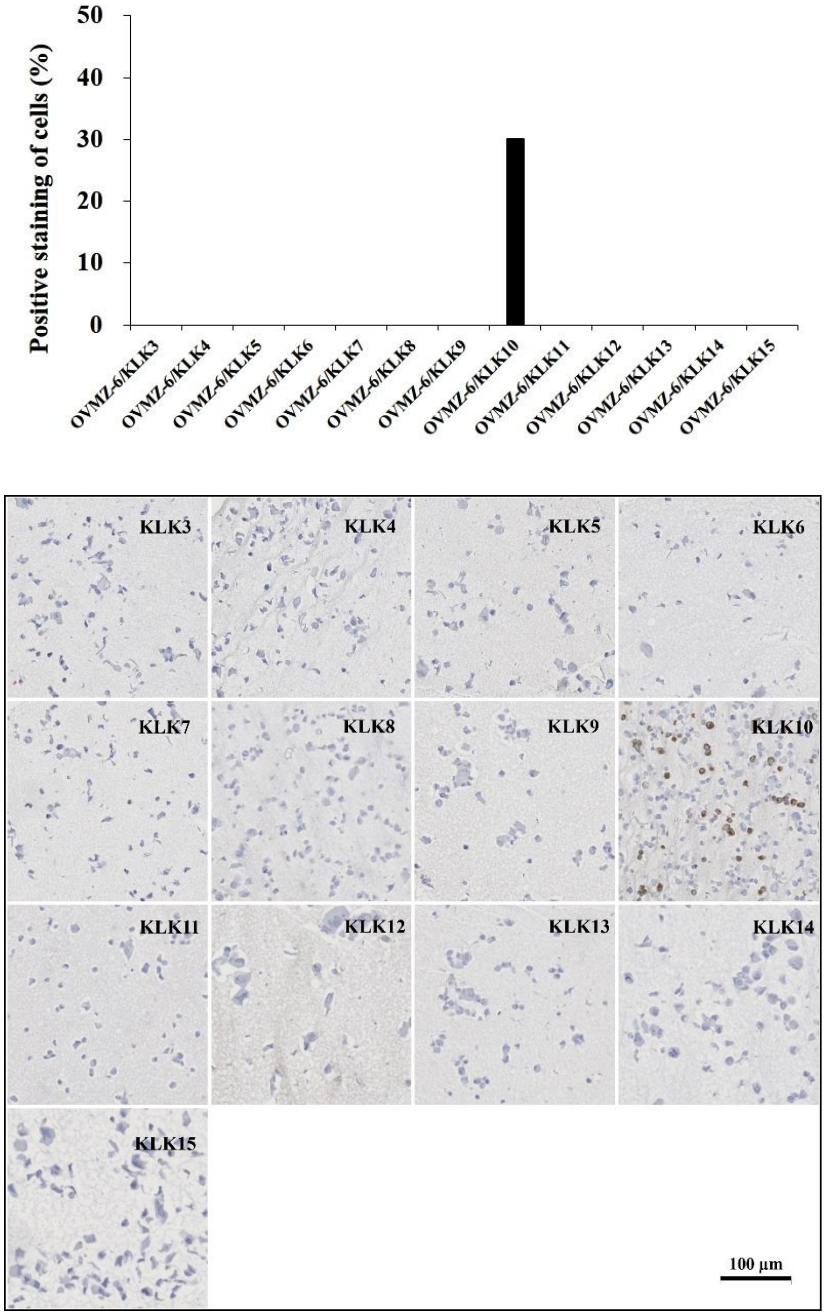

Figure 13. CMA analysis demonstrating the specificity of the KLK10-directed pAb HPA017195.

The CMA was immunohistochemically stained with the KLK10-directed pAb HPA017195. The CMA encompasses 13 OV-MZ-6 cell lines separately transfected with KLK3-15. Positive staining was only observed in KLK10-overexpressing OV-MZ-6 cells, while the rest did not show any staining. Overexpression of the individual KLKs has previously been proven by ELISA measurements in cell culture supernatants (E. P. Diamandis, pers. comm.). The parental cell line OV-MZ-6 does not express any of the 13 KLKs.

4.2.2 Protein expression of KLK10 in advanced high-grade serous ovarian cancer tissues and the association with clinical parameters

To evaluate the clinical value of KLK10 protein expression in this major ovarian cancer subtype, ovarian cancer TMAs, including 159 tumor specimens of advanced high-grade serous ovarian cancer (cohort 2, for details see chapter 3.1; Geng et al., 2018), were immunohistochemically stained with the KLK10-specific pAb HPA017195. Then, the stained TMAs were imaged by the Hamamatsu NanoZoomer Digital Pathology virtual microscope. Finally, KLK10 protein expression levels were determined by an automated quantitative scoring system based on software ImageJ (Java 1.8.0, 64 bit) plus IHC Profiler plugin.

KLK10 protein expression was predominantly observed in the cytoplasm of tumor cells (**Figure 14**; Geng et al., 2018). With the utility of the automated quantitative scoring system, the immunohistochemical staining intensity for each TMA core was assigned with an immunoreactive score (IRS), ranging from 29.64 to 121.50 (median = 42.46). The histogram shown in **Figure 15** gives an overview of KLK10 protein expression in tumor tissue of the patient cohort, demonstrating that KLK10 protein is highly expressed in the most samples. This is in line with its mRNA expression pattern in this subgroup of ovarian cancer. Next, KLK10 protein expression levels were initially categorized into a low-expressing group (tertile T1) and a high-expressing group (tertiles T2+3). Results obtained by using dichotomization by T1 versus T2+3 have been published in Geng et al., 2018. In the present work, the cut-off was further optimized with respect to patient prognosis, resulting in the use of the 32^{nd} instead of the 33^{rd} percentile for categorization into a low- versus high-expressing group.

As cohort 1 partially overlapped with cohort 2, the relationship of KLK10 mRNA and protein expression could be explored in the overlapping samples (n = 60). We found that KLK10 protein expression was positively correlated with its mRNA expression (r_s = 0.453, $p < 0.001$). In box plot analysis the association between KLK10 mRNA and protein levels only showed a trend towards significance (Mann-Whitney test; p = 0.060; **Figure 16A**).

Within the present project, KLK11 protein expression was also determined in the same cohort (X. Geng, pers. comm.). Concordant with the coordinate expression of KLK10 and KLK11 at mRNA level, Spearman correlation analysis demonstrated a moderate correlation between KLK10 and KLK11 expression at the protein level (r_s = 0.403, p =

0.001; Geng et al., 2018). This finding was validated by the box plot analysis, KLK11 protein expression was significantly increased in the KLK10 high group and vice versa (Mann-Whitney test; $p < 0.001$; **Figure 16B**).

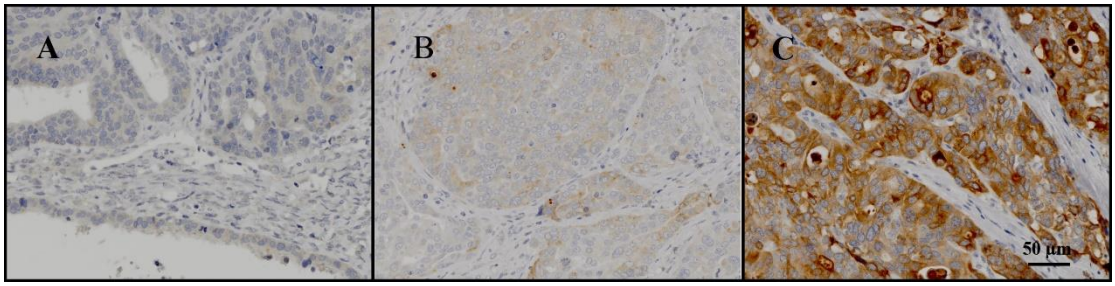

Figure 14. Immunohistochemical staining of KLK10 applying pAb HPA017195 in ovarian tumor tissues

Tissue microarrays were immunohistochemically stained with KLK10-directed pAb HPA017195 (Sigma, 1:200). Micrographs A, B, and C separately represent low, moderate, and high KLK10 immunoexpression in ovarian cancer cells. All micrographs are imaged by Hamamatsu Nanozoomer XT virtual microscope. Figures are published in Geng et al., 2018.

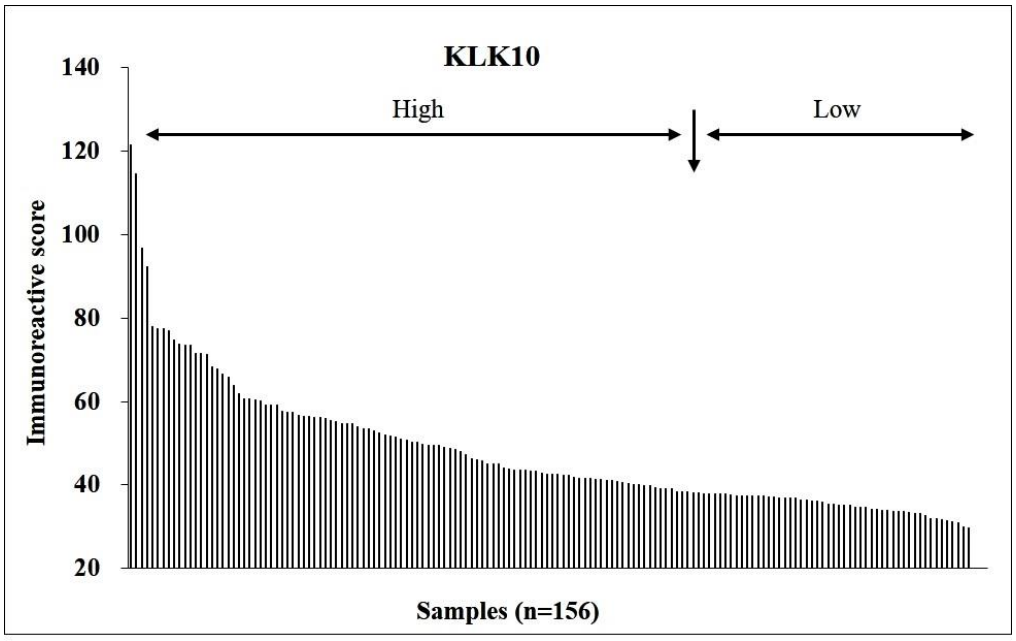

Figure 15. KLK10 protein expression levels in advanced high-grade serous ovarian cancer (FIGO III/IV) (cohort 2)

The majority of the samples display a robust KLK10 protein expression. KLK10 IRSs were dichotomized into a low- and high-expressing group by the 32nd percentile.

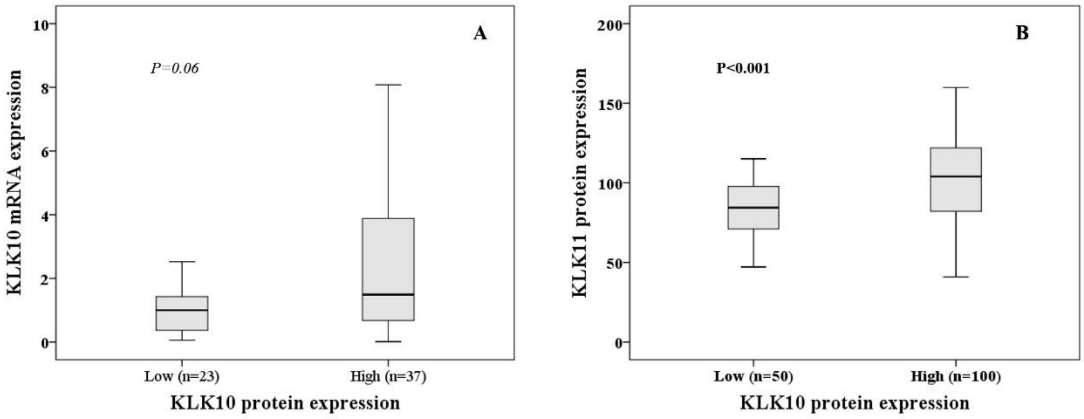

Figure 16. Association of KLK10 protein expression with its mRNA expression and KLK11 protein expression in tumor tissues of advanced high-grade serous ovarian cancer patients.

(A) Association between KLK10 mRNA and protein levels showed a trend towards significance (Mann-Whitney test; p = 0.060); (B) KLK11 protein levels (given as IRS values) are significantly increased in the KLK10 high group and vice versa (Mann-Whitney test; p < 0.001).

Table 9. Associations of tumor biological markers with clinical parameters of advanced high-grade serous ovarian cancer patients (FIGO III/IV)

Clinical parameters	KLK10[a]	KLK10+KLK11[a, b]
	Low/high	Low/high
Age	p = 0.651	p = 0.382
≤ 60 years	17/40	22/33
> 60 years	33/66	45/50
Residual tumor mass	*p = 0.074*	*p = 0.075*
0 mm	20/58	29/47
> 0 mm	29/45	37/33
Ascitic fluid volume	p = 0.108	p = 0.220
≤ 500 ml	24/64	36/51
> 500 ml	25/38	30/28

[a] Chi-square test (KLK10 protein expression levels were dichotomized into low and high groups by the 32nd percentile; KLK11 protein expression levels were dichotomized into low and high groups by the 25th percentile);

[b] Chi-square test (dichotomized into KLK10 low and/or KLK11 low versus KLK10 high and KLK11 high);

Italics indicate trends towards significance (p ≤ 0.08).

Owing to the correlation of KLK10 and KLK11, the protein levels of both factors were further dichotomized into a KLK10+KLK11 high group (both protein levels above respective cutoff value; cut-off KLK10: 32nd percentile; KLK11: 25th percentile) versus a KLK10+KLK11 low group (KLK10 and/or KLK11 protein levels below the respective cutoff value) for statistical analysis. As depicted in **Table 9**, no significant associations of KLK10 or KLK10+KLK11 with clinical parameters were observed, aside from a trend towards significance for high KLK10 and high KLK10+KLK11 in postoperative tumor-free patients versus patients with residual tumor mass (KLK10, p = 0.074; KLK10+KLK11, p = 0.075).

4.2.3 Association of KLK10 protein expression levels and clinical parameters with PFS and OS

In univariate Cox regression analysis (**Table 10**; see also Geng et al., 2018), residual tumor mass left after debulking surgery and pre-operative amounts of ascitic fluid were prognostic factors for PFS and OS, while age did not display any prognostic power for outcome. Compared to tumor-free cases, patients with residual tumor mass (>0 mm) had an increased probability for tumor progression (HR, 2.87; 95% CI, 1.85-4.46; p <0.001) as well as cancer-related death (HR, 4.10; 95% CI, 2.38-7.06; p <0.001). High ascitic fluid volume was associated with an elevated probability of cancer-related death (HR, 1.80; 95% CI, 1.12-2.90; p = 0.016) and an increased risk of disease progression (HR, 1.95; 95% CI, 1.26-3.30; p = 0.003).

As shown in **Table 10**, KLK10 protein expression turned out to represent a pronounced prognostic factor for OS (HR, 0.57; 95% CI, 0.35-0.91; p = 0.020), but not for PFS (HR, 1.13; 95% CI, 0.70-1.84; p = 0. 623), in the patients afflicted with advanced high-grade serous ovarian cancer. Patients with elevated KLK10 protein expression had an approximately two-fold reduced probability of cancer-related death. Also, the patients in KLK10+KLK11 high group displayed a remarkably decreased risk of cancer-related death (HR, 0.41; 95% CI, 0.25-0.67; p < 0.001). Moreover, compared to KLK10 alone, the combination of KLK10+KLK11 could obviously increase the predictive power for OS. The impact of these factors on prognosis is also visualized by respective Kaplan-Meier survival curves (**Figure 17**): patients with high KLK10 expression have a prolonged OS, while KLK10 protein expression not associated with PFS; similarly, the

cases in KLK10+KLK11 high group display a prolonged OS, whereas the association with PFS remains not significant.

Table 10. Univariate Cox regression analysis of tumor biological markers and clinical parameters for the prediction of clinical outcome in advanced high-grade serous ovarian cancer patients (FIGO III/IV)

Clinical parameters	PFS			OS		
	No[a]	HR (95% CI)[b]	p	No[a]	HR (95% CI)[b]	p
Age			0.704			0.337
≤ 60 years	43	1		51	1	
> 60 years	76	1.09 (0.70-1.70)		93	1.28 (0.78-2.09)	
Residual tumor mass			**< 0.001**			**< 0.001**
0 mm	69	1		72	1	
> 0 mm	48	2.87 (1.85-4.46)		68	4.10 (2.38-7.06)	
Ascitic fluid volume			**0.003**			**0.016**
≤ 500 ml	70	1		81	1	
> 500 ml	45	1.95 (1.26-3.30)		58	1.80 (1.12-2.90)	
KLK10 IRS[c]			0.623			**0.020**
low	34	1		46	1	
high	84	1.13 (0.70-1.84)		96	0.57 (0.35-0.91)	
KLK10+KLK11 IRS[c, d]			0.791			**< 0.001**
low	49	1		63	1	
high	67	0.94 (0.61-1.46)		76	0.41 (0.25-0.67)	

[a] Number of patients;

[b] HR: hazard ratio (CI: confidence interval) of univariate Cox regression analysis;

[c] KLK10 protein expression levels were dichotomized into low and high groups by the 32nd percentile; KLK11 protein expression levels were dichotomized into low and high groups by the 25th percentile;

[d] Dichotomized into KLK10 low and/or KLK11 low versus by KLK10 high and KLK11 high;

Bold value indicates statistical significance ($p < 0.05$).

The data concerning age, residual tumor mass, ascitic fluid volume and their association with OS are presented in Geng et al., 2018.

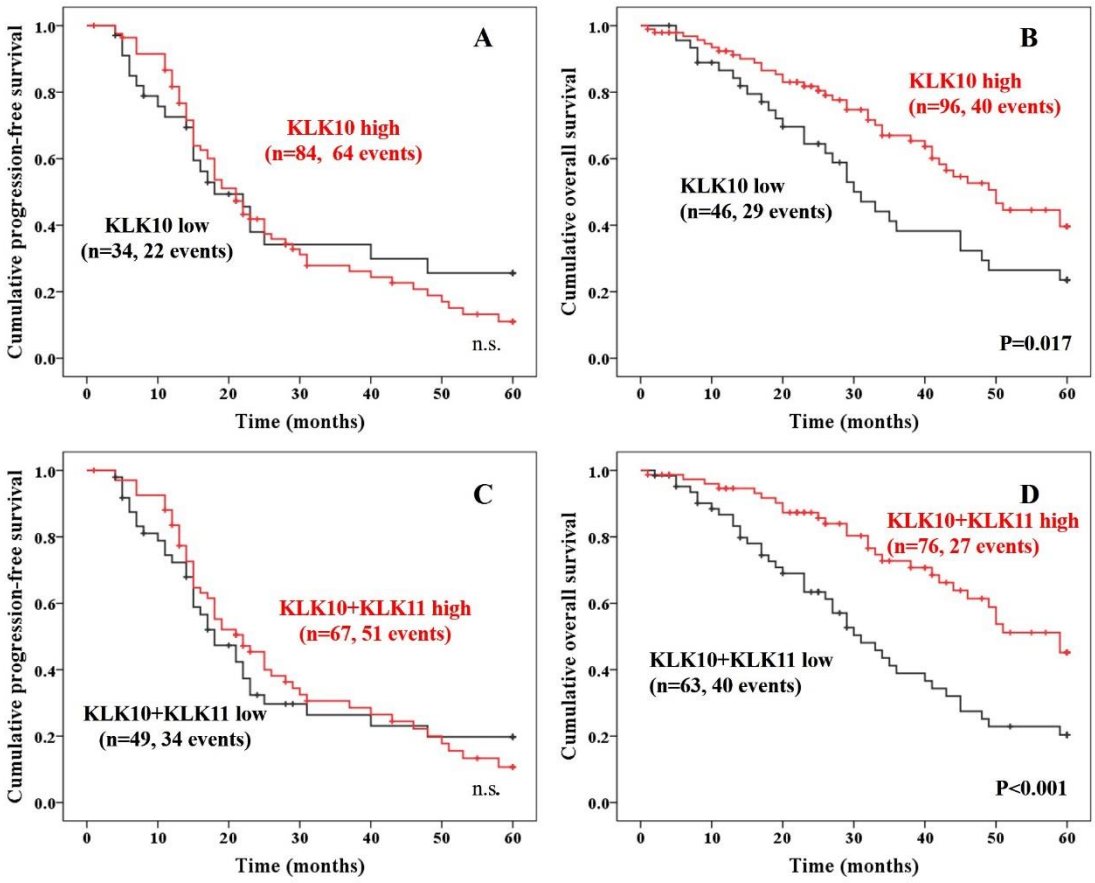

Figure 17. Kaplan–Meier survival curves for the cohort of advanced high-grade serous ovarian cancer patients (FIGO III/IV).

(A, B) Patients with high KLK10 expression have a prolonged OS, while KLK10 protein expression is not associated with PFS. (C, D) Patients in the KLK10+KLK11 high group have a prolonged OS, while the association with PFS remains not significant.

Multivariate Cox regression analysis was applied to test for an independent relationship of KLK10 protein levels with OS (**Table 11**). First, we established a base model containing age, ascitic fluid volume, and residual tumor mass. When the base model was subjected to multivariable analysis, residual tumor mass still showed predictive power for OS (HR, 3.58; 95% CI, 1.99-6.43; $p < 0.001$). Next, KLK10 protein expression was added to the base model for multivariate Cox regression analysis, illustrating KLK10 is an independent favorable predictor of OS (HR, 0.59; 95% CI, 0.35-0.98; $p = 0.043$). Additionally, a separate multivariate analysis including KLK10+KLK11 values and the base model was developed, indicative of the independence of KLK10+KLK11 values in the prediction of OS (HR, 0.41; 95% CI, 0.24-0.70; $p = 0.001$).

Table 11. Multivariate Cox regression analysis of tumor biological markers and clinical parameters for the prediction of overall survival (OS) in advanced high-grade serous ovarian cancer patients (FIGO III/IV)

Clinical parameters	OS		
	No[a]	HR (95% CI)[b]	p
Age			0.964
≤ 60 years	49	1	
> 60 years	82	1.01 (0.60-1.71)	
Residual tumor mass			**< 0.001**
0 mm	68	1	
> 0 mm	63	3.58 (1.99-6.43)	
Ascitic fluid volume			0.749
≤ 500 ml	78	1	
> 500 ml	53	1.09 (0.65-1.84)	
KLK10 IRS[c]			**0.043**
low	44	1	
high	87	0.59 (0.35-0.98)	
KLK10+KLK11 IRS[c, d]			**0.001**
low	61	1	
high	70	0.41 (0.24-0.70)	

The hazard ratios of tumor markers were adjusted for the base model, including age, residual tumor mass, and ascitic fluid volume. The data concerning the base model and its association with OS are presented in Geng et al., 2018. Bold value indicates statistical significance ($p < 0.05$).

[a] Number of patients;

[b] HR: hazard ratio (CI: confidence interval) of univariate Cox regression analysis;

[c] KLK10 protein expression levels were dichotomized into low and high groups by the 32nd percentile; KLK11 protein expression levels were dichotomized into low and high groups by the 25th percentile;

[d] Dichotomized into KLK10 low and/or KLK11 low versus KLK10 high and KLK11 high.

4.3 Assessment of KLK10 mRNA expression by qPCR in breast cancer

4.3.1 KLK10 mRNA expression in tumor tissues of triple-negative breast cancer (TNBC) and hormone receptor-positive breast cancer (HRPBC) patients

KLK10 mRNA expression was determined by the newly established qPCR assay in 127 cases of triple-negative breast cancer tissues (cohort 3, for details see chapter 3.2) and 27 cases of hormone receptor-positive breast cancer tissues. The values of relative

KLK10 mRNA expression ranged from 0.00 to 10.53 (median: 0.15) in the TNBC cohort and from 0.00 to 0.79 (median: 0.02) in the HRPBC cohort, respectively. Most of the tumor tissues display low KLK10 mRNA expression in the two subtypes of breast cancer (**Figure 18, Figure 19**). Therefore, KLK10 mRNA expression levels were categorized into a low-expressing group (tertiles 1+2) and a high-expressing group (tertile 3) in both cases. Box plot analysis demonstrated that TNBC samples showed significantly higher KLK10 mRNA levels, compared to HRPBC cases (Mann-Whitney test; $p < 0.001$; **Figure 20**).

KLK11 mRNA expression levels were also quantified in the identical breast cancer cohorts (X. Geng, pers. comm.). Remarkable positive correlations between KLK10 and KLK11 mRNA were observed both in the TNBC cohort ($r_s = 0.724$, $p < 0.001$) and the HRPBC cohort ($r_s = 0.766$, $p < 0.001$) by Spearman correlation analysis, indicative of their coordinate expression also in these tumor entities. Moreover, box plot analysis was employed to validate their correlation at the mRNA level, showing that high KLK10 mRNA expression was notably associated with increased KLK11 expression in HRPBC (Mann-Whitney test; $p = 0.001$; **Figure 21A**) as well as TNBC (Mann-Whitney test; $p < 0.001$; **Figure 21B**).

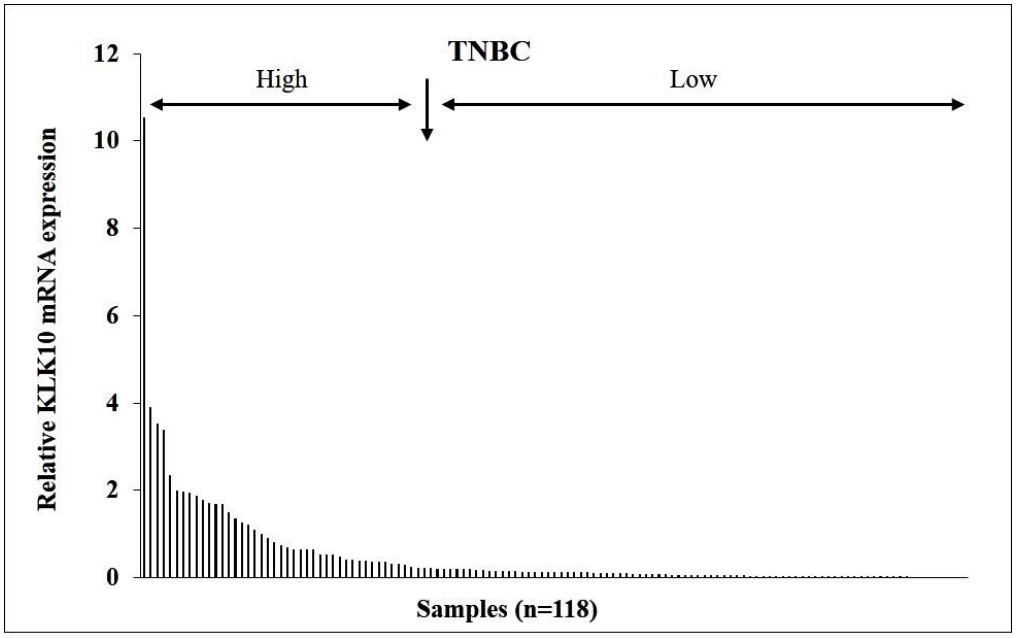

Figure 18. Expression levels of KLK10 mRNA in triple-negative breast cancer (TNBC)

The majority of the samples displayed low KLK10 mRNA expression. KLK10 mRNA expression levels were categorized into a low-expressing group (tertiles 1+2) versus a high-expressing group (tertile 3) by the 66th percentile.

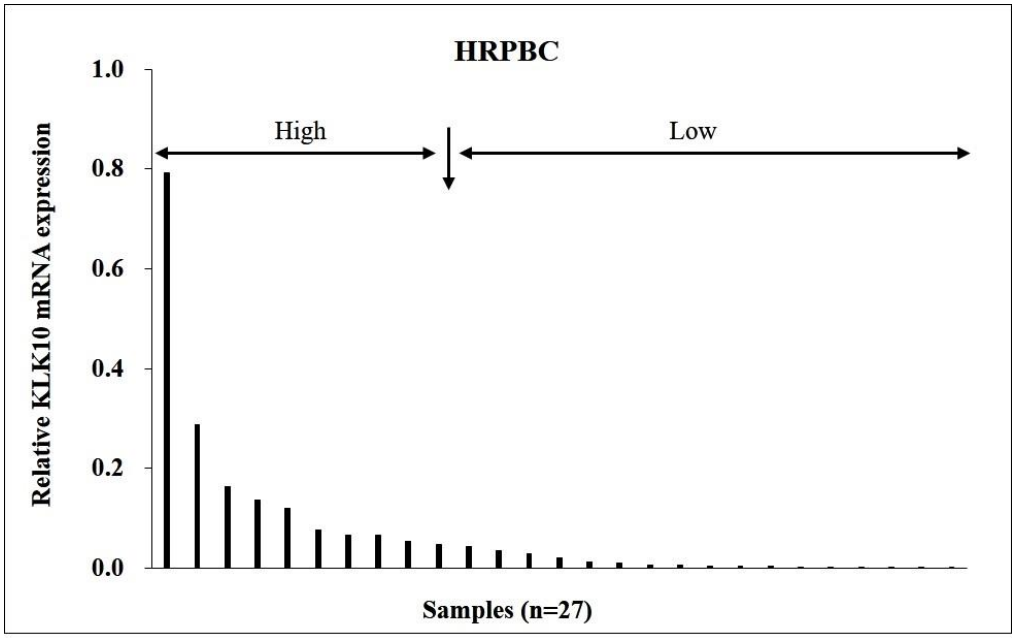

Figure 19. Expression levels of KLK10 mRNA in hormone receptor-positive breast cancer (HRPBC)

The majority of the samples displayed low KLK10 mRNA expression. KLK10 mRNA expression levels were categorized into a low-expressing group (tertiles 1+2) versus a high-expressing group (tertile 3) by the 66th percentile.

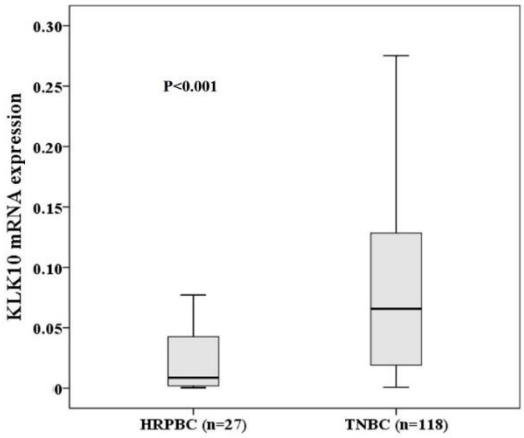

Figure 20. Expression levels of KLK10 mRNA in hormone receptor-positive and triple-negative breast cancer tissues.

Compared to HRPBC, KLK10 mRNA expression was remarkably increased in TNBC samples (Mann-Whitney test; $p < 0.001$).

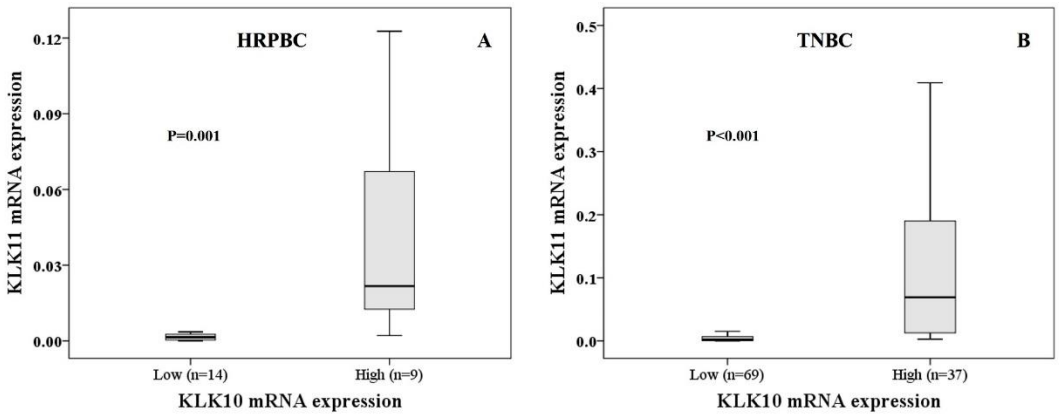

Figure 21. Association of KLK10 and KLK11 mRNA expression in tumor tissues of hormone receptor-positive breast cancer and triple-negative breast cancer.
Enhanced KLK10 mRNA expression is significantly associated with high KLK11 expression in tumor tissues of hormone receptor-positive breast cancer ($p < 0.001$, Mann-Whitney test) and triple-negative breast cancer patients ($p < 0.001$, Mann-Whitney test).

4.3.2 Association of KLK10 mRNA expression levels with clinicopathological parameters and its prognostic impact on disease-free survival (DFS) in TNBC

We investigated the associations of KLK10 mRNA levels with established clinicopathological parameters in 127 cases of TNBC patients (cohort 3; for details see chapter 3.2). Due to the observed correlation of KLK10 and KLK11 expression in TNBC, the mRNA levels of the two factors were dichotomized into a KLK10+KLK11 low group (both KLK10 and KLK11 mRNA levels below the respective cutoff value) and a KLK10+KLK11 high group (KLK10 and/or KLK11 protein levels above the respective cutoff value) for further analysis. As can be seen in **Table 12,** KLK10 as well as KLK10+KLK11 were not associated with clinicopathological parameters of TNBC, including age, lymph node status, tumor size, and histological grade.

Univariate Cox regression analysis was performed to evaluate the prognostic relevance of KLK10, KLK10+KLK11, and the clinicopathological parameters regarding DFS in the TNBC cohort (**Table 13)**. Among the clinical variables, age was the only univariate predictor for DFS. Patients with advanced age (>60 years) experienced an increased probability of disease recurrence and/or death (HR, 2.39; 95% CI, 1.38-4.13; $p = 0.002$). Lymph node status displayed a trend towards significance (N_+ vs N_0: HR, 1.59; 95% CI, 0.93-2.72; $p = 0.090$).

KLK10 mRNA levels represented a significant predictive marker for DFS (HR, 1.81; 95% CI, 1.02-3.21; $p = 0.044$), displaying an approximate two-fold increased risk of

disease progression in the KLK10 high group. KLK10+KLK11 high was also significantly associated with an elevated probability of disease progression (HR, 1.98; 95% CI, 1.07-3.65; p = 0.029). Compared to KLK10 alone, the combined KLK10+KLK11 values could mildly increase the predictive power for DFS. Furthermore, the impact of these factors on DFS were also confirmed by Kaplan-Meier estimation. As shown by the respective survival curves (**Figure 22**), high KLK10 and high KLK10+KLK11 were notably related with shortened DFS (log-rank test; KLK10, p = 0.041; KLK10+KLK11, p = 0.026).

Finally, multivariate Cox regression analysis was performed to estimate the independence of KLK10 and KLK10+KLK11 as prognostic factors in TNBC (**Table 14**). Similar to the analysis of the advanced serous ovarian cancer, we also established a base model containing age, lymph node status, tumor size, and histological grade. In the multivariate Cox regression analysis of the base model, age is the only clinical parameter displaying predictive power for DFS (HR, 2.39; 95% CI, 1.27-4.48; p = 0.007). After adjustment for the base model, KLK10 mRNA expression turned out to represent an independent unfavorable predictor of DFS (HR, 2.51; 95% CI, 1.33-4.74; p = 0.005). KLK10+KLK11 values were found to significantly contribute to the base model for DFS (HR, 2.35; 95% CI, 1.23-4.51; p = 0.010), as well indicative of its independence in the prediction of DFS.

Table 12. Associations of tumor biological markers with clinicopathological parameters of triple-negative breast cancer

Clinicopathological parameters	KLK10[a] Low/high	KLK10+KLK11[b] Low/high
Age	p = 0.276	p = 0.579
≤ 60 years	42/24	33/30
> 60 years	38/14	26/19
Lymph node status	p = 0.672	p = 0.765
N_0	43/22	33/26
N_+	37/16	26/23
Tumor Size	p = 0.633	p = 0.609
≤20 mm	22/9	18/13
>20 mm	57/29	40/36
Histological grade	p = 0.769	p = 0.342
Grade I or II	13/7	8/10
Grade III	67/31	51/39

[a] Chi-square test (dichotomized into low and high groups by the 66th percentile);
[b] Chi-square test (dichotomized into low group by KLK10 low and KLK11 low, and high group by KLK10 high and/or KLK11 high).

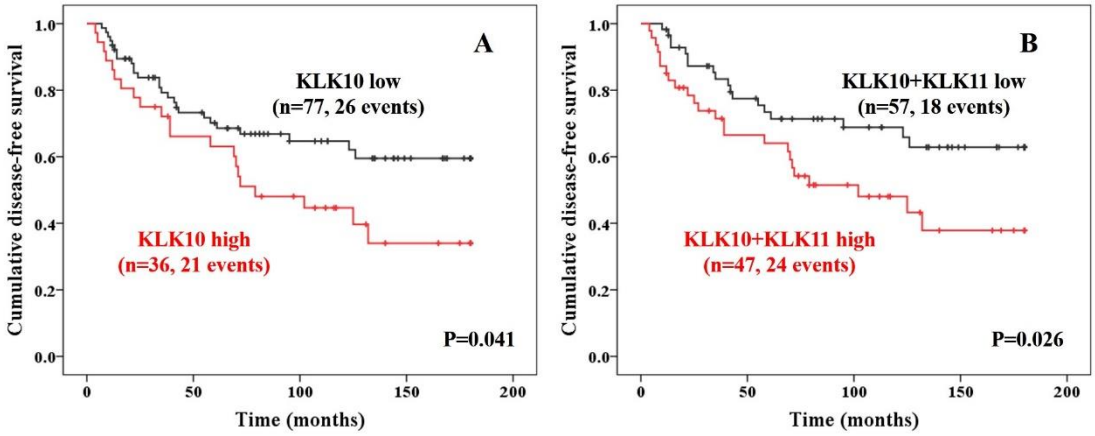

Figure 22. Kaplan–Meier survival curves for the cohort of triple-negative breast cancer.
(A) Patients with KLK10 high expression were significantly associated with shortened DFS (log-rank test, p = 0.041). (B) Patients in KLK10+KLK11 high group were notably related with shortened DFS (log-rank test, p = 0.026).

Table 13. Univariate Cox regression analysis of tumor biological markers and clinicopathological parameters for the prediction of disease-free survival (DFS) in triple-negative breast cancer

Clinicopathological parameters	DFS		
	No[a]	HR (95% CI)[b]	p
Age			**0.002**
≤ 60 years	67	1	
> 60 years	55	2.39 (1.38-4.13)	
Lymph node status			*0.090*
N0	68	1	
N1/N2/N3	54	1.59 (0.93-2.72)	
Tumor Size			0.134
≤20 mm	32	1	
>20 mm	89	1.69 (0.85-3.37)	
Histological grade			0.409
Grade I or II	20	1	
Grade III	102	1.40 (0.63-3.09)	
KLK10 mRNA[c]			**0.044**
low	77	1	
high	36	1.81 (1.02-3.21)	
KLK10+KLK11 mRNA[d]			**0.029**
low	57	1	
high	47	1.98 (1.07-3.65)	

[a] Number of patients;

[b] HR: hazard ratio (CI: confidence interval) of univariate Cox regression analysis;

[c] Dichotomized into low and high groups by the 66th percentile;

[d] Dichotomized into low group by KLK10 low and KLK11 low, and high group by KLK10 high and/or KLK11 high;

Bold value indicates statistical significance ($p < 0.05$). Italics indicate trends towards significance ($p \leq 0.09$).

Table 14. Multivariate Cox regression analysis of tumor biological markers and clinical parameters for the prediction of disease-free survival (DFS) in triple-negative breast cancer

Clinicopathological parameters	DFS		
	No[a]	HR (95% CI)[b]	p
Age			**0.007**
≤ 60 years	62	1	
> 60 years	44	2.39 (1.27-4.48)	
Lymph node status			0.290
N0	59	1	
N1/N2/N3	47	1.41 (0.75-2.64)	
Tumor Size			0.491
≤20 mm	30	1	
>20 mm	76	1.30 (0.61-2.77)	
Histological grade			0.340
Grade I or II	18	1	
Grade III	88	1.59 (0.62-4.10)	
KLK10 mRNA[c]			**0.005**
low	68	1	
high	38	2.51 (1.33-4.74)	
KLK10+KLK11 mRNA[d]			**0.010**
low	58	1	
high	48	2.35 (1.23-4.51)	

The hazard ratios of tumor markers were adjusted for the base model, including age, lymph node status, tumor Size, and histological grade.

[a] Number of patients;

[b] HR: hazard ratio (CI: confidence interval) of univariate Cox regression analysis;

[c] Dichotomized into low and high group by the 66th percentile;

[d] Dichotomized into low group by KLK10 low and KLK11 low, and high group by KLK10 high and/or KLK11 high;

Bold value indicates statistical significance ($p < 0.05$).

5 Discussion

Accumulative evidence strongly indicates that kallikrein-related peptidases may serve as diagnostic and prognostic biomarkers in various malignancies such as ovarian, breast, prostate, lung, gastric, and colorectal cancer (Zhang et al., 2011; Olkhov-Mitsel et al., 2012; Petraki et al., 2012; Michaelidou et al., 2015; Ahmed et al., 2016; Kolin et al., 2016). Nevertheless, the investigation of the impact of KLKs in cancer is still progressing and, moreover, often has resulted in conflicting results, especially in ovarian and breast cancer. The contradictory findings concerning clinical relevance of individual KLKs were speculated to be due to the patient cohorts analyzed, which generally included different clinical stages and histological subtypes. However, ovarian and breast cancer both represent heterogeneous diseases and are composed of several distinct subtypes exhibiting a tremendous variety in their histopathological, clinical, and molecular genetic pattern (Jelovac and Armstrong, 2011; Cedolini et al., 2014). Thus, in the present study, we focused on the analysis of tumor-relevant KLK expression in more homogenous ovarian (advanced high-grade serous ovarian cancer) and breast cancer (triple-negative breast cancer) cohorts and evaluated their clinical relevance in these well-defined subgroups.

5.1 Clinical relevance of KLK9 mRNA expression in advanced high-grade serous ovarian cancer (FIGO stage III/IV)

It has been reported that KLK9 mRNA expression is distinctly lower in breast cancer patients with advanced stage tumors compared to the early stage patients, as well as in patients with large versus small tumor size (Yousef et al., 2003). In ovarian cancer, low KLK9 expression was observed to be associated with advanced disease stages (III/IV) and suboptimal tumor debulking rather than optimal debulking (Yousef et al., 2001). In the current study, KLK9 displayed low mRNA expression in the majority of advanced high-grade serous ovarian cancer samples. Still, because we did not analyze the expression pattern in early stage patients, it cannot be concluded that repressed KLK9 expression represents be a marker for the more aggressive subtype of ovarian cancer. Interestingly, KLK9 and KLK15 were coordinately expressed at the mRNA level (r_s = 0.716), indicating that their regulation was controlled by a similar mechanism. All 15 genes of KLK family are tightly arranged within a single locus of approximately 0.3 Mbp on the long arm of chromosome 19q13.4, comprising the largest tandem protease gene cluster of human genome. The regulatory mechanism of a single locus control

region, seems improbable owing to the fact that tissue-specific expression profiles of specific KLKs has been well established in human body, *i.e.*KLK6 primarily expressed in central nervous system while KLK5 and KLK7 abundant in skin (Shaw and Diamandis, 2007). Accumulating evidence supported that the transcription of each KLK is independently modulated by conserved regulatory elements (Kroon et al., 1997; Lawrence et al., 2010). Indeed, the KLK locus is strongly responsive to androgens, estrogens, and other hormones, in which previous researches identified more than 14 functional hormone response elements (Lawrence et al., 2010). Thus, hormone-related regulatory mechanisms are speculated to underlie coordinate expression of several KLKs, including KLK9 and KLK15. In fact, Yousef and Diamandis demonstrated that KLK9 and KLK15 were simultaneously upregulated in BT-474 breast cancer cells when subjected to androgens (Yousef and Diamandis, 2000; Yousef et al., 2002). Moreover, both high KLK9 and KLK15 expression was demonstrated to represent favorable prognostic biomarkers in breast cancer (Yousef et al., 2002, 2003).

Regarding clinical relevance, KLK9 has been shown to represent a predictive biomarker in other type cancer as well. In contrast to breast cancer, in glioma patients with higher KLK9 protein expression were reported to have a poor outcome (Drucker et al., 2015). In line with the breast cancer data, in ovarian cancer, overexpression of KLK9 mRNA has been demonstrated to represent an independent biomarker of favorable prognosis (Yousef et al., 2001). However, in contrast to this latter finding, in the present study KLK9 mRNA levels did not display any prognostic power in the OS or PFS of advanced high-grade serous ovarian cancer patients. Moreover, applying *in silico* analysis we analyzed the publicly available mRNA expression profiles of advanced high-grade serous ovarian cancer patients from TCGA (Gyorffy et al., 2012), confirming the lack of any significant prognostic power of KLK9 mRNA levels (**Figure 11**). This contradictory observations in ovarian cancer may be attributed to the heterogeneous patient cohorts previously investigated. Whereas the patient cohort analyzed by Yousef et al. (Yousef et al., 2001) encompassed early/advanced stage, low/high grade, serous, endometrioid, mucinous, clear cell, and undifferentiated histological types of ovarian cancer patients, the patient cohort of the present study consisted of a homogenous subgroup, advanced high-grade serous ovarian cancer.

5.2 Assessment of KLK10 as a potential prognostic biomarker in advanced high-grade serous ovarian cancer (FIGO III/IV)

In case of KLK10, we not only quantified its mRNA expression in a cohort of 139 patients suffering advanced high-grade serous ovarian cancer (FIGO stage III/IV) via qPCR, but also assessed its protein expression by immunohistochemistry (IHC) in a partially overlapping cohort including 159 cases of the same subtype of ovarian cancer.

When employed for detecting protein expression in tissue, IHC exhibits unique and apparent advantages: it is of low cost, widely used in research and clinical practice, and capable of differentiating the expression in epithelial cells vs. stromal cells vs. extracellular matrix, or cytoplasm vs. nuclear (Kolin et al., 2016). However, manual scoring of IHC staining intensity can be challenging, due to its inter- and intra-observer variability. Therefore, we applied an automated quantitative scoring method based on the software ImageJ plus the IHC Profiler plugin, which was previously used by others for IHC analysis in gastric and breast cancer (Chatterjee et al., 2013; Kolin et al., 2016). The automated scoring method not only elevates the reliability of the measurement by avoiding the variability from inter- and intra-observer, but also improves the sensibility in distinguishing the differences of staining (Kolin et al., 2014). It, e.g., allows the subclassification of staining intensity (normally categorized as =, 1+, 2+, and 3+ in manual evaluation), which may be important one or more of the categories are too large. The use of TMAs allows to simultaneously stain and screen numerous tumors tissues under identical conditions, which thus provides a high degree of standardization.

Prior studies indicated that compared to normal ovary, KLK10 expression is upregulated in ovarian cancer and its overexpression is associated with more advanced stage (Luo et al., 2001; El Sherbini et al., 2011; Koh et al., 2011). In line with these previous studies, most of the advanced high-grade serous ovarian cancer tissues showed robust KLK10 mRNA and protein expression (**Figure 8** and **Figure 15**). Based on this expression pattern, the KLK10 mRNA and protein levels were initially categorized into a low group and a high group by the same cutoff (33^{rd} percentile; Geng et al., 2018), respectively. In the present work, the cut-off for KLK10 protein expression levels was further optimized with respect to patient prognosis, resulting in the use of the 32nd instead of the 33^{rd} percentile for categorization into a low- versus high-expressing group. In addition, we found KLK10 mRNA levels were significantly positively correlated with its protein levels ($r_s = 0.453$) in advanced high-grade serous ovarian cancer, which

was further validated by box plot analysis (**Figure 16A**). Likewise, a similar correlation of KLK10 mRNA and protein expression was previously reported in gastric cancer with an r_s value of 0.514 (Lei et al., 2012).

KLK11 mRNA and protein expression levels have also been quantified in the identical ovarian cancer cohorts (X. Geng, pers. comm.). A pronounced correlation was identified between KLK10 and KLK11 at the mRNA level ($r_s = 0.647$) as well as at the protein level ($r_s = 0.403$), suggesting KLK10 and KLK11 were coordinately expressed in advanced high-grade serous ovarian cancer. In fact, coordinate expression of KLK10 and KLK11 has been previously reported in non-small-cell lung cancer as well as in breast cancer (Yousef et al., 2004; Planque et al., 2006). It is tempting to speculate that a similar modulatory mechanism underlies their coordinate expression in these different tumor types. As discussed in **chapter 5.1** concerning correlation of KLK9 and KLK15, a hormone-related regulatory mechanism may contribute to coordinate expression of these KLKs, rather than the existence of a common single control region within KLK locus. Paliouras and Diamandis proved that androgens could simultaneously upregulate KLK10 and KLK11 protein expression through RAS/MEK/ERK and PI3K/AKT signaling pathways in breast cancer cells (Paliouras and Diamandis, 2008). In this tumor entity, both KLK10 and KLK11 expression was reported to be elevated upon estrogen stimulation. Furthermore, androgen was observed to synergistically enhance the estrogen-induced upregulation of KLK10 and KLK11 (Paliouras and Diamandis, 2008).

In the present study, we investigated the associations of KLK10 mRNA and protein expression with clinical parameters in advanced high-grade serous ovarian cancer, demonstrating that KLK10 protein levels displayed a tendency to be associated with residual tumor mass ($p = 0.074$). An increased proportion of KLK10 protein high expression was observed in the tumor-free patients (73%, 58/78, **Table 9**), compared to the cases with residual tumor (60%, 45/74, **Table 9**), which may point to a tumor-suppressing role of KLK10. This observation is in agreement with the previous finding by Pepin, showing that artificially re-expressed KLK10 was capable to diminish the aggressivity of ES-2 ovarian cancer cells as defined by decreased colony formation *in vitro* and oncogenicity *in vivo* (Pepin et al., 2011).

It should be noted, however, that KLK10 expression in tumor tissue has been proposed as an independent biomarker of poor prognosis in advanced (FIGO stage III/IV) ovarian

cancer (Luo et al., 2001), as well as in other type cancer like gastric, colon, and endometrial cancer (Santin et al., 2006; Alexopoulou et al., 2013; Jiao et al., 2013). Moreover, increased KLK10 protein levels in sera were also observed to be associated with high risk of relapse and death in a cohort containing 146 patients with ovarian cancer of all stages, low/high grade, and mixed histotypes (Luo et al., 2003). Additionally, White *et al.* depleted KLK10 expression in OVCAR-3 ovarian cancer cells by targeting miRNAs, leading to a significant decrease in the proliferation rate of the cancer cells (White et al., 2010). All these evidences implied a tumor-favoring role of KLK10, which thus supported the observation of KLK10 serving as a predicative marker of poor prognosis in ovarian cancer. Nevertheless, in the current study, no significant association of KLK10 mRNA levels with outcome was observed. Furthermore, like KLK9, the prognostic power of KLK10 was also investigated by *in silico* analysis using the mRNA expression profiles from TCGA (Gyorffy et al., 2012), which corroborates our findings (**Figure 11**).

Concerning the prognostic impact of KLK10 protein, a contrary result from prior findings was observed in our study. Here, high KLK10 protein levels represent an independent biomarker of prolonged overall survival in advanced high-grade serous ovarian cancer. It seems to be consistent with the study by Dorn and co-workers (Dorn et al., 2007) investigating KLK10 protein levels by ELISA in the primary tumor tissue extracts of 142 ovarian cancer patients, illustrating KLK10 protein was a decisive (favorable) clinical determinant of OS. Moreover, Pepin and co-workers (2011) reported the mice injected with ovarian cancer cell ES-2 clones overexpressing KLK10 had significantly longer survival than the empty vector control group in an intraperitoneal xenograft model. This anti-tumorigenic effect of KLK10 was further validated via exogenous administration of recombinant KLK10 which also conferred a survival advantage.

These discrepant findings of the prognostic impact of KLK10 in ovarian cancer may be due to the fact that, firstly, the current study analyzed the mRNA and protein levels of KLK10 in tumor specimen tissues rather than in sera of patients (Luo, et al., 2003). Secondly, our cohort only enrolled patients afflicting with advanced stage (FIGO stage III/IV), high-grade, and serous ovarian cancer, whereas the cohorts previously investigated by Luo et al. (2001, 2003) including heterogeneous subtypes of ovarian cancer. It should be noted, however, that although the results of the study by Dorn et al. (Dorn et al., 2007) is accordance with ours, the analyzed cohort also included the

ovarian cancer of all stages, low/high-grade, and mixed histological subtypes.

There are serval possible mechanisms to explain that KLK10 may act as a suppressor in cancer progression. Zheng *et al.* (2012) showed that up-regulation of KLK10 in human tongue cancer cells repressed proliferation and invasiveness. In SGC-7901 gastric cancer cells, elevated KLK10 expression was reported to decelerate tumor growth *in vivo* (Huang et al., 2008). Furthermore, overexpression of KLK10 suppressed proliferation and glucose metabolism of PC3 prostate cancer cells, accompanied with increased apoptosis rate, through modulating expression of Bcl-2 and HK-2 (Hu et al., 2015). Moreover, overexpression of KLK10 (as well as KLK6/10) repressed colony formation of ES-2 ovarian cancer cells in CD-1 nu/nu mice, whereas up-regulation of KLK6 alone conferred positive impact on colony formation (Pepin et al., 2011). Co-expression of KLK6/10 in ES-2 cells represented a similar impact as overexpression of KLK10 alone, suggesting that KLK10 can diminish the tumor-promoting role of KLK6 in ES-2 cells. The reduced colony formation in KLK10 and KLK6/10 expressing cells was accompanied by a shortened survival rate and lesser ascitic volume.

5.3 Quantitative assessment of KLK10 mRNA expression in tumor tissues of triple negative breast cancer: correlation with clinical outcome

As stated above, we have observed that KLK10 and KLK11 are coordinately expressed at the mRNA and protein level in ovarian cancer, which may be ascribed to hormone-related regulatory mechanisms. Interestingly, their expression was also reported to be modulated by androgen and estrogen in breast cancer cells (Luo et al., 2000; Paliouras and Diamandis, 2007, 2008). Thus, it may be tempting to hypothesize KLK10 and KLK11 may be also coordinately expressed in a steroid hormone-dependent manner in breast cancer. In the present breast cancer-related project, KLK10 mRNA expression was quantified in both triple-negative breast cancer (TNBC) and hormone receptor-positive breast cancer (HRPBC) samples applying the newly established qPCR assay. Again, my colleague X. Geng (pers. comm.) determined KLK11 mRNA expression levels in the identical cohorts. A pronounced, positive correlation between KLK10 and KLK11 was observed in both the TNBC cohort ($r_s = 0.724$) and HRPBC cohort ($r_s = 0.766$). In box plot analysis, high KLK10 mRNA levels were significantly associated with elevated KLK11 expression in TNBC ($p < 0.001$; **Figure 20A**) and HRPBC ($p < 0.001$; **Figure 20B**), illuminating KLK10 and KLK11 were also co-expressed in these subtypes of breast cancer.

Since co-expression of KLK10 and KLK11 has been proposed to be regulated in a steroid hormone-dependent manner, it is not surprising that coordinate expression was observed in hormone receptor-positive breast cancer (HRPBC) samples. Interestingly, however, coordinate expression was also observed in TNBC, which is characterized with the lack of estrogen receptor (ER) and progesterone receptor (PR) in tumor cells, indicating that neither estrogen nor progesterone are the cause for their coordinate expression in TNBC. Of note, androgen was previously reported to prominently upregulate KLK10 and KLK11 expression as well through direct and indirect mechanisms in breast cancer (Luo et al., 2000, 2003; Paliouras and Diamandis, 2007). Applying the so-called ChIP (chromatin immunoprecipitation assay) method, androgen receptor (AR) binding regions were identified within the promoters of KLK10 (-2,000 to -2,500 bp and +1,000 to +1,500 bp) and KLK11 (-1,000 to -1,500 bp and +1 to +500 bp), possibly representing androgen response elements (AREs). Indeed, T47D breast cancer cells displayed increased KLK10 and KLK11 expression when subjected to androgen alone (Paliouras and Diamandis, 2008). Regarding the indirect modulatory effects of androgens, co-stimulation with androgens and estrogens led to a far more increased KLK10 and KLK11 expression than the additive impact of the respective hormone stimulation. Further studies revealed that androgens enhanced Akt-dependent ER activity through membrane-bound AR, thereby synergistically elevating the estrogen-induced KLK10 and KLK11 expression (Paliouras and Diamandis, 2008).

Although expression of numerous KLKs is responsive to estrogens in breast cancer cell lines, estrogens are not essential for the modulation of KLK expression in the human body (Lawrence et al., 2010). ER-negative breast cancer cells, for instance MDA-MB-231, MDA-MB-468, and BT-20 express KLK5-11 (Paliouras and Diamandis, 2007; Shaw and Diamandis, 2008). Moreover, several studies reported no correlation between ER status and KLK9, 11, and 15 expressions in breast cancer tissues (Yousef et al., 2002, 2003; Sano et al., 2007). In case of KLK10, it is more frequently expressed in ER-negative breast cancer tissues rather than ER-positive cases; elevated KLK10 protein levels were found to be significantly associated with tamoxifen resistance (Luo et al., 2002). In line with these previous finding, we detected higher KLK10 mRNA levels in ER-negative TNBC samples than ER-positive HRPBC samples ($p < 0.001$; **Figure 19**). Importantly, also, microarray data from 586 breast cancer specimens revealed the same trend that estrogen-responsive KLKs including KLK10 were higher expressed in ER-negative versus ER-positive breast cancer samples (Lawrence et al.,

2010). Furthermore, it was also reported that KLK10 overexpression was more often observed in “basal-like” (ER-negative) breast cancer tissues than ER-positive “luminal” cases (Richardson et al., 2006). Consistent with the expression pattern in tumor specimens, KLK10 were also more highly expressed in “basal-like” cell lines, compared to “luminal” cell lines (Neve et al., 2006). Taken together, co-expression of KLK10 and KLK11 in TNBC may be regulated in an androgen-dependent manner.

KLK10 was reported to be highly expressed in normal breast tissue, with downregulation in cancerous breast tissues (Dhar et al., 2001; Yousef et al., 2004). Similarly, the current study showed most of the TNBC and HRPBC specimens displayed rather low KLK10 mRNA expression. The reduction of KLK10 in breast cancer is supposed to be due to CpG island hypermethylation (Pasic et al., 2012). Biocomputational and *in silico* analyses indicate that the KLK10 sequence contains 4 CpG islands, of which the largest one is located within the third exon (Pampalakis and Sotiropoulou, 2006). A robust association of exon 3 hypermethylation with loss of KLK10 expression was indeed observed in breast cancer tissues and cell lines, implicating that DNA methylation can modulate transcription of KLK10 (Li et al., 2001). When treated with 5-aza-2′-deoxycytidine, a cytosine analog that reduces DNA methylation, KLK10-negative breast cancer cell lines, like MDA-MB-231 and MDA-MB-435, were found to regain KLK10 expression, suggesting methylation is responsible for the loss of KLK10 expression in these cells (Li et al., 2001; Sidiropoulos et al., 2005). In line with the proposed relationship of KLK10 expression and methylation in cell lines, Kioulafa et al. (Kioulafa et al., 2009) revealed that whereas KLK10 was not methylated in normal breast tissues, half of the cancerous breast specimens were detected with KLK10 gene methylation.

Additionally, KLK10 gene methylation in tumor tissue has been described as an prognostic factor not only for breast cancer (Kioulafa et al., 2009), but also for other types of cancer (Huang et al., 2007; Lu et al., 2009; Zhang et al., 2010, 2011). Thus, KLK10 mRNA, as the downstream factor of gene methylation, could also represent predictive power for the outcome of cancer patients. In the current study, we firstly evaluated the potential predictive power of KLK10 mRNA in triple-negative breast cancer, demonstrating that elevated KLK10 mRNA levels were significantly associated with shortened DFS and turned out to represent an independent predictive marker in TNBC. A similar trend was previously also reported by Wang et al. (Wang et al., 2016) investigating the mRNA data of 434 HER2-positive breast cancer patients from the

TCGA database, illustrating that high KLK10 expression was significantly associated with poor prognosis in this breast cancer subset. The observation was further supported by KLK10 mRNA expression profiling, comparing herceptin-responsive versus herceptin-resistant BT474 breast cancer cells. Here, enhanced KLK10 expression was the leading cause contributing to the herceptin resistance. After depletion of KLK10 by siRNA treatment in herceptin-resistant cells, herceptin successfully induced G1 arrest. Thus, KLK10 represents a therapeutic target of reversing herceptin resistance (Wang et al., 2016). Furthermore, Luo et al. (Luo et al., 2002) determined KLK10 protein levels in cytosolic tumor tissue extracts from 242 patients receiving tamoxifen as first-line treatment for advanced disease and observed an association of high KLK10 protein levels with shortened progression-free and post-relapse overall survival. Our data show that in TNBC, the breast cancer subtype with worst prognosis, KLK10 mRNA levels are significantly higher than in HRPBC displaying relatively favorable prognosis. Altogether, more and more evidence is evolving regarding KLK10 as an unfavorable prognostic marker in breast cancer.

It seems contradictory that KLK10 expression is, on one hand, downregulated in cancerous breast tissues, but, on the other, represents an indicator of unfavorable prognosis in breast cancer. Actually, in breast cancer, down-regulation is frequently observed among KLK family, like KLK5, KLK7, KLK8, and KLK14 (**Table 3)**. In fact, these KLKs described to display reduced expression in cancerous breast tissues, still serve as unfavorable predictive markers for breast cancer patients (Yousef et al., 2002, 2002; Talieri et al., 2004; Michaelidou et al., 2015). Of note, besides KLKs, many other genes contributing to cancer pathways are frequently characterized by lower expression in cancerous than normal breast tissues (Schummer et al., 2010).

There are several mechanisms which may explain why KLK10 favors tumorigenicity. KLK10 silencing in Eca-109 esophagus cancer cells was found to induce S-phase arrest, accompanied with repressed cyclin A and CDK2 activity, resulting in suppressed proliferation of the tumor cells (Li et al., 2015). In OVCAR-3 ovarian cancer cells, miRNA-mediated KLK10 downregulation caused inhibition of tumor cell proliferation as well (White et al., 2010). KLK10, being a serine protease, is commonly hypothesized to be able to facilitate tumor metastasis by degradation of extracellular matrix proteins (Petraki et al., 2012). Besides, KLK10 was reported to lower the cisplatin-induced apoptosis in esophageal cancer cells, suggesting that KLK10 represents a potential therapeutic target for reversing cisplatin resistance (Li et al., 2015). Last but not least,

Tang and co-workers (Tang et al., 2017) established herceptin-resistant gastric cancer cell line SGC7901-TR and BGC-823-TR and found that KLK10 expression was significantly increased in these herceptin-resistant cells. Also, in these established herceptin-resistant cells, suppressing KLK10 expression or inhibiting PI3K/AKT pathway could diminish the herceptin resistance, while overexpression displayed the reverse effects, demonstrating KLK10 favors herceptin resistance through the PI3K/AKT signaling pathway.

5.4 KLK10 and KLK11 are coordinately expressed and displayed distinct and convert effects in ovarian and breast cancer

As demonstrated above, KLK10 and KLK11 are coordinately expressed in advanced high-grade serous ovarian cancer as well as in triple-negative breast cancer. This raised the possibility that KLK10 and KLK11 might be involved in synergetic mechanisms affecting tumor pathogenesis. Notably, the combination of KLK10 and KLK11 expression levels (*e.g.* KLK10 low and/or KLK11 low group versus KLK10 high and KLK11 high group in ovarian cancer) predicted patient prognosis with better accuracy than KLK10 or KLK11 alone in both advanced high-grade serous ovarian cancer (**Figure 17**) and TNBC (**Figure 22**). Again, this supported that they are both involved in tumorigenicity and jointly perform the impact in these tumor entities. Similarly, prior study from our lab also reported that KLK6 alone displayed predictive power for OS in advanced high-grade serous ovarian cancer, whereas the combination of KLK6 and KLK8 could aid to identify patients with better OS and PFS (Ahmed et al., 2016). All these findings may indicate that KLKs are implicated in KLK cascades contributing to tumor-relevant processes.

Importantly, in ovarian versus breast cancer, KLK10 and KLK11 display distinct and contrary effects on prognosis in ovarian and breast cancer, which has been also observed in case of other KLKs like KLK8, 14, and 15 (**Table 2** and **3**). Substrates of these proteases may substantially differ in tumor tissues depending on cancer (sub-) type, which may explain that the given protease could elicit a tumor-supporting role in one (sub-) type of cancer or a tumor-suppressing role in another one. Therefore, the prognostic impact of biomarkers should be evaluated and employed only in the context of homogenous subgroups/types of cancer rather than in mixed cohorts.

In advanced high-grade serous ovarian cancer and triple negative breast cancer, KLK10 shows the potential to aid clinical therapy decisions by the identification of patients

with unfavorable outcome. Further studies to identify the mechanisms how KLK10 influences distinct tumor-relevant processes may result in an improvement of anti-cancer strategies, from which patients afflicted with these diseases will benefit.

6 Summary

Several members of the KLK family have previously been reported to be dysregulated in different types of malignancies and to be involved in the modulation of tumor-relevant processes. Furthermore, many members of the KLK family were shown to represent diagnostic and prognostic markers in ovarian and breast cancer. Nevertheless, the impact of some KLKs on prognosis in a given tumor entity was often described to be paradoxical, which may be attributable to rather heterogeneous patient cohorts previously analyzed. Therefore, the current project aimed at investigating tumor-relevant KLK expression in more homogenous ovarian (advanced high-grade serous ovarian cancer) and breast (triple-negative breast cancer) cancer cohorts and correlating the expression levels with clinical outcome.

In advanced high-grade serous ovarian cancer, qPCR and immunohistochemistry were carried out to analyze expression of KLK9 and/or KLK10. KLK9 and KLK10 mRNA expression was quantified in 139 cases of advanced high-grade serous ovarian cancer specimens. Together with available KLK11 and KLK15 mRNA data in the identical cohort, pronounced correlations were found between KLK10 and KLK11 mRNA (r_s = 0.647, $p < 0.001$) as well as KLK9 and KLK15 mRNA (r_s = 0.716, $p < 0.001$). Univariate Cox regression analysis demonstrated that KLK9 and KLK10 mRNA levels did not show any predictive power in this tumor entity, which was further confirmed by *in silico* analysis based on the publicly available mRNA expression profiles from The Cancer Genome Atlas.

Regarding immunohistochemistry, a quantitative and automated scoring system based on ImageJ plus the IHC Profiler plugin was applied for evaluating immunohistochemical staining intensity. With the assistance of this scoring system, we assessed KLK10 protein expression in tissue microarrays including 159 tumor specimens of advanced high-grade serous ovarian cancer. KLK10 protein expression was significantly correlated with the mRNA expression (r_s = 0.453, $p < 0.001$). KLK10 protein expression was also correlated with KLK11 at protein level (r_s = 0.403, p = 0.001), strongly supporting the notion that KLK10 and KLK11 are coordinately expressed in this tumor entity. Patients with elevated KLK10 protein levels displayed prolonged overall survival (hazard ratio [HR] = 0.57, p = 0.020), but did not show any statistically significant difference in progression-free survival (PFS). In addition, applying dichotomization by KLK10+KLK11 (KLK10 low and/or KLK11 low versus

KLK10 high and KLK11 high) increased the predictive power for OS (HR = 0.41, $p < 0.001$), whereas it remained not associated with PFS. In multivariate Cox regression analysis, KLK10 and KLK10+KLK11 both turned out independent favorable predictors of OS (KLK10, HR = 0.59, p = 0.043; KLK10+KLK11, HR = 0.41, p = 0.001), when adjusted for age, residual tumor mass, and ascitic fluid volume.

In addition, we selected a cohort including 127 patients afflicted with triple-negative breast cancer (TNBC) and assessed KLK10 mRNA expression in tumor tissues by quantitative PCR. Tumors from the TNBC subgroup are characterized by the lack of estrogen receptor (ER) and progesterone receptor (PR) expression, and by normal or reduced levels of human epidermal growth factor receptor type 2 (HER2). Since the patients cannot be treated with endocrine therapy or therapies targeted to HER2, they display a worse outcome compared to other breast cancer subtypes like hormone receptor-positive breast cancer (HRPBC: ER and PR positive, HER2 negative). The latter is associated with a relatively favorable prognosis. We determined KLK10 expression in 27 specimens of HRPBC, showing that KLK10 mRNA expression was significantly higher in TNBC than HPRBC ($p < 0.001$), which may point to a negative impact of KLK10 expression on prognosis in breast cancer. In addition to the findings in advanced high-grade serous ovarian cancer, remarkable associations between KLK10 and KLK11 mRNA were also observed in TNBC ($r_s = 0.724$, $P < 0.001$) and HRPBC ($r_s = 0.766$, $p < 0.001$), suggesting that a coordinated expression also exists in these subtypes of breast cancer. Univariate Cox regression analysis showed that elevated KLK10 mRNA levels are significantly related with shortened disease-free survival (HR = 1.81, p = 0.044). Moreover, compared to KLK10 alone, combined KLK10+KLK11 increased the predictive power for DFS (HR = 1.98, p = 0.029). In multivariable Cox analysis, both KLK10 and KLK10+KLK11, apart from age, remained an independent predictive marker for disease-free survival (KLK10, HR = 2.51, p = 0.005; KLK10+KLK11, HR = 2.35, p = 0.010).

In conclusion, for the first time, the clinical relevance of KLK10 was investigated in homogenous ovarian cancer and breast cancer cohorts, illustrating KLK10 can serve as an independent prognostic marker in these tumor types. In triple-negative breast cancer, elevated KLK10 levels are associated with unfavorable prognosis, which contrasts the observed association of KLK10 with favorable outcome in advanced high-grade serous ovarian cancer. Thus, in future, studies to identify the tumor-relevant pathways in which KLK10 is implicated may lead to an improvement of anti-cancer strategies.

7 Acknowledgment

First, I would like to offer my honest gratefulness to my supervisor, Prof. Dr. rer. nat. Viktor Magdolen. Until now, I still remember the feeling of great happiness when the invitation letter to join his laboratory arrived. Before that, I was confused about the future and then he provided me an amazing opportunity of better knowing science and world. Moreover, thanks to his guidance and counseling, I never felt frustrated and hesitated on my doctoral road. Moreover, he was always willing to offer help no matter in life or science. I really appreciate his help and encouragement of my academic career.

I also would like to thank Prof. Dr. Manfred Schmitt for introducing me to my supervisor. He always encouraged me to follow my dream of studying abroad.

I would like to offer my gratitude to Dr. Rudolf Napieralski and Dr. Sandra Diersch. Due to their technical and statistical guidance, we figured out many problems during the qPCR experiments and data analyses, conducting my research smoothly.

I acknowledge Sabine Creutzburg, Anke Benge and Daniela Hellmann for their technical support. Their great experience concerning WB and IHC experiments really helped me a lot. Also, I would like to thanks Elisabeth Schueren for her help in cell culture; Dr. Tobias Dreyer for preparation of the patient data list and doctoral thesis correction; Dr. Natalie Falkenberg for sharing transfected cancer cell lines; Dr. Christof Seidl for his suggestions on my doctoral thesis and the presentations at international meeting and doctoral thesis correction; PD Dr. med. Julia Dorn for her co-leadership of the studies on the clinical relevance of KLKs, together with Prof. Viktor Magdolen, her help in paper correction, and clinical data preparation.

I am really lucky to be with so many nice colleagues and friends, who gave me various support and encouragement in work and life, especially, Xiaocong Geng, Weiwei Gong, Shengjia Wang, Nancy Ahmed, Ping Wang, Shuo Zhao, Sarah Preis, Larissa Dettmar, and Christoph Stange.

Last but not least, my sincerest gratefulness is for my parents and my wife Weiwei Gong for their unlimited love and support in my life. Their belief and expectation on me is always my motivation for being better in myself and career, encouraging me to strive to overcome any difficulties.

8 List of publications

Thesis-related publications:

1. Geng X*, Liu Y*, Diersch S, Kotzsch M, Weichert W, Kiechle1 M, Magdolen V, Dorn J (2017). Clinical relevance of kallikrein-related peptidase 9, 10, 11, and 15 mRNA expression in advanced high-grade serous ovarian cancer. PLoS One 12: e0186847. * contributed equally

2. Geng X*, Liu Y*, Dreyer T, Bronger H, Drecoll E, Magdolen V, Dorn J (2018) Elevated tumor tissue protein expression levels of kallikrein-related peptidases KLK10 and KLK11 are associated with a better prognosis in advanced high-grade serous ovarian cancer patients. Am J Cancer Res8:1856-64. * contributed equally

Oral presentations at international meetings:

1. Liu Y, Geng X, Diersch S, Kotzsch M, Weichert W, Kiechle1 M, Magdolen V, Dorn J. Clinical relevance of kallikrein-related peptidase 9, 10, 11, and 15 mRNA expression in advanced high-grade serous ovarian cancer. 7th International Symposium on Kallikreins and kallikrein-related peptidases. 2017, Tours, France. Oral presentation.

2. Liu Y, Geng X, Preis S, Kiechle M, Magdolen V, Dorn J. Quantitative assessment of KLK10 and KLK11 mRNA expression in triple-negative breast cancer (TNBC): KLK10 is a novel independent prognostic marker for disease-free survival in this major breast cancer subtype. 34th Winter School on Proteases and Inhibitors. 2017, Tiers, Italy. Oral presentation.

Further KLK-related publications:

Gong W*, Liu Y*, Seidl C, Diamandis EP, Kiechle M, Drecoll E, Kotzsch M, Dorn J, Magdolen V (2018) Quantitative assessment and clinical relevance of kallikrein-related peptidase 5 mRNA expression in advanced high-grade serous ovarian cancer. Submitted for publication in BMC Cancer.

Further publications:

1. Bao X, Zhao S, Liu T, Liu Y, Liu Y, Yang X. Overexpression of PRMT5 promotes tumor cell growth and is associated with poor disease prognosis in epithelial ovarian cancer. J Histochem Cytochem. 2013. 61(3): 206-17.

2. Liu T, Liu Y, Bao X, Tian J, Liu Y, Yang X. Overexpression of TROP2 predicts poor prognosis of patients with cervical cancer and promotes the proliferation and invasion of cervical cancer cells by regulating ERK signaling pathway. PLoS One. 2013. 8(9): e75864.

3. Liu Y, Liu T, Bao X, He M, Li L, Yang X. Increased EZH2 expression is associated with proliferation and progression of cervical cancer and indicates a poor prognosis. Int J Gynecol Pathol. 2014. 33(3): 218-24.

9 Appendix

9.1 Ovarian cancer FIGO stage description from the Féderation Internationale de Gynécologie et d'Obstétrique (FIGO)

Stage		Description
I		Tumor confined to ovaries or fallopian tube(s).
	IA	Tumor limited to one ovary (capsule intact) or fallopian tube; no tumor on ovarian or fallopian tube surface; no malignant cells in the ascites or peritoneal washings.
	IB	Tumor limited to both ovaries (capsules intact) or fallopian tubes; no tumor on ovarian or fallopian tube surface; no malignant cells in the ascites or peritoneal washings.
	IC	Tumor limited to one or both ovaries or fallopian tubes, with any of the following:
	IC1	Surgical spill intraoperatively.
	IC2	Capsule ruptured before surgery or tumor on ovarian or fallopian tube surface.
	IC3	Malignant cells in the ascites or peritoneal washings.
II		Tumor involves one or both ovaries with pelvic extension (below the pelvic brim) or primary peritoneal cancer
	IIA	Extension and/or implant on uterus and/or Fallopian tubes
	IIB	Extension to other pelvic intraperitoneal tissues
III		Tumor involves one or both ovaries, or fallopian tubes, or primary peritoneal cancer, with cytologically or histologically confirmed spread to the peritoneum outside of the pelvis and/or metastasis to the retroperitoneal lymph nodes.
	IIIA	Metastasis to the retroperitoneal lymph nodes with or without microscopic peritoneal involvement beyond the pelvis.
	IIIA(i)	Positive retroperitoneal lymph nodes only (cytologically or histologically proven).
	IIIA(ii)	Metastasis >10 mm in greatest dimension.
	IIIA2	Microscopic extrapelvic (above the pelvic brim) peritoneal involvement with or without positive retroperitoneal lymph nodes.
	IIIB	Macroscopic peritoneal metastases beyond the pelvic brim ≤2 cm in greatest dimension, with or without metastasis to the retroperitoneal lymph nodes.
	IIIC	Macroscopic peritoneal metastases beyond the pelvic brim >2 cm in greatest dimension, with or without metastases to the retroperitoneal nodes.
IV		Distant metastasis excluding peritoneal metastases
	IVA	Pleural effusion with positive cytology
	IVB	Metastases to extra-abdominal organs (including inguinal lymph nodes and lymph nodes outside of the abdominal cavity).

Adapted from the Féderation Internationale de Gynécologie et d'Obstétrique (Mutch and Prat, 2014).

9.2 Ovarian cancer grading system

Grade	Description
GX:	Grade cannot be assessed (undetermined grade)
G1	Well differentiated (low grade)
G2	Moderately differentiated (intermediate grade)
G3	Poorly differentiated (high grade)
G4	Undifferentiated (high grade)

Adapted from (Edge and Compton, 2010).

10 Abbreviations

ACPT	testicular acid phosphatase
Acry / Bis	acrylamide-bisacrylamide
APS	ammonium persulfate
AREs	androgen response elements
CA-125	serum Cancer Antigen 125
cDNA	complementary deoxyribonucleic acid
CI	confidence interval
CMAs	cell microarrays
Ct	cycle threshold
D	aspartic
DAB	3,3'-diaminobenzidine
DFS	disease-free survival
DMEM	Dulbecco's Modified Eagle Medium
DMSO	dimethylsulfoxid
DNA	desoxyriunicleic acid
dNTP	deoxyribonucleoside triphosphate
E	efficiency
ECM	extracellular matrix
EDTA	ethylene diamine tretraccetic acid
EGF	epidermal growth factor
EGFR	epidermal growth factor receptor
EMT	epithelial-mesenchymal transition
EOC	epithelial ovarian cancer
ER	estrogen receptor
FBS	fetal bovine serum
FFPE	formalin-fixed, paraffin-embedded
FGF	fibroblast growth factor
FIGO	Féderation Internationale de Gynécologie et d'Obstétrique
H	histidine
h	hour
H&E	hematoxylin-eosin
HEPES	4-(2-hydroxyethyl)-1-piperazineethanesulfonic acid
HER2	the human epidermal growth factor receptor 2
HPRT	hypoxanthine-guaninephosphoribosyltransferase
HR	hazard ratio
HRP	horseradish peroxidase
HRPBC	hormone receptor-positive breast cancer
IGF	insulin-like growth factor
IGFBPs	insulin-like growth factor binding proteins
IHC	immunohistochemistry
kDa	kilo Dalton

KLK	kallikrein-related peptidase
MAPK	mitogen-activated protein kinases
min	minute
MMPs	matrix metalloproteinases
OS	overall survival
PAA	polyacrylamide
PARs	protease-activated receptors
PFS	progression-free survival
PR	progesterone receptor
PSA	prostate-specific antigen
PVDF	polyvinylidene difluoride
qPCR	quantity polymerase chain reaction
RNA	ribonucleic acid
RT	room temperature
S	serine
SDS	sodium dodecyl sulfate
SIGLEC9	sialic acid-binding Ig-like lectin 9
TCGA	The Cancer Genome Atlas
TEMED	tetramethylethylenediamine
TGF-ß	transforming growth factor beta
TMA	tissue microarrays
TNBC	triple-negative breast cancer
tPA	tissue-type plasminogen activator
uPA	urokinase plasminogen activator
VEGF	vascular endothelial growth factor

11 References

Adib TR, Henderson S, Perrett C, Hewitt D, Bourmpoulia D, Ledermann J, Boshoff C. 2004. Predicting biomarkers for ovarian cancer using gene-expression microarrays. Br J Cancer. 90(3): 686-92.

Ahmed N, Dorn J, Napieralski R, Drecoll E, Kotzsch M, Goettig P, Zein E, Avril S, Kiechle M, Diamandis EP, Schmitt M, Magdolen V. 2016. Clinical relevance of kallikrein-related peptidase 6 (KLK6) and 8 (KLK8) mRNA expression in advanced serous ovarian cancer. Biol Chem. 397(12): 1265-1276.

Alexopoulou DK, Papadopoulos IN, Scorilas A. 2013. Clinical significance of kallikrein-related peptidase (KLK10) mRNA expression in colorectal cancer. Clin Biochem. 46(15): 1453-61.

Au KK, Josahkian JA, Francis JA, Squire JA, Koti M. 2015. Current state of biomarkers in ovarian cancer prognosis. Future Oncol. 11(23): 3187-95.

Bast RC. 2011. Molecular approaches to personalizing management of ovarian cancer. Ann Oncol. 22 Suppl 8: viii5-viii15.

Bayés A, Tsetsenis T, Ventura S, Vendrell J, Aviles FX, Sotiropoulou G. 2004. Human kallikrein 6 activity is regulated via an autoproteolytic mechanism of activation/inactivation. Biol Chem. 385(6): 517-24.

Black MH, Diamandis EP. 2000. The diagnostic and prognostic utility of prostate-specific antigen for diseases of the breast. Breast Cancer Res Treat. 59(1): 1-14.

Blazquez-Medela AM, Garcia-Sanchez O, Quiros Y, Blanco-Gozalo V, Prieto-Garcia L, Sancho-Martinez SM, Romero M, Duarte JM, Lopez-Hernandez FJ, Lopez-Novoa JM, Martinez-Salgado C. 2015. Increased Klk9 Urinary Excretion Is Associated to Hypertension-Induced Cardiovascular Damage and Renal Alterations. Medicine (Baltimore). 94(41): e1617.

Bonzanini M, Morelli L, Bonandini EM, Leonardi E, Pertile R, Dalla Palma P. 2012. Cytologic features of triple-negative breast carcinoma. Cancer Cytopathol. 120(6): 401-9.

Borgono CA, Diamandis EP. 2004. The emerging roles of human tissue kallikreins in cancer. Nat Rev Cancer. 4(11): 876-90.

Borgono CA, Michael IP, Diamandis EP. 2004. Human tissue kallikreins: physiologic roles and

applications in cancer. Mol Cancer Res. 2(5): 257-80.

Borgoño CA, Fracchioli S, Yousef GM, Rigault de la Longrais IA, Luo LY, Soosaipillai A, Puopolo M, Grass L, Scorilas A, Diamandis EP, Katsaros D. 2003. Favorable prognostic value of tissue human kallikrein 11 (hK11) in patients with ovarian carcinoma. Int J Cancer. 106(4): 605-10.

Borgoño CA, Grass L, Soosaipillai A, Yousef GM, Petraki CD, Howarth DH, Fracchioli S, Katsaros D, Diamandis EP. 2003. Human kallikrein 14: a new potential biomarker for ovarian and breast cancer. Cancer Res. 63(24): 9032-41.

Borgoño CA, Kishi T, Scorilas A, Harbeck N, Dorn J, Schmalfeldt B, Schmitt M, Diamandis EP. 2006. Human kallikrein 8 protein is a favorable prognostic marker in ovarian cancer. Clin Cancer Res. 12(5): 1487-93.

Bustin SA, & Nolan T. (2013). Analysis of mRNA expression by real-time PCR. Real-time PCR: advanced technologies and applications. Caister Academic Press, Norfolk, United Kingdom, 51-88.

Cameron D, Casey M, Oliva C, Newstat B, Imwalle B, Geyer CE. 2010. Lapatinib plus capecitabine in women with HER-2-positive advanced breast cancer: final survival analysis of a phase III randomized trial. Oncologist. 15(9): 924-34.

Cedolini C, Bertozzi S, Londero AP, Bernardi S, Seriau L, Concina S, Cattin F, Risaliti A. 2014. Type of breast cancer diagnosis, screening, and survival. Clin Breast Cancer. 14(4): 235-40.

Chang A, Yousef GM, Scorilas A, Grass L, Sismondi P, Ponzone R, Diamandis EP. 2002. Human kallikrein gene 13 (KLK13) expression by quantitative RT-PCR: an independent indicator of favourable prognosis in breast cancer. Br J Cancer. 86(9): 1457-64.

Chatterjee S, Malhotra R, Varghese F, Bukhari AB, Patil A, Budrukkar A, Parmar V, Gupta S, De A. 2013. Quantitative immunohistochemical analysis reveals association between sodium iodide symporter and estrogen receptor expression in breast cancer. PLoS One. 8(1): e54055.

Chou RH, Lin SC, Wen HC, Wu CW, Chang WS. 2011. Epigenetic activation of human kallikrein 13 enhances malignancy of lung adenocarcinoma by promoting N-cadherin expression and laminin degradation. Biochem Biophys Res Commun. 409(3): 442-7.

Clements J, Hooper J, Dong Y, Harvey T. 2001. The expanded human kallikrein (KLK) gene family: genomic organisation, tissue-specific expression and potential functions. Biol Chem.

382(1): 5-14.

Dhar S, Bhargava R, Yunes M, Li B, Goyal J, Naber SP, Wazer DE, Band V. 2001. Analysis of normal epithelial cell specific-1 (NES1)/kallikrein 10 mRNA expression by in situ hybridization, a novel marker for breast cancer. Clin Cancer Res. 7(11): 3393-8.

Diamandis EP, Borgoño CA, Scorilas A, Harbeck N, Dorn J, Schmitt M. 2004. Human kallikrein 11: an indicator of favorable prognosis in ovarian cancer patients. Clin Biochem. 37(9): 823-9.

Diamandis EP, Borgoño CA, Scorilas A, Yousef GM, Harbeck N, Dorn J, Schmalfeldt B, Schmitt M. 2003. Immunofluorometric quantification of human kallikrein 5 expression in ovarian cancer cytosols and its association with unfavorable patient prognosis. Tumour Biol. 24(6): 299-309.

Diamandis EP, Okui A, Mitsui S, Luo LY, Soosaipillai A, Grass L, Nakamura T, Howarth DJ, Yamaguchi N. 2002. Human kallikrein 11: a new biomarker of prostate and ovarian carcinoma. Cancer Res. 62(1): 295-300.

Diamandis EP, Yousef GM, Soosaipillai AR, Bunting P. 2000. Human kallikrein 6 (zyme/protease M/neurosin): a new serum biomarker of ovarian carcinoma. Clin Biochem. 33(7): 579-83.

Dominek P, Campagnolo P, H-Zadeh M, Kränkel N, Chilosi M, Sharman JA, Caporali A, Mangialardi G, Spinetti G, Emanueli C, Pignatelli M, Madeddu P. 2010. Role of human tissue kallikrein in gastrointestinal stromal tumour invasion. Br J Cancer. 103(9): 1422-31.

Dong Y, Kaushal A, Brattsand M, Nicklin J, Clements JA. 2003. Differential splicing of KLK5 and KLK7 in epithelial ovarian cancer produces novel variants with potential as cancer biomarkers. Clin Cancer Res. 9(5): 1710-20.

Dong Y, Kaushal A, Bui L, Chu S, Fuller PJ, Nicklin J, Samaratunga H, Clements JA. 2001. Human kallikrein 4 (KLK4) is highly expressed in serous ovarian carcinomas. Clin Cancer Res. 7(8): 2363-71.

Dorn J, Beaufort N, Schmitt M, Diamandis EP, Goettig P, Magdolen V. 2014. Function and clinical relevance of kallikrein-related peptidases and other serine proteases in gynecological cancers. Crit Rev Clin Lab Sci. 51(2): 63-84.

Dorn J, Bronger H, Kates R, Slotta-Huspenina J, Schmalfeldt B, Kiechle M, Diamandis EP,

Soosaipillai A, Schmitt M, Harbeck N. 2015. OVSCORE - a validated score to identify ovarian cancer patients not suitable for primary surgery. Oncol Lett. 9(1): 418-424.

Dorn J, Schmitt M, Kates R, Schmalfeldt B, Kiechle M, Scorilas A, Diamandis EP, Harbeck N. 2007. Primary tumor levels of human tissue kallikreins affect surgical success and survival in ovarian cancer patients. Clin Cancer Res. 13(6): 1742-8.

Drucker KL, Gianinni C, Decker PA, Diamandis EP, Scarisbrick IA. 2015. Prognostic significance of multiple kallikreins in high-grade astrocytoma. BMC Cancer. 15: 565.

Edge SB, Compton CC. 2010. The American Joint Committee on Cancer: the 7th edition of the AJCC cancer staging manual and the future of TNM. Ann Surg Oncol. 17(6): 1471-4.

El Sherbini MA, Sallam MM, Shaban EA, El-Shalakany AH. 2011. Diagnostic value of serum kallikrein-related peptidases 6 and 10 versus CA125 in ovarian cancer. Int J Gynecol Cancer. 21(4): 625-32.

Elliott MB, Irwin DM, Diamandis EP. 2006. In silico identification and Bayesian phylogenetic analysis of multiple new mammalian kallikrein gene families. Genomics. 88(5): 591-9.

Ewan King L, Li X, Cheikh Saad Bouh K, Pedneault M, Chu CW. 2007. Human kallikrein 10 ELISA development and validation in breast cancer sera. Clin Biochem. 40(13-14): 1057-62.

Feng B, Xu WB, Zheng MH, Ma JJ, Cai Q, Zhang Y, Ji J, Lu AG, Qu Y, Li JW, Wang ML, Hu WG, Liu BY, Zhu ZG. 2006. Clinical significance of human kallikrein 10 gene expression in colorectal cancer and gastric cancer. J Gastroenterol Hepatol. 21(10): 1596-603.

Ferlay J, Soerjomataram I, Dikshit R, Eser S, Mathers C, Rebelo M, Parkin DM, Forman D, Bray F. 2015. Cancer incidence and mortality worldwide: sources, methods and major patterns in GLOBOCAN 2012. Int J Cancer. 136(5): E359-86.

Ferlay J, Steliarova-Foucher E, Lortet-Tieulent J, Rosso S, Coebergh JW, Comber H, Forman D, Bray F. 2013. Cancer incidence and mortality patterns in Europe: estimates for 40 countries in 2012. Eur J Cancer. 49(6): 1374-403.

Filippou PS, Farkona S, Brinc D, Yu Y, Prassas I, Diamandis EP. 2017. Biochemical and Functional Characterization of the Human Tissue Kallikrein 9. Biochemical Journal. 474(14): 2417-2433.

Foulkes WD, Smith IE, Reis-Filho JS. 2010. Triple-negative breast cancer. N Engl J Med.

363(20): 1938-48.

Geng X, Liu Y, Diersch S, Kotzsch M, Grill S, Weichert W, Kiechle M, Magdolen V, Dorn J. 2017. Clinical relevance of kallikrein-related peptidase 9, 10, 11, and 15 mRNA expression in advanced high-grade serous ovarian cancer. PLoS One. 12(11): e0186847.

Geng X, Liu Y, Dreyer T, Bronger H, Drecoll E, Magdolen V, Dorn J. 2018. Elevated tumor tissue protein expression levels of kallikrein-related peptidases KLK10 and KLK11 are associated with a better prognosis in advanced high-grade serous ovarian cancer patients. Am J Cancer Res. 8(9): 1856.

Geyer FC, Marchio C, Reis-Filho JS. 2009. The role of molecular analysis in breast cancer. Pathology. 41(1): 77-88.

Giuliano AE, Hunt KK, Ballman KV, Beitsch PD, Whitworth PW, Blumencranz PW, Leitch AM, Saha S, McCall LM, Morrow M. 2011. Axillary dissection vs no axillary dissection in women with invasive breast cancer and sentinel node metastasis: a randomized clinical trial. JAMA. 305(6): 569-75.

Goettig P, Magdolen V, Brandstetter H. 2010. Natural and synthetic inhibitors of kallikrein-related peptidases (KLKs). Biochimie. 92(11): 1546-67.

Guo S, Skala W, Magdolen V, Brandstetter H, Goettig P. 2014. Sweetened kallikrein-related peptidases (KLKs): glycan trees as potential regulators of activation and activity. Biol Chem. 395(9): 959-76.

Gyorffy B, Lánczky A, Szállási Z. 2012. Implementing an online tool for genome-wide validation of survival-associated biomarkers in ovarian-cancer using microarray data from 1287 patients. Endocr Relat Cancer. 19(2): 197-208.

Harbeck N, Gnant M. 2017. Breast cancer. Lancet. 389(10074): 1134-1150.

Harter P, Sehouli J, Lorusso D, Reuss A, Vergote I, Marth C, Kim JW, Raspagliesi F, Lampe B, Landoni F, Meier W, Cibula D, Mustea A, Mahner S, Runnebaum IB, Schmalfeldt B, Burges A, Kimmig R, Wagner UAG, Du Bois A. 2017. LION: Lymphadenectomy in ovarian neoplasms—A prospective randomized AGO study group led gynecologic cancer intergroup trial. Journal of Clinical OncologyJournal of Clinical OncologyJCO. 35(15_suppl): 5500-5500.

Harvey TJ, Hooper JD, Myers SA, Stephenson SA, Ashworth LK, Clements JA. 2000. Tissue-specific expression patterns and fine mapping of the human kallikrein (KLK) locus on proximal

19q13.4. J Biol Chem. 275(48): 37397-406.

Hicks DG, Short SM, Prescott NL, Tarr SM, Coleman KA, Yoder BJ, Crowe JP, Choueiri TK, Dawson AE, Budd GT, Tubbs RR, Casey G, Weil RJ. 2006. Breast cancers with brain metastases are more likely to be estrogen receptor negative, express the basal cytokeratin CK5/6, and overexpress HER2 or EGFR. Am J Surg Pathol. 30(9): 1097-104.

Holzscheiter L, Biermann JC, Kotzsch M, Prezas P, Farthmann J, Baretton G, Luther T, Tjan-Heijnen VC, Talieri M, Schmitt M, Sweep FC, Span PN, Magdolen V. 2006. Quantitative reverse transcription-PCR assay for detection of mRNA encoding full-length human tissue kallikrein 7: prognostic relevance of KLK7 mRNA expression in breast cancer. Clin Chem. 52(6): 1070-9.

Howlader N, Noone AM, Krapcho M, Neyman N, Aminou R, Waldron W, Altekruse SF, Kosary CL, Ruhl J, Tatalovich Z, Cho H, Mariotto A, Eisner MP, Lewis DR, Chen HS, Feuer EJ, & Cronin KA. 2015. SEER Cancer Statistics Review, 1975-2011, National Cancer Institute; Bethesda [Web page] Retrieved from http://seer.cancer.gov/csr/1975_2009_pops09/.

Hu J, Lei H, Fei X, Liang S, Xu H, Qin D, Wang Y, Wu Y, Li B. 2015. NES1/KLK10 gene represses proliferation, enhances apoptosis and down-regulates glucose metabolism of PC3 prostate cancer cells. Sci Rep. 5: 17426.

Huang W, Zhong J, Wu LY, Yu LF, Tian XL, Zhang YF, Li B. 2007. Downregulation and CpG island hypermethylation of NES1/hK10 gene in the pathogenesis of human gastric cancer. Cancer Lett. 251(1): 78-85.

Shih IM, Kurman RJ. 2004. Ovarian tumorigenesis: a proposed model based on morphological and molecular genetic analysis. Am J Pathol. 164(5): 1511-8.

Jayson GC, Kohn EC, Kitchener HC, Ledermann JA. 2014. Ovarian cancer. Lancet. 384(9951): 1376-88.

Jelovac D, Armstrong DK. 2011. Recent progress in the diagnosis and treatment of ovarian cancer. CA Cancer J Clin. 61(3): 183-203.

Jiao X, Lu HJ, Zhai MM, Tan ZJ, Zhi HN, Liu XM, Liu CH, Zhang DP. 2013. Overexpression of kallikrein gene 10 is a biomarker for predicting poor prognosis in gastric cancer. World J Gastroenterol. 19(48): 9425-31.

Kalinska M, Meyer-Hoffert U, Kantyka T, Potempa J. 2016. Kallikreins - The melting pot of

activity and function. Biochimie. 122: 270-82.

Kapadia C, Chang A, Sotiropoulou G, Yousef GM, Grass L, Soosaipillai A, Xing X, Howarth DH, Diamandis EP. 2003. Human kallikrein 13: production and purification of recombinant protein and monoclonal and polyclonal antibodies, and development of a sensitive and specific immunofluorometric assay. Clin Chem. 49(1): 77-86.

Kassam F, Enright K, Dent R, Dranitsaris G, Myers J, Flynn C, Fralick M, Kumar R, Clemons M. 2009. Survival outcomes for patients with metastatic triple-negative breast cancer: implications for clinical practice and trial design. Clin Breast Cancer. 9(1): 29-33.

Kim JJ, Kim JT, Yoon HR, Kang MA, Kim JH, Lee YH, Kim JW, Lee SJ, Song EY, Myung PK, Lee HG. 2012. Upregulation and secretion of kallikrein-related peptidase 6 (KLK6) in gastric cancer. Tumour Biol. 33(3): 731-8.

Kim JT, Song EY, Chung KS, Kang MA, Kim JW, Kim SJ, Yeom YI, Kim JH, Kim KH, Lee HG. 2011. Up-regulation and clinical significance of serine protease kallikrein 6 in colon cancer. Cancer. 117(12): 2608-19.

Kioulafa M, Kaklamanis L, Stathopoulos E, Mavroudis D, Georgoulias V, Lianidou ES. 2009. Kallikrein 10 (KLK10) methylation as a novel prognostic biomarker in early breast cancer. Ann Oncol. 20(6): 1020-5.

Kipps E, Tan DS, Kaye SB. 2013. Meeting the challenge of ascites in ovarian cancer: new avenues for therapy and research. Nat Rev Cancer. 13(4): 273-82.

Kishi T, Grass L, Soosaipillai A, Scorilas A, Harbeck N, Schmalfeldt B, Dorn J, Mysliwiec M, Schmitt M, Diamandis EP. 2003. Human kallikrein 8, a novel biomarker for ovarian carcinoma. Cancer Res. 63(11): 2771-4.

Koh SC, Razvi K, Chan YH, Narasimhan K, Ilancheran A, Low JJ, Choolani M. 2011. The association with age, human tissue kallikreins 6 and 10 and hemostatic markers for survival outcome from epithelial ovarian cancer. Arch Gynecol Obstet. 284(1): 183-90.

Kolin DL, Sy K, Rotondo F, Bassily MN, Kovacs K, Brezden-Masley C, Streutker CJ, Yousef GM. 2016. Prognostic significance of human tissue kallikrein-related peptidases 11 and 15 in gastric cancer. Tumour Biol. 37(1): 437-46.

Kolin DL, Sy K, Rotondo F, Bassily MN, Kovacs K, Brezden-Masley C, Streutker CJ, Yousef GM. 2014. Prognostic significance of human tissue kallikrein-related peptidases 6 and 10 in

gastric cancer. Biol Chem. 395(9): 1087-93.

Kountourakis P, Psyrri A, Scorilas A, Camp R, Markakis S, Kowalski D, Diamandis EP, Dimopoulos MA. 2008. Prognostic value of kallikrein-related peptidase 6 protein expression levels in advanced ovarian cancer evaluated by automated quantitative analysis (AQUA). Cancer Sci. 99(11): 2224-9.

Kountourakis P, Psyrri A, Scorilas A, Markakis S, Kowalski D, Camp RL, Diamandis EP, Dimopoulos MA. 2009. Expression and prognostic significance of kallikrein-related peptidase 8 protein levels in advanced ovarian cancer by using automated quantitative analysis. Thromb Haemost. 101(3): 541-6.

Krishnamurti U, Silverman JF. 2014. HER2 in breast cancer: a review and update. Adv Anat Pathol. 21(2): 100-7.

Kroon E, MacDonald RJ, Hammer RE. 1997. The transcriptional regulatory strategy of the rat tissue kallikrein gene family. Genes Funct. 1(5-6): 309-19.

Kryza T, Silva ML, Loessner D, Heuze-Vourc'h N, Clements JA. 2015. The kallikrein-related peptidase family: Dysregulation and functions during cancer progression. Biochimie. 122: 283-299.

Kurman RJ. 2013. Origin and molecular pathogenesis of ovarian high-grade serous carcinoma. Ann Oncol. 24 Suppl 10: x16-21.

Kurman RJ, Shih IM. 2011. Molecular pathogenesis and extraovarian origin of epithelial ovarian cancer--shifting the paradigm. Hum Pathol. 42(7): 918-31.

Lai J, Kedda MA, Hinze K, Smith RL, Yaxley J, Spurdle AB, Morris CP, Harris J, Clements JA. 2007. PSA/KLK3 AREI promoter polymorphism alters androgen receptor binding and is associated with prostate cancer susceptibility. Carcinogenesis. 28(5): 1032-9.

Lawrence MG, Lai J, Clements JA. 2010. Kallikreins on steroids: structure, function, and hormonal regulation of prostate-specific antigen and the extended kallikrein locus. Endocr Rev. 31(4): 407-46.

Lei KF, Liu BY, Zhang XQ, Jin XL, Guo Y, Ye M, Zhu ZG. 2012. Development of a survival prediction model for gastric cancer using serine proteases and their inhibitors. Exp Ther Med. 3(1): 109-116.

Li B, Goyal J, Dhar S, Dimri G, Evron E, Sukumar S, Wazer DE, Band V. 2001. CpG methylation as a basis for breast tumor-specific loss of NES1/kallikrein 10 expression. Cancer Res. 61(21): 8014-21.

Li L, Xu N, Fan N, Meng Q, Luo W, Lv L, Ma W, Liu X, Liu L, Xu F, Wang H, Mao W, Li Y. 2015. Upregulated KLK10 inhibits esophageal cancer proliferation and enhances cisplatin sensitivity in vitro. Oncol Rep. 34(5): 2325-32.

Li X, Liu J, Wang Y, Zhang L, Ning L, Feng Y. 2009. Parallel underexpression of kallikrein 5 and kallikrein 7 mRNA in breast malignancies. Cancer Sci. 100(4): 601-7.

Linardoutsos D, Gazouli M, Machairas A, Bramis I, Zografos GC. 2014. Kallikrein-related peptidases in cancers of gastrointestinal tract: an inside view of their role and clinical significance. J BUON. 19(1): 53-9.

Lu CY, Hsieh SY, Lu YJ, Wu CS, Chen LC, Lo SJ, Wu CT, Chou MY, Huang TH, Chang YS. 2009. Aberrant DNA methylation profile and frequent methylation of KLK10 and OXGR1 genes in hepatocellular carcinoma. Genes Chromosomes Cancer. 48(12): 1057-68.

Lundwall A, Band V, Blaber M, Clements JA, Courty Y, Diamandis EP, Fritz H, Lilja H, Malm J, Maltais LJ, Olsson AY, Petraki C, Scorilas A, Sotiropoulou G, Stenman UH, Stephan C, Talieri M, Yousef GM. 2006. A comprehensive nomenclature for serine proteases with homology to tissue kallikreins. Biol Chem. 387(6): 637-41.

Lundwall A, Brattsand M. 2008. Kallikrein-related peptidases. Cell Mol Life Sci. 65(13): 2019-38.

Luo LY, Bunting P, Scorilas A, Diamandis EP. 2001. Human kallikrein 10: a novel tumor marker for ovarian carcinoma. Clin Chim Acta. 306(1-2): 111-8.

Luo LY, Diamandis EP, Look MP, Soosaipillai AP, Foekens JA. 2002. Higher expression of human kallikrein 10 in breast cancer tissue predicts tamoxifen resistance. Br J Cancer. 86(11): 1790-6.

Luo LY, Grass L, Diamandis EP. 2003. Steroid hormone regulation of the human kallikrein 10 (KLK10) gene in cancer cell lines and functional characterization of the KLK10 gene promoter. Clin Chim Acta. 337(1-2): 115-26.

Luo LY, Grass L, Diamandis EP. 2000. The normal epithelial cell-specific 1 (NES1) gene is up-regulated by steroid hormones in the breast carcinoma cell line BT-474. Anticancer Res.

20(2A): 981-6.

Luo LY, Grass L, Howarth DJ, Thibault P, Ong H, Diamandis EP. 2001. Immunofluorometric assay of human kallikrein 10 and its identification in biological fluids and tissues. Clin Chem. 47(2): 237-46.

Luo LY, Katsaros D, Scorilas A, Fracchioli S, Bellino R, van Gramberen M, de Bruijn H, Henrik A, Stenman UH, Massobrio M, van der Zee AG, Vergote I, Diamandis EP. 2003. The serum concentration of human kallikrein 10 represents a novel biomarker for ovarian cancer diagnosis and prognosis. Cancer Res. 63(4): 807-11.

Luo LY, Katsaros D, Scorilas A, Fracchioli S, Piccinno R, Rigault de la Longrais IA, Howarth DJ, Diamandis EP. 2001. Prognostic value of human kallikrein 10 expression in epithelial ovarian carcinoma. Clin Cancer Res. 7(8): 2372-9.

Luo LY, Rajpert-De Meyts ER, Jung K, Diamandis EP. 2001. Expression of the normal epithelial cell-specific 1 (NES1; KLK10) candidate tumour suppressor gene in normal and malignant testicular tissue. Br J Cancer. 85(2): 220-4.

Magklara A, Scorilas A, Katsaros D, Massobrio M, Yousef GM, Fracchioli S, Danese S, Diamandis EP. 2001. The human KLK8 (neuropsin/ovasin) gene: identification of two novel splice variants and its prognostic value in ovarian cancer. Clin Cancer Res. 7(4): 806-11.

Mangé A, Desmetz C, Berthes ML, Maudelonde T, Solassol J. 2008. Specific increase of human kallikrein 4 mRNA and protein levels in breast cancer stromal cells. Biochem Biophys Res Commun. 375(1): 107-12.

Mauri D, Pavlidis N, Ioannidis JP. 2005. Neoadjuvant versus adjuvant systemic treatment in breast cancer: a meta-analysis. J Natl Cancer Inst. 97(3): 188-94.

Meinhold-Heerlein I, Hauptmann S. 2014. The heterogeneity of ovarian cancer. Arch Gynecol Obstet. 289(2): 237-9.

Michael IP, Kurlender L, Memari N, Yousef GM, Du D, Grass L, Stephan C, Jung K, Diamandis EP. 2005. Intron retention: a common splicing event within the human kallikrein gene family. Clin Chem. 51(3): 506-15.

Michael IP, Pampalakis G, Mikolajczyk SD, Malm J, Sotiropoulou G, Diamandis EP. 2006. Human tissue kallikrein 5 is a member of a proteolytic cascade pathway involved in seminal clot liquefaction and potentially in prostate cancer progression. J Biol Chem. 281(18): 12743-

50.

Michael IP, Sotiropoulou G, Pampalakis G, Magklara A, Ghosh M, Wasney G, Diamandis EP. 2005. Biochemical and enzymatic characterization of human kallikrein 5 (hK5), a novel serine protease potentially involved in cancer progression. J Biol Chem. 280(15): 14628-35.

Michaelidou K, Ardavanis A, Scorilas A. 2015. Clinical relevance of the deregulated kallikrein-related peptidase 8 mRNA expression in breast cancer: a novel independent indicator of disease-free survival. Breast Cancer Res Treat. 152(2): 323-36.

Michel N, Heuzé-Vourc'h N, Lavergne E, Parent C, Jourdan ML, Vallet A, Iochmann S, Musso O, Reverdiau P, Courty Y. 2014. Growth and survival of lung cancer cells: regulation by kallikrein-related peptidase 6 via activation of proteinase-activated receptor 2 and the epidermal growth factor receptor. Biol Chem. 395(9): 1015-25.

Millikan RC, Newman B, Tse CK, Moorman PG, Conway K, Dressler LG, Smith LV, Labbok MH, Geradts J, Bensen JT, Jackson S, Nyante S, Livasy C, Carey L, Earp HS, Perou CM. 2008. Epidemiology of basal-like breast cancer. Breast Cancer Res Treat. 109(1): 123-39.

Mize GJ, Wang W, Takayama TK. 2008. Prostate-specific kallikreins-2 and -4 enhance the proliferation of DU-145 prostate cancer cells through protease-activated receptors-1 and -2. Mol Cancer Res. 6(6): 1043-51.

Moasser MM. 2007. The oncogene HER2: its signaling and transforming functions and its role in human cancer pathogenesis. Oncogene. 26(45): 6469-87.

Mutch DG, Prat J. 2014. 2014 FIGO staging for ovarian, fallopian tube and peritoneal cancer. Gynecol Oncol. 133(3): 401-4.

Neve RM, Chin K, Fridlyand J, Yeh J, Baehner FL, Fevr T, Clark L, Bayani N, Coppe JP, Tong F, Speed T, Spellman PT, DeVries S, Lapuk A, Wang NJ, Kuo WL, Stilwell JL, Pinkel D, Albertson DG, Waldman FM, McCormick F, Dickson RB, Johnson MD, Lippman M, Ethier S, Gazdar A, Gray JW. 2006. A collection of breast cancer cell lines for the study of functionally distinct cancer subtypes. Cancer Cell. 10(6): 515-27.

Obiezu CV, Diamandis EP. 2005. Human tissue kallikrein gene family: applications in cancer. Cancer Lett. 224(1): 1-22.

Obiezu CV, Scorilas A, Katsaros D, Massobrio M, Yousef GM, Fracchioli S, Rigault de la Longrais IA, Arisio R, Diamandis EP. 2001. Higher human kallikrein gene 4 (KLK4)

expression indicates poor prognosis of ovarian cancer patients. Clin Cancer Res. 7(8): 2380-6.

Olkhov-Mitsel E, Van der Kwast T, Kron KJ, Ozcelik H, Briollais L, Massey C, Recker F, Kwiatkowski M, Fleshner NE, Diamandis EP, Zlotta AR, Bapat B. 2012. Quantitative DNA methylation analysis of genes coding for kallikrein-related peptidases 6 and 10 as biomarkers for prostate cancer. Epigenetics. 7(9): 1037-45.

Paliouras M, Diamandis EP. 2008. Androgens act synergistically to enhance estrogen-induced upregulation of human tissue kallikreins 10, 11, and 14 in breast cancer cells via a membrane bound androgen receptor. Mol Oncol. 1(4): 413-24.

Paliouras M, Diamandis EP. 2007. Coordinated steroid hormone-dependent and independent expression of multiple kallikreins in breast cancer cell lines. Breast Cancer Res Treat. 102(1): 7-18.

Paliouras M, Diamandis EP. 2008. Intracellular signaling pathways regulate hormone-dependent kallikrein gene expression. Tumour Biol. 29(2): 63-75.

Palma G, Frasci G, Chirico A, Esposito E, Siani C, Saturnino C, Arra C, Ciliberto G, Giordano A, D'Aiuto M. 2015. Triple negative breast cancer: looking for the missing link between biology and treatments. Oncotarget. 6(29): 26560-74.

Pampalakis G, Prosnikli E, Agalioti T, Vlahou A, Zoumpourlis V, Sotiropoulou G. 2009. A tumor-protective role for human kallikrein-related peptidase 6 in breast cancer mediated by inhibition of epithelial-to-mesenchymal transition. Cancer Res. 69(9): 3779-87.

Pampalakis G, Sotiropoulou G. 2006. Multiple mechanisms underlie the aberrant expression of the human kallikrein 6 gene in breast cancer. Biol Chem. 387(6): 773-82.

Papachristopoulou G, Avgeris M, Charlaftis A, Scorilas A. 2011. Quantitative expression analysis and study of the novel human kallikrein-related peptidase 14 gene (KLK14) in malignant and benign breast tissues. Thromb Haemost. 105(1): 131-7.

Pasic MD, Olkhov E, Bapat B, Yousef GM. 2012. Epigenetic regulation of kallikrein-related peptidases: there is a whole new world out there. Biol Chem. 393(5): 319-30.

Pasic MD, Sotiropoulou G, Yousef GM. 2015. The miRNA-Kallikrein interactions: adding a new dimension. Cell Cycle. 14(5): 691-2.

Paulsen T, Kaern J, Kjaerheim K, Tropé C, Tretli S. 2005. Symptoms and referral of women

with epithelial ovarian tumors. Int J Gynaecol Obstet. 88(1): 31-7.

Pepin D, Shao ZQ, Huppe G, Wakefield A, Chu CW, Sharif Z, Vanderhyden BC. 2011. Kallikreins 5, 6 and 10 differentially alter pathophysiology and overall survival in an ovarian cancer xenograft model. PLoS One. 6(11): e26075.

Petraki C, Youssef YM, Dubinski W, Lichner Z, Scorilas A, Pasic MD, Komborozos V, Khalil B, Streutker C, Diamandis EP, Yousef GM. 2012. Evaluation and prognostic significance of human tissue kallikrein-related peptidase 10 (KLK10) in colorectal cancer. Tumour Biol. 33(4): 1209-14.

Pfaffl MW. (2012). Quantification strategies in real-time polymerase chain reaction. Quantitative real-time PCR. Appl Microbiol, 53-62.

Planque C, Aïnciburu M, Heuzé-Vourc'h N, Régina S, de Monte M, Courty Y. 2006. Expression of the human kallikrein genes 10 (KLK10) and 11 (KLK11) in cancerous and non-cancerous lung tissues. Biol Chem. 387(6): 783-8.

Psyrri A, Kountourakis P, Scorilas A, Markakis S, Camp R, Kowalski D, Diamandis EP, Dimopoulos MA. 2008. Human tissue kallikrein 7, a novel biomarker for advanced ovarian carcinoma using a novel in situ quantitative method of protein expression. Ann Oncol. 19(7): 1271-7.

Radulovic M, Yoon H, Larson N, Wu J, Linbo R, Burda JE, Diamandis EP, Blaber SI, Blaber M, Fehlings MG, Scarisbrick IA. 2013. Kallikrein cascades in traumatic spinal cord injury: in vitro evidence for roles in axonopathy and neuron degeneration. J Neuropathol Exp Neurol. 72(11): 1072-89.

Reis-Filho JS, Tutt AN. 2008. Triple negative tumours: a critical review. Histopathology. 52(1): 108-18.

Richardson AL, Wang ZC, De Nicolo A, Lu X, Brown M, Miron A, Liao X, Iglehart JD, Livingston DM, Ganesan S. 2006. X chromosomal abnormalities in basal-like human breast cancer. Cancer Cell. 9(2): 121-32.

Romond EH, Perez EA, Bryant J, Suman VJ, Geyer CE, Davidson NE, Tan-Chiu E, Martino S, Paik S, Kaufman PA, Swain SM, Pisansky TM, Fehrenbacher L, Kutteh LA, Vogel VG, Visscher DW, Yothers G, Jenkins RB, Brown AM, Dakhil SR, Mamounas EP, Lingle WL, Klein PM, Ingle JN, Wolmark N. 2005. Trastuzumab plus adjuvant chemotherapy for operable

HER2-positive breast cancer. N Engl J Med. 353(16): 1673-84.

Ross JS, Slodkowska EA, Symmans WF, Pusztai L, Ravdin PM, Hortobagyi GN. 2009. The HER-2 receptor and breast cancer: ten years of targeted anti-HER-2 therapy and personalized medicine. Oncologist. 14(4): 320-68.

Ruijter JM, Pfaffl MW, Zhao S, Spiess AN, Boggy G, Blom J, Rutledge RG, Sisti D, Lievens A, De Preter K, Derveaux S, Hellemans J, Vandesompele J. 2013. Evaluation of qPCR curve analysis methods for reliable biomarker discovery: bias, resolution, precision, and implications. Methods. 59(1): 32-46.

Samaan S, Lichner Z, Ding Q, Saleh C, Samuel J, Streutker C, Yousef GM. 2014. Kallikreins are involved in an miRNA network that contributes to prostate cancer progression. Biol Chem. 395(9): 991-1001.

Sano A, Sangai T, Maeda H, Nakamura M, Hasebe T, Ochiai A. 2007. Kallikrein 11 expressed in human breast cancer cells releases insulin-like growth factor through degradation of IGFBP-3. Int J Oncol. 30(6): 1493-8.

Santin AD, Diamandis EP, Bellone S, Marizzoni M, Bandiera E, Palmieri M, Papasakelariou C, Katsaros D, Burnett A, Pecorelli S. 2006. Overexpression of kallikrein 10 (hK10) in uterine serous papillary carcinomas. Am J Obstet Gynecol. 194(5): 1296-302.

Schedlich LJ, Bennetts BH, Morris BJ. 1987. Primary structure of a human glandular kallikrein gene. DNA. 6(5): 429-37.

Schummer M, Green A, Beatty JD, Karlan BY, Karlan S, Gross J, Thornton S, McIntosh M, Urban N. 2010. Comparison of breast cancer to healthy control tissue discovers novel markers with potential for prognosis and early detection. PLoS One. 5(2): e9122.

Scorilas A, Borgoño CA, Harbeck N, Dorn J, Schmalfeldt B, Schmitt M, Diamandis EP. 2004. Human kallikrein 13 protein in ovarian cancer cytosols: a new favorable prognostic marker. J Clin Oncol. 22(4): 678-85.

Seiz L, Kotzsch M, Grebenchtchikov NI, Geurts-Moespot AJ, Fuessel S, Goettig P, Gkazepis A, Wirth MP, Schmitt M, Lossnitzer A, Sweep FC, Magdolen V. 2010. Polyclonal antibodies against kallikrein-related peptidase 4 (KLK4): immunohistochemical assessment of KLK4 expression in healthy tissues and prostate cancer. Biol Chem. 391(4): 391-401.

Senkus E, Kyriakides S, Ohno S, Penault-Llorca F, Poortmans P, Rutgers E, Zackrisson S,

Cardoso F. 2015. Primary breast cancer: ESMO Clinical Practice Guidelines for diagnosis, treatment and follow-up. Ann Oncol. 26 Suppl 5: v8-30.

Seoane J, Gomis RR. 2017. TGF-β Family Signaling in Tumor Suppression and Cancer Progression. Cold Spring Harb Perspect Biol. 9(12).

Shan SJ, Scorilas A, Katsaros D, Diamandis EP. 2007. Transcriptional upregulation of human tissue kallikrein 6 in ovarian cancer: clinical and mechanistic aspects. Br J Cancer. 96(2): 362-72.

Shan SJ, Scorilas A, Katsaros D, Rigault de la Longrais I, Massobrio M, Diamandis EP. 2006. Unfavorable prognostic value of human kallikrein 7 quantified by ELISA in ovarian cancer cytosols. Clin Chem. 52(10): 1879-86.

Shaw JL, Diamandis EP. 2007. Distribution of 15 human kallikreins in tissues and biological fluids. Clin Chem. 53(8): 1423-32.

Shaw JL, Diamandis EP. 2008. Regulation of human tissue kallikrein-related peptidase expression by steroid hormones in 32 cell lines. Biol Chem. 389(11): 1409-19.

Sher YP, Chou CC, Chou RH, Wu HM, Wayne Chang WS, Chen CH, Yang PC, Wu CW, Yu CL, Peck K. 2006. Human kallikrein 8 protease confers a favorable clinical outcome in non-small cell lung cancer by suppressing tumor cell invasiveness. Cancer Res. 66(24): 11763-70.

Shigemasa K, Gu L, Tanimoto H, O'Brien TJ, Ohama K. 2004. Human kallikrein gene 11 (KLK11) mRNA overexpression is associated with poor prognosis in patients with epithelial ovarian cancer. Clin Cancer Res. 10(8): 2766-70.

Sidiropoulos M, Pampalakis G, Sotiropoulou G, Katsaros D, Diamandis EP. 2005. Downregulation of human kallikrein 10 (KLK10/NES1) by CpG island hypermethylation in breast, ovarian and prostate cancers. Tumour Biol. 26(6): 324-36.

Siegel RL, Miller KD, Jemal A. 2017. Cancer Statistics, 2017. CA Cancer J Clin. 67(1): 7-30.

Skacel M, Skilton B, Pettay JD, Tubbs RR. 2002. Tissue microarrays: a powerful tool for high-throughput analysis of clinical specimens: a review of the method with validation data. Appl Immunohistochem Mol Morphol. 10(1): 1-6.

Sundar S, Neal RD, Kehoe S. 2015. Diagnosis of ovarian cancer. BMJ. 351: h4443.

Talieri M, Devetzi M, Scorilas A, Pappa E, Tsapralis N, Missitzis I, Ardavanis A. 2012. Human kallikrein-related peptidase 12 (KLK12) splice variants expression in breast cancer and their clinical impact. Tumour Biol. 33(4): 1075-84.

Talieri M, Diamandis EP, Gourgiotis D, Mathioudaki K, Scorilas A. 2004. Expression analysis of the human kallikrein 7 (KLK7) in breast tumors: a new potential biomarker for prognosis of breast carcinoma. Thromb Haemost. 91(1): 180-6.

Tang L, Long Z, Feng G, Guo X, Yu M. 2017. NES1/KLK10 promotes trastuzumab resistance via activation of PI3K/AKT signaling pathway in gastric cancer. J Cell Biochem. 119(8): 6398-6407.

Thiery JP, Acloque H, Huang RY, Nieto MA. 2009. Epithelial-mesenchymal transitions in development and disease. Cell. 139(5): 871-90.

Torre LA, Bray F, Siegel RL, Ferlay J, Lortet-Tieulent J, Jemal A. 2015. Global cancer statistics, 2012. CA Cancer J Clin. 65(2): 87-108.

Varghese F, Bukhari AB, Malhotra R, De A. 2014. IHC Profiler: an open source plugin for the quantitative evaluation and automated scoring of immunohistochemistry images of human tissue samples. PLoS One. 9(5): e96801.

Veveris-Lowe TL, Lawrence MG, Collard RL, Bui L, Herington AC, Nicol DL, Clements JA. 2005. Kallikrein 4 (hK4) and prostate-specific antigen (PSA) are associated with the loss of E-cadherin and an epithelial-mesenchymal transition (EMT)-like effect in prostate cancer cells. Endocr Relat Cancer. 12(3): 631-43.

Walker JL, Powell CB, Chen LM, Carter J, Bae Jump VL, Parker LP, Borowsky ME, Gibb RK. 2015. Society of Gynecologic Oncology recommendations for the prevention of ovarian cancer. Cancer. 121(13): 2108-20.

Wang Z, Ruan B, Jin Y, Zhang Y, Li J, Zhu L, Xu W, Feng L, Jin H, Wang X. 2016. Identification of KLK10 as a therapeutic target to reverse trastuzumab resistance in breast cancer. Oncotarget. 7(48): 79494.

Waziri A, Schevon CA, Cappell J, Emerson RG, McKhann GM, Goodman RR. 2009. Initial surgical experience with a dense cortical microarray in epileptic patients undergoing craniotomy for subdural electrode implantation. Neurosurgery. 64(3): 540-5; discussion 545.

White NM, Chow TF, Mejia-Guerrero S, Diamandis M, Rofael Y, Faragalla H, Mankaruous

M, Gabril M, Girgis A, Yousef GM. 2010. Three dysregulated miRNAs control kallikrein 10 expression and cell proliferation in ovarian cancer. Br J Cancer. 102(8): 1244-53.

Yang F, Aubele M, Walch A, Gross E, Napieralski R, Zhao S, Ahmed N, Kiechle M, Reuning U, Dorn J, Sweep F, Magdolen V, Schmitt M. 2017. Tissue kallikrein-related peptidase 4 (KLK4), a novel biomarker in triple-negative breast cancer. Biol Chem. 398(10): 1151-1164.

Yoon H, Blaber SI, Debela M, Goettig P, Scarisbrick IA, Blaber M. 2009. A completed KLK activome profile: investigation of activation profiles of KLK9, 10, and 15. Biol Chem. 390(4): 373-7.

Yoon H, Blaber SI, Evans DM, Trim J, Juliano MA, Scarisbrick IA, Blaber M. 2008. Activation profiles of human kallikrein-related peptidases by proteases of the thrombostasis axis. Protein Sci. 17(11): 1998-2007.

Yoon H, Blaber SI, Li W, Scarisbrick IA, Blaber M. 2013. Activation profiles of human kallikrein-related peptidases by matrix metalloproteinases. Biol Chem. 394(1): 137-47.

Yoon H, Laxmikanthan G, Lee J, Blaber SI, Rodriguez A, Kogot JM, Scarisbrick IA, Blaber M. 2007. Activation profiles and regulatory cascades of the human kallikrein-related peptidases. J Biol Chem. 282(44): 31852-64.

Yousef GM, Borgoño CA, Scorilas A, Ponzone R, Biglia N, Iskander L, Polymeris ME, Roagna R, Sismondi P, Diamandis EP. 2002. Quantitative analysis of human kallikrein gene 14 expression in breast tumours indicates association with poor prognosis. Br J Cancer. 87(11): 1287-93.

Yousef GM, Chang A, Diamandis EP. 2000. Identification and characterization of KLK-L4, a new kallikrein-like gene that appears to be down-regulated in breast cancer tissues. J Biol Chem. 275(16): 11891-8.

Yousef GM, Diamandis EP. 2000. The expanded human kallikrein gene family: locus characterization and molecular cloning of a new member, KLK-L3 (KLK9). Genomics. 65(2): 184-94.

Yousef GM, Diamandis EP. 2001. The new human tissue kallikrein gene family: structure, function, and association to disease. Endocr Rev. 22(2): 184-204.

Yousef GM, Fracchioli S, Scorilas A, Borgoño CA, Iskander L, Puopolo M, Massobrio M, Diamandis EP, Katsaros D. 2003. Steroid hormone regulation and prognostic value of the

human kallikrein gene 14 in ovarian cancer. Am J Clin Pathol. 119(3): 346-55.

Yousef GM, Kyriakopoulou LG, Scorilas A, Fracchioli S, Ghiringhello B, Zarghooni M, Chang A, Diamandis M, Giardina G, Hartwick WJ, Richiardi G, Massobrio M, Diamandis EP, Katsaros D. 2001. Quantitative expression of the human kallikrein gene 9 (KLK9) in ovarian cancer: a new independent and favorable prognostic marker. Cancer Res. 61(21): 7811-8.

Yousef GM, Magklara A, Chang A, Jung K, Katsaros D, Diamandis EP. 2001. Cloning of a new member of the human kallikrein gene family, KLK14, which is down-regulated in different malignancies. Cancer Res. 61(8): 3425-31.

Yousef GM, Magklara A, Diamandis EP. 2000. KLK12 is a novel serine protease and a new member of the human kallikrein gene family-differential expression in breast cancer. Genomics. 69(3): 331-41.

Yousef GM, Obiezu CV, Luo LY, Magklara A, Borgoño CA, Kishi T, Memari N, lP M, Sidiropoulos M, Kurlender L, Economopolou K, Kapadia C, Komatsu N, Petraki C, Elliott M, Scorilas A, Katsaros D, Levesque MA, Diamandis EP. 2005. Human tissue kallikreins: from gene structure to function and clinical applications. Adv Clin Chem. 39: 11-79.

Yousef GM, Polymeris ME, Grass L, Soosaipillai A, Chan PC, Scorilas A, Borgoño C, Harbeck N, Schmalfeldt B, Dorn J, Schmitt M, Diamandis EP. 2003. Human kallikrein 5: a potential novel serum biomarker for breast and ovarian cancer. Cancer Res. 63(14): 3958-65.

Yousef GM, Polymeris ME, Yacoub GM, Scorilas A, Soosaipillai A, Popalis C, Fracchioli S, Katsaros D, Diamandis EP. 2003. Parallel overexpression of seven kallikrein genes in ovarian cancer. Cancer Res. 63(9): 2223-7.

Yousef GM, Scorilas A, Katsaros D, Fracchioli S, Iskander L, Borgono C, Rigault de la Longrais IA, Puopolo M, Massobrio M, Diamandis EP. 2003. Prognostic value of the human kallikrein gene 15 expression in ovarian cancer. J Clin Oncol. 21(16): 3119-26.

Yousef GM, Scorilas A, Kyriakopoulou LG, Rendl L, Diamandis M, Ponzone R, Biglia N, Giai M, Roagna R, Sismondi P, Diamandis EP. 2002. Human kallikrein gene 5 (KLK5) expression by quantitative PCR: an independent indicator of poor prognosis in breast cancer. Clin Chem. 48(8): 1241-50.

Yousef GM, Scorilas A, Magklara A, Memari N, Ponzone R, Sismondi P, Biglia N, Abd Ellatif M, Diamandis EP. 2002. The androgen-regulated gene human kallikrein 15 (KLK15) is an

independent and favourable prognostic marker for breast cancer. Br J Cancer. 87(11): 1294-300.

Yousef GM, Scorilas A, Nakamura T, Ellatif MA, Ponzone R, Biglia N, Maggiorotto F, Roagna R, Sismondi P, Diamandis EP. 2003. The prognostic value of the human kallikrein gene 9 (KLK9) in breast cancer. Breast Cancer Res Treat. 78(2): 149-58.

Yousef GM, Yacoub GM, Polymeris ME, Popalis C, Soosaipillai A, Diamandis EP. 2004. Kallikrein gene downregulation in breast cancer. Br J Cancer. 90(1): 167-72.

Yu H, Levesque MA, Clark GM, Diamandis EP. 1998. Prognostic value of prostate-specific antigen for women with breast cancer: a large United States cohort study. Clin Cancer Res. 4(6): 1489-97.

Yu Y, Prassas I, Diamandis EP. 2014. Putative kallikrein substrates and their (patho)biological functions. Biol Chem. 395(9): 931-43.

Yunes MJ, Neuschatz AC, Bornstein LE, Naber SP, Band V, Wazer DE. 2003. Loss of expression of the putative tumor suppressor NES1 gene in biopsy-proven ductal carcinoma in situ predicts for invasive carcinoma at definitive surgery. Int J Radiat Oncol Biol Phys. 56(3): 653-7.

Zeppernick F, Meinhold-Heerlein I. 2014. The new FIGO staging system for ovarian, fallopian tube, and primary peritoneal cancer. Arch Gynecol Obstet. 290(5): 839-42.

Zhang Y, Bhat I, Zeng M, Jayal G, Wazer DE, Band H, Band V. 2006. Human kallikrein 10, a predictive marker for breast cancer. Biol Chem. 387(6): 715-21.

Zhang Y, Song H, Miao Y, Wang R, Chen L. 2010. Frequent transcriptional inactivation of Kallikrein 10 gene by CpG island hypermethylation in non-small cell lung cancer. Cancer Sci. 101(4): 934-40.

Zhang Y, Wang R, Song H, Huang G, Yi J, Zheng Y, Wang J, Chen L. 2011. Methylation of multiple genes as a candidate biomarker in non-small cell lung cancer. Cancer Lett. 303(1): 21-8.

Zheng H, Zhang W, Wang X, Zhao G. 2012. Enhancement of kallikrein-related peptidase 10 expression attenuates proliferation and invasiveness of human tongue cancer cells in vitro. Nan Fang Yi Ke Da Xue Xue Bao. 32(12): 1796-9.